Title
Signaling Scaffolds in Cardiovascular Development and Disease

Permalink
https://escholarship.org/uc/item/9ns2x7cc

Author
Spindler, Matthew

Publication Date
2011

Peer reviewed|Thesis/dissertation

Signaling Scaffolds in Cardiovascular Development and Disease

by

Matthew J. Spindler

DISSERTATION

Submitted in partial satisfaction of the requirements for the degree of

DOCTOR OF PHILOSOPHY

in

Pharmaceutical Sciences and Pharmacogenomics

in the

GRADUATE DIVISION

of the

UNIVERSITY OF CALIFORNIA, SAN FRANCISCO

Acknowledgments

Publication Reprints

Personal Acknowledgments

I have built strong personal connections with many of these scientists and highly value all of these friendships. I also met many wonderful people at Gladstone, UCSF, and in San Francisco that provided a good work-play balance. A special thank you to all of my classmates and fellow PSPG students, especially Ryan Owens, Leslie Chinn, Eric Peters, Jason Gow, Ben Lauffer, Jim Shima, and Jeff and Molly Kraft for all of the enjoyable kickball, softball, and volleyball games and hiking excursions. I also would like to thank my great friends Nathan Wilson and Matthew Wanat for introducing me to San Francisco and helping me maintain my sanity during the many years of school.

I am especially grateful to my family; if it wasn't for their love, support, and sacrifices, I wouldn't be where I am today. My parents, Charles and Linda, taught me the importance of hard work and perseverance. By following their example, I was able to successfully complete my doctoral degree despite the many ups and downs along the way. To my sisters Erin and Holly, growing up on the farm with you was a wonderful experience, and though we are all now far from home you still provide levity when we return.

Finally, to the love of my life, Erin, thank you for all of your love and support throughout my time here. I am truly indebted to you. You always had faith in me and have shown incredible patience as I plodded through my research. I am so lucky to have shared this time and this wonderful city with you and am excited to conquer our next adventure together.

Abstract

Signaling Scaffolds in Cardiovascular Development and Disease

Matthew J. Spindler

Background: G-protein signaling pathways regulate many aspects of cardiovascular development and disease. A-kinase anchoring proteins (AKAPs) are scaffolding molecules that coordinate and integrate these signaling events into specific physiological processes. One family member, AKAP13, integrates G_s, $G_{q/11}$, and $G_{12/13}$ signals through binding of protein kinase A, C (PKC), and D (PKD) and encoding an active Rho-guanine nucleotide exchange factor (Rho-GEF) domain. AKAP13 is required for mouse development as null embryos die by E10.5 and exhibit cardiovascular defects. Additionally, the Rho-GEF and PKC-PKD binding domains mediate cardiomyocyte hypertrophy in isolated cardiomyocytes. However, the specific developmental processes regulated by AKAP13 and the requirements for the Rho-GEF and PKC-PKD binding domains during development and cardiac hypertrophy are unknown.

Methodology/Principal Findings: We used an RNAi, loss-of-function approach, to determine if AKAP13 mediates differentiation of mouse embryonic stem (ES) cells or angiogenic processes in human umbilical vein endothelial cells (HUVECs). We found that AKAP13 knockdown did not decrease ES cell differentiation into Nkx2.5-GFP-positive cardiac mesodermal cells or functionally beating cardiomyocytes. Similarly, the expression of endodermal, endothelial, or

cardiac structural marker genes was not affected. We also found that AKAP13-deficient HUVECs had normal tube formation, VEGF-induced wound healing, and VEGF-induced PKD phosphorylation. We then generated AKAP13-truncation mutant mice to determine if the Rho-GEF and PKC-PKD binding domains are required for development. Surprisingly, homozygous mutant mice were born at normal Mendelian ratios and had normal survival, fertility, and cardiac structure. Finally, to determine if these domains mediate β-adrenergic-induced cardiac hypertrophy, we stressed the mice with isoproterenol. We found that heart size increased normally in mice lacking the Rho-GEF and PKC-PKD binding domains. However, these hearts failed to increase cardiac ejection fraction or fractional shortening.

Conclusions: These results indicate that AKAP13 is not required for differentiation into cardiovascular tissue, the formation of functional cardiomyocytes, or angiogenic processes. They also indicate that the AKAP13 Rho-GEF and PKC-PKD binding domains are not required for mouse development or the cardiac structural response to β-adrenergic-induced hypertrophy. However, these domains are required for the proper cardiac functional response to β-adrenergic stimulation.

Table of Contents

Chapter 4

AKAP13 Rho-GEF and PKC-PKD Binding Domain-Deficient Mice Develop Normally Yet Fail to Induce a Functional Cardiac Response to β-Adrenergic Stimulation **134**

List of Tables

List of Figures

Chapter 1

Introduction: Using A-Kinase Anchoring Proteins (AKAPs) to Elucidate G-Protein Signaling Events During Cardiovascular Development and Disease

1.1 G-protein signaling regulates many aspects of development and adult physiology.

G-protein signaling pathways have been extensively studied in the context of adult physiology and disease and are known to regulate a vast array of physiological processes, including the senses of smell, taste, and sight, hormonal and neurotransmitter signaling, cardiovascular function, chemotaxis, and development [1,2,3]. The G-protein signaling pathways are activated by seven-transmembrane G-protein-coupled receptors (GPCRs) that transduce extracellular signals into intracellular events. The GPCR family contains over 800 genes, with about half encoding for odorant receptors [4], and GPCRs alone are targeted by 30% of marketed small-molecule drugs with many additional drugs targeting proteins downstream of GPCRs [5]. For example, drugs that target the GPCR pathways for angiotensin II (ACE inhibitors) and β-adrenergic (β-blockers) receptors and have become common for treating hypertension and heart failure [6]. Despite extensive research in identifying GPCRs and downstream signaling pathways important for adult physiology and disease, little is known about the pathways important for development. The enormous number of GPCRs and the signaling redundancy between them present a problem for studying their specific functions during development. However, a signaling bottleneck occurs

downstream of GPCRs as the receptors signal through four common pathways by coupling to heterotrimeric G-proteins.

Heterotrimeric G-proteins consist of an α-, β-, and γ-subunit and the signaling pathways activated are classically defined by the α-subunit in the complex (Figure 1.1). The stimulatory and inhibitory Gα-proteins (Gα_s and Gα_i) regulate the production of cyclic AMP (cAMP), a second messenger, by adenylyl cyclase (AC). Downstream cellular signaling then occurs by cAMP activation of cAMP-dependent protein kinase A (PKA) and/or exchange proteins activated by cAMP (Epac) [1,7]. The G$\alpha_{q/11}$ proteins stimulate phospholipase C (PLC) to produce the second messengers inositol trisphosphate (IP$_3$) and diacylglycerol (DAG), which stimulate the release of calcium (Ca^{++}) and the activation of protein kinase C (PKC), respectively [8,9]. Finally, the G$\alpha_{12/13}$ proteins stimulate the Rho family of small GTPases through the activation of Rho-selective guanine nucleotide exchange factors (Rho-GEFs) [10,11,12].
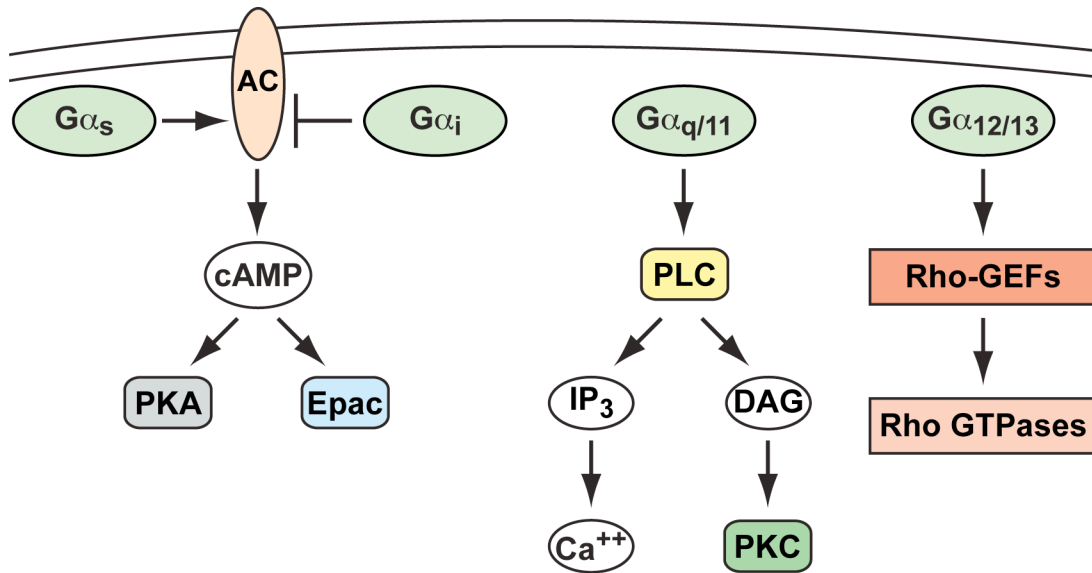
Figure 1.1. The classical G-protein signaling pathways. G-protein-coupled receptors (GPCRs) activate heterotrimeric G-proteins to transduce extracellular signals into intracellular events. Classically, the signaling cascade induced by the GPCR depends on the specific α-subunit within the GPCR-bound heterotrimeric G-protein. The stimulatory (Gα$_s$) and inhibitory (Gα$_i$) G-proteins regulate the production of the second messenger cyclic AMP (cAMP) through the regulation of adenylyl cyclase (AC). In turn, cAMP can activate cAMP-dependent protein kinase A (PKA) and the exchange factor directly activated by cAMP (Epac) to mediate cellular physiological responses. Gα$_{q/11}$ proteins stimulate phospholipase C (PLC) to hydrolyze phosphatidylinositol 4,5-bisphosphate into the second messengers inositol trisphosphate (IP$_3$) and diacylglycerol (DAG), which stimulate the release of calcium (Ca^{++}) and the activation of protein kinase C (PKC). Finally, Gα$_{12/13}$ proteins activate Rho-specific guanine nucleotide exchange factors (Rho-GEFs) that then activate the Rho family of small GTPases.

Interestingly, disruptions of the Gα-subunits for any of these four G-protein signaling pathways cause embryonic death in mice, and three of them display defects in cardiovascular development, with the fourth lacking a phenotypic description [3]. It is not surprising that disruption of the ubiquitously important G-protein signaling pathways would yield cardiovascular phenotypes, since the cardiovascular system is the first to form during development and is required for subsequent stages of development. These G-protein pathways are also important for neuronal, bone, and adipocyte development, asymmetry, planar cell polarity, and Wnt signaling [2]. Targeted disruption of the mouse Gα_s gene, *Gnas*, results in death by embryonic day E10.5 of development [13,14], and an ENU-induced mutation mapped to *Gnas* suggests that this gene regulates cardiac development [15]. A double knockout for the Gα_i genes, *Gnai2* and *Gnai3*, results in embryonic lethality; however, the cause of death has not been reported [3]. A double knockout for the G$\alpha_{q/11}$ genes, *Gnaq* and *Gna11*, results in embryonic lethality at E10.5 and display myocardial hypoplasia, with a thin ventricular myocardium, and edema [16]. Finally, knockout for the G$\alpha_{12/13}$ gene, *Gna13*, results in embryonic lethality at E9.5 from defective angiogenesis and the mice lack properly formed blood vessels in the yolk sac and embryo [17].

In addition to these requirements for Gα-proteins, many of the signaling molecules directly downstream of them play important roles during cardiac development. A global increase in basal PKA activity results in mouse embryos dying by E9.5 with reduced mesoderm formation and no heart tube [18], while a cardiac specific increase causes embryonic death at E11.5 from heart failure and

these embryos display thin ventricular walls and reduced trabeculation [19].

Similar to the $G\alpha_{q/11}$ double knockout, inhibition of PKC *in vitro* prevents

differentiation of ES cells into functional cardiomyocytes [20,21]. Finally, RhoA, a

member of the Rho GTPase family, is required for heart-tube closure in the chick

[22], and cardiac specific inhibition of the Rho GTPase family (RhoA, Rac1, and

Cdc42) causes embryonic death at E10.5 and defects in cardiac morphogenesis,

ventricular maturation, and cellular proliferation [23]. Despite these studies

demonstrating the importance of G-protein signaling pathways for cardiovascular

development, little is known about the molecular mechanisms that control these

processes.

   G-protein signaling pathways rely on second messengers (cAMP, IP_3, DAG,

and calcium) to propagate and amplify receptor stimulation. The second

messengers in turn induce intracellular signaling processes through the

activation of protein kinases (PKA and PKC), small GTPases, and ion channels.

However, these second messengers and downstream effecters are promiscuous

and can affect many cellular processes including metabolism, transcription, ion

channel activity, cytoskeletal organization, and contractility. Activation of specific

cellular processes by particular cell-surface receptors requires tight control of the

signal transduction pathway. Scaffolding molecules such as the A-kinase

anchoring protein (AKAP) family regulate the subcellular distribution of second

messenger signaling, thus providing signaling specificity [24].

1.2 AKAPs organize multiprotein complexes to provide signaling specificity.

The AKAP family consists of a very diverse set of at least 22 genes that encode for over 50 proteins [25]. This family of scaffolding molecules is classified by the ability to bind the regulatory region of PKA [26]. However, these scaffolds can bind many other important proteins, including protein kinases C and D (PKC & PKD), phosphotases, phosphodiesterases, ion channels, GPCRs, cytoskeletal components, and other signaling molecules and effectors, and localize them to specific cellular compartments [27,28]. Thus, AKAPs coordinate the induction of specific physiological effects by creating multiprotein complexes, controlling subcellular localization and target specificity, and integrating multiple upstream signals (Figure 1.2). This coordination of multiple proteins into a single signaling complex creates a focal point for regulating cellular physiology. Thus, disrupting these signaling focal points by mutagenesis of specific AKAPs can elucidate the physiological effects controlled by these signaling complexes. In fact, mutagenesis in model systems and cell culture indicates that AKAPs regulate aspects of reproduction, fertilization, embryonic development, neuronal activity, and cardiac structure and function [29].

AKAPs have been extensively studied in the cardiac system; however, much of this work has been limited to cell culture. Thirteen AKAPs have cardiac expression, and they regulate aspects of cardiac growth and remodeling, excitation-contraction coupling, and calcium and potassium regulation (Table 1.1). Despite this work, very little is known about the role of these AKAPs during

cardiac development. Given the importance of G-protein signaling for embryonic

development and specifically cardiovascular formation, it is reasonable to

hypothesize that AKAPs are also required for these processes. Interestingly,

many of the signaling pathways involved in AKAP-mediated cardiac remodeling

are also important in the developing heart. Additionally, there are indications that

certain AKAP knockouts cause embryonic lethality; however, they have not yet

been described [29].
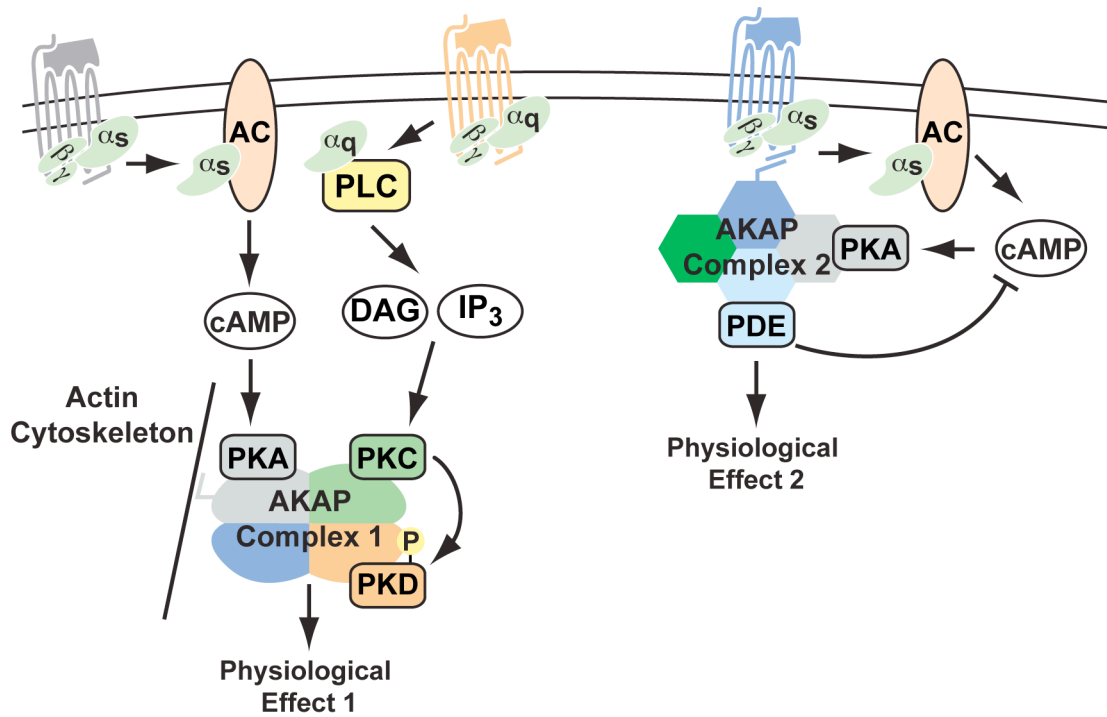
Figure 1.2. Cartoon of AKAP-coordinated signaling complexes. AKAPs organize multi-protein signaling complexes at specific subcellular locations to provide G-protein signaling specificity. AKAPs are categorized by their ability to bind PKA, but they can bind additional proteins such as PKC, PKD, and phosphodiesterases (PDE). This allows AKAPs to integrate multiple upstream signaling pathways into a specific physiological effect. These unique signaling complexes also provide a mechanism for common second messengers (cAMP, IP$_3$, and DAG) to produce specific physiological effects.

1.3 Embryonic stem (ES) cell differentiation is an ideal model for studying early cardiac developmental processes.

During mammalian development, the heart is the first organ to form and its proper function is required for further development. The heart derives from mesodermal cells that migrate out of the primitive streak and form the cardiac crescent which then become cells of the primary and secondary heart fields [30,31,32]. Complex signaling events involving the BMP, FGF, Wnt, Sonic hedgehog, G-protein, and Notch pathways regulate the differentiation of these heart field cells into the diverse set of cells in the mature heart [2,33]. In addition, many of the elegant transcriptional networks involved in cardiac differentiation and morphogenesis have been delineated [34,35].

Studying these early developmental processes in mice can be difficult. However, ES cells can be used as a model for these processes because they can differentiate into the three germ layers (endoderm, mesoderm, and ectoderm) and can be driven into many cell types [36] (Figure 1.3). In particular, ES cell differentiation through embryoid bodies (EBs) results in the formation of functional cardiomyocytes that spontaneously contract [37]. These ES cell-derived cardiomyocytes can form areas of rhythmically beating cells and display the electrical properties of atrial-, ventricular-, and nodal-like cardiomyocytes [38]. The process of ES cell differentiation into cardiomyocytes faithfully models *in vivo* cardiac development as the same genes, signaling molecules, and pathways regulate both processes [39,40,41]. Additionally, the ES cell–derived cardiomyocytes can model physiological processes and diseases including heart-

rate regulation [42], electrical activity [38], long-QT syndrome [43,44], and hypertrophy [45]. Thus, the ES cell differentiation model offers an ideal system for studying the role of G-protein signaling pathways and AKAPs in regulating cardiomyocyte differentiation and disease.

Another advantage that ES cells provide over *in vivo* developmental systems is that they are a very tractable cell system and can be easily mutated. Mouse ES cell have long been used to introduce genetic mutations into mouse lines through gene targeting for knockouts and knock-ins and random mutagenesis by gene-trapping [46,47,48]. These approaches often affect only one allele and require mating the mice to homozygosity for phenotypes to become apparent. This takes lots of time, space, and resources to accomplish. However, the advent of gene knockdown by RNA interference (RNAi) combined with lentiviral delivery of short hairpin RNA (shRNA) to mediate RNAi have created a strategy to quickly and efficiently reduce gene expression in ES cells [49,50]. Furthermore, this lentiviral-mediated RNAi strategy has been used to assess gene function during ES cell differentiation into cardiac tissue [51]. Thus, this RNAi strategy in ES cells offers an ideal system for studying the function of genes during tissue development and physiology.
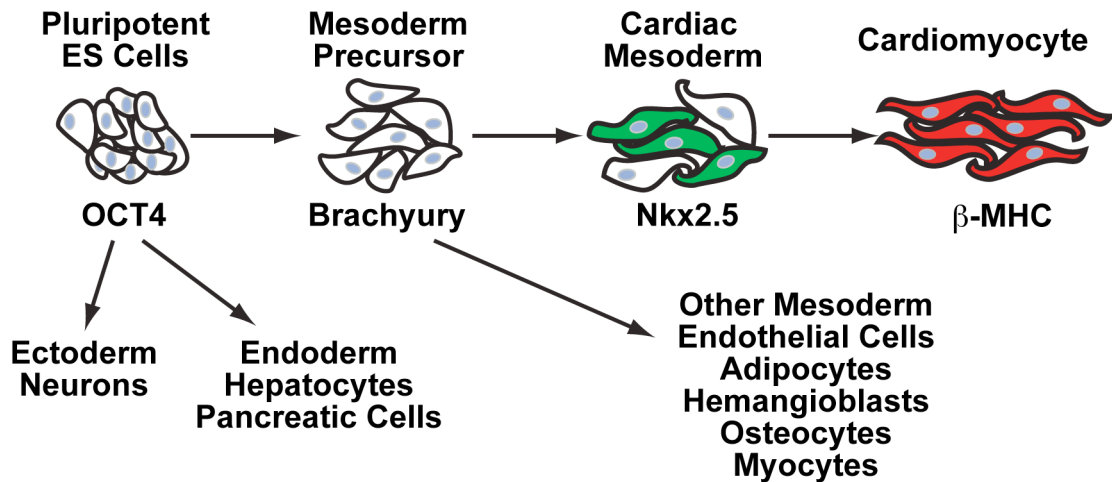
Figure 1.3. Pluripotent ES cells can differentiate into all three germ layers as well as functional cardiomyocytes. ES cells can differentiate into the three embryonic germ layers that give rise to all cells of an adult organism: ectoderm (e.g. neurons), endoderm (e.g. hepatocytes and pancreatic cells), and mesoderm (e.g. myocytes, adipocytes, osteocytes, and cardiomyocytes). ES cell–derived cardiomyocytes form groups of cells that rhythmically contract and express important structural proteins such as β-myosin heavy chain (β-MHC). The differentiation of functional cardiomyocytes from ES cells progresses through a mesoderm precursor (marked by Brachyury expression) and cardiac mesoderm (marked by the transcription factor Nkx2.5). The mesoderm precursor cells can also differentiate into many other mesodermal cell types including endothelial and smooth muscle cells.

1.4 Many AKAPs are expressed in ES cells and are regulated during mouse development and ES cell differentiation.

Since ES cell differentiation recapitulates early embryonic developmental processes, we hypothesized that AKAPs up-regulated during both processes are important for mammalian development. To identify candidate AKAP family members important for development, we analyzed publicly available microarray datasets for expression changes during mouse embryonic development [52] and ES cell differentiation [53]. Our main interest was in cardiovascular development, so we further hypothesized that AKAPs important for this process would be expressed in cardiac tissue. Thus, we conducted a literature review to identify AKAPs that are expressed in cardiac tissue and that are associated with cardiac phenotypes. Finally, we identified the AKAPs expressed in mouse ES cells and the available truncation mutant cell lines for these AKAPs that could be made into mice. We did this by analyzing the gene-trap events for each AKAP gene with the International Gene Trap Consortium sequence tag alignment track on the UCSC Genome Browser [54,55].

The gene-trap constructs stably integrate into the ES cell genome in a random fashion and generate protein truncation mutants. For ES cell selection of the gene-trap insertional event, the endogenous gene needs to be expressed and splicing from an endogenous exon to the splice acceptor of the gene-trap cassette needs to occur [48]. Thus, the likelihood and frequency of a gene being trapped using a splice acceptor cassette depends on gene length and ES cell expression [56]. Therefore, the number of unique gene-trap events for a given

AKAP correlates with the genomic size and ES cell expression level of that AKAP gene. The gene-trap event generates a truncation mutant by creating a fusion protein that contains a portion of the amino-terminus for the endogenous protein fused to the β-Geo cassette (β-galactosidase and neomycin resistance) from the gene-trap construct [48]. These mutations are heterozygous in ES cells and can produce phenotypes in cell culture [42]; however, the gene-trap cell lines are mostly used to generate mutant mouse lines. Unlike traditional gene knockouts that create null alleles, the gene-trap events often create hypomorphic alleles that retain some functionality. Thus, a series of truncation mutant mice can be generated if a gene has been trapped multiple times. This series of mutant mice can then be used to identify the functional importance of specific domains for a protein *in vivo*.

We found that many AKAPs are expressed and regulated during mouse development [52] and mouse ES cell differentiation [53] (Table 1.1). Of the 22 AKAP genes, only seven had expression information for both data sets. We found that only AKAP13 expression increased during mouse development and ES cell differentiation. Conversely, three of these seven genes (i.e., AKAP1, AKAP9, and Pericentrin) were down-regulated in both data sets. The remaining three genes (i.e., AKAP8, AKAP11, and Wasf1) were down-regulated during ES cell differentiation but were unchanged (AKAP8) or up-regulated during mouse development (AKAP11 and Wasf1). Unfortunately, there was no expression data for nine of the AKAP genes, and six genes had expression data for only one of the two data sets. Of these six AKAP genes, five had data for mouse

13

development only; in this data set, AKAP12 expression increased, AKAP7, AKAP10, and Ezrin expression decreased, and AKAP6 was expressed but this expression was unchanged over the developmental time course. The remaining gene, AKAP2, showed increased gene expression during ES cell differentiation.

The analysis of gene-trap events provided additional data on AKAP expression in ES cells as well as information on mutant cell lines that could be used to study gene function. Several genes that lacked expression data for the ES cell differentiation data set were trapped (AKAP6, AKAP7, AKAP8l, AKAP10, AKAP12, Map2, and Ezrin). Thus, these genes are expressed in ES cells. Additionally, many of the AKAP genes have several unique gene-trap events suggesting that these genes have a high level of expression in ES cells. In particular, Pericentrin had 15 unique exons trapped and AKAP13 had 10. Both of these genes are quite large with more than 40 exons in each and the high number of gene-traps indicates that they are also highly expressed in ES cells. The high level of Pericentrin expression in ES cells agrees with its functional role as a critical component of the centrosome and required protein for general mouse embryonic growth [57]. However, the reason for high expression levels of AKAP13, a cytoskeletal associated protein, in ES cells is unclear. Finally, the high number of uniquely trapped exons for Pericentrin and AKAP13 indicate that multiple truncation mutant mice could be generated. These truncation mutant mice could be used to dissect protein function and identify important protein domains *in vivo*.

The last piece of analysis we conducted was a literature review to identify AKAPs expressed in cardiac tissue and those associated with cardiac phenotypes either in cell culture or whole organisms. From this review, we identified 13 AKAP genes that are expressed in cardiac tissue and seven of these are associated with cardiac phenotypes. Most of the identified cardiac phenotypes indicate that AKAPs function to control proper cardiac excitation-contraction coupling and electrical activity through the regulation of cellular calcium (AKAP5, 6, & 7) and potassium (AKAP9) levels. Moreover, human mutations in several AKAPs cause changes in cardiac function, including AKAP9, which leads to type 1 long-QT syndrome (LQT1) [58], and AKAP10, which regulates heart rate and heart-rate variability [42,59]. AKAPs also regulate cardiomyocyte structure and growth as three AKAPs (AKAP1, 6, & 13) function in regulating cardiomyocyte hypertrophic processes. In particular, AKAP1 appears to play a protective role in the heart by inhibiting hypertrophy in isolated cardiomyocytes [60] and promoting mitochondrial function and cell survival *in vitro* and *in vivo* [61]. Contrary to AKAP1, AKAP6 [62] and AKAP13 [63,64] regulate the induction of hypertrophy by multiple receptors including adrenergic (AKAP6 & 13), angiotensin II (Ang II; AKAP13) and endothelin-1 (ET-1; AKAP13) receptors in isolated cardiomyocytes. Furthermore, both AKAP6 and AKAP13 are required for the induced expression of hypertrophic genes, such as atrial natriuretic factor (ANF). Finally, we learned that *Akap13*-null mice die during embryonic development and display cardiac hypoplasia [65]. However, this initial

information came from a poster abstract and we did not have phenotypic data to

indicate what part of cardiac development was affected.

Table 1.1. Analysis of cardiac and developmental expression and gene-trap events for the AKAP family

Gene	Aliases	Cardiac Expression	Cardiac Phenotype	Mouse Development [52]	ES Cell Differentiation [53]	Unique Gene Trapped Exons
AKAP1	D-AKAP1, S-AKAP84, AKAP121, AKAP149	+ [66,67]	Hyper [60,61]	-8.70	-2.31	5
AKAP2	AKAP-KL, PALM2				3.97	3
AKAP3	AKAP110, FSP95, SOB1					0
AKAP4	AKAP82, FSC1					0
AKAP5	AKAP75, AKAP79, AKAP150	+ [67]	Ca^{2+} [68]			0
AKAP6	mAKAP, AKAP100	+ [67,69,70,71]	Hyper [62], Ca^{2+} [72,73]	P		1
AKAP7	AKAP15, AKAP18	+ [74,75]	Ca^{2+} [76,77]	-2.14		1
AKAP8	AKAP95	+ [67,78]		P	-4.02	2
AKAP8l	NAKAP95, HAP95					4
AKAP9	AKAP350, AKAP450, Yotiao, Hyperion, CG-NAP	+ [79,80]	K^+ [58,81]	-2.26	-2.23	3
AKAP10	D-AKAP2	+ [82]	Arrhythmia [42]	-2.40		5
AKAP11	AKAP220, Gm80	+ [67,83]		2.17	-3.43	1
AKAP12	AKAP250, Gravin, SSeCKS	+ [84,85]		2.16		5
AKAP13	AKAP-Lbc, BRX, LBC, Ht31	+ [86,87]	Dev [65], Hyper [63,64]	1.88	3.69	10
AKAP14	AKAP28					0
Map2	Mtap2					1
Ezr	Ezrin, Villin-2			-7.56		4
Pcnt	Pericentrin, Kendrin			-1.94	-4.73	15
Wasf1	WAVE1, Scar			12.76	-2.04	1
Synm	Synemin, Desmuslin	+ [88]				0
Cmya5	Myospryn, Tims, Srfsd	+ [89,90]				0
Sphkap	SPHK1 interactor, Skip	+ [91]				0

A literature review identified AKAPs expressed in cardiac tissue and that have cardiac phenotypes in cell culture or animals. The type of cardiac phenotype is indicated: Hyper = hypertrophy, Ca^{2+} = calcium regulation, K^+ = potassium regulation, Dev = development. Publicly available microarray data sets were mined to determine the expression of AKAPs during mouse development and embryonic stem (ES) cell

differentiation. Absolute fold changes are reported when greater than 1.8, and expressed, but unchanged, genes are marked as present (P). The number of uniquely trapped exons for each AKAP gene is indicated.

1.5 Discussion: AKAP13 is our top candidate for regulating cardiovascular development in mice.

We identified AKAP13 as our top candidate for regulating cardiovascular development from our expression and literature analysis. The expression analysis showed that AKAP13 is up-regulated during both mouse development and ES cell differentiation. Additionally, AKAP13 appears to be highly expressed in undifferentiated ES cells because it has multiple gene-trapped exons. From a literature analysis, we found that AKAP13 is highly expressed in adult heart tissue and has a much lower level of expression in other tissue types [86,87]. AKAP13 also functions in promoting cardiac growth by propagating hypertrophic signals in isolated cardiomyocytes [63,64]. Finally, AKAP13 appears to be required for proper cardiovascular development and mouse embryonic survival [65].

AKAP13 coordinates signaling pathways that induce cardiomyocyte hypertrophy and these pathways may also be important for cardiovascular development. AKAP13 integrates multiple G-protein signaling pathways ($G\alpha_s$, $G\alpha_{12/13}$, and $G\alpha_{q/11}$) by binding PKA, PKC, PKD, and the chaperon protein 14-3-3 and encoding for a RhoA-specific GEF domain [87,92,93,94] (Figure 1.4 A). In isolated rat ventricular cardiomyocytes, AKAP13 integrates these signals to

18

induce a hypertrophic response that increases cell size and turns on the expression of hypertrophic genes (i.e., the "fetal" gene program). In these cells, stimulation of the α1-adrenergic receptor (α1-AR) by phenylephrine (PE) activates the G$\alpha_{q/11}$ and G$\alpha_{12/13}$ pathways which both signal through AKAP13 to mediate the hypertrophic response [63,64]. The G$\alpha_{q/11}$ pathway induces myocyte enhancer factor 2 (MEF2) transcriptional activity through a PKC-PKD-class II histone deacetylase (HDAC) phosphorylation cascade [64]. The α1-AR-coupling to the G$\alpha_{q/11}$ pathway signals through PLC to activate PKC, which then phosphorylates co-bound PKD to make it active. The activated PKD then phosphorylates class II HDACs, and the phosphorylated HDACs translocate from the nucleus to the cytoplasm and become bound to the chaperon protein 14-3-3. This translocation of HDACs derepresses MEF2 transcriptional activity and turns on the expression of MEF2 responsive genes. Additionally, coupling to the G$\alpha_{12/13}$ pathway activates the Rho-GEF domain of AKAP13 which in turn activates RhoA, and this activation of RhoA appears to be important for cardiomyocyte hypertrophy [63]. However, the molecular events downstream of G$\alpha_{12/13}$-AKAP13 activation of RhoA that lead to cardiac hypertrophy are unknown. The GPCR agonists Ang II and ET-1 also induce hypertrophy in isolated cardiomyocytes through an AKAP13-dependent manner [63,64]; however, the specific AKAP13-mediated signaling events required for this are not known.

AKAP13-bound PKA appears to modulate these two AKAP13-mediated signaling pathways by regulating the phosphorylation state of AKAP13 (Figure

1.4 B). AKAP13-bound PKA can be activated by isoproterenol (Iso) stimulation of the $G\alpha_s$-coupled β-adrenergic receptor in isolated cardiomyocytes, and this induces PKA phosphorylation of AKAP13 at the carboxy-terminal PKD-binding domain [92]. This phosphorylation event appears to enhance the PKC-mediated activation of PKD by decreasing the AKAP13 binding affinity for PKD and potentially increasing the turnover rate of AKAP13-bound PKD. Conversely, AKAP13-bound PKA inhibits Rho-GEF activity by phosphorylating the 14-3-3 binding site on AKAP13. This phosphorylation event allows 14-3-3 to bind to AKAP13, and this binding inhibits AKAP13 Rho-GEF activity [93]. It is unknown if PKA-mediated phosphorylation of the 14-3-3 binding site is also induced by the β-adrenergic receptor. It is also unclear if AKAP13-bound PKA regulates any additional signaling processes during cardiomyocyte hypertrophy or cardiovascular development.
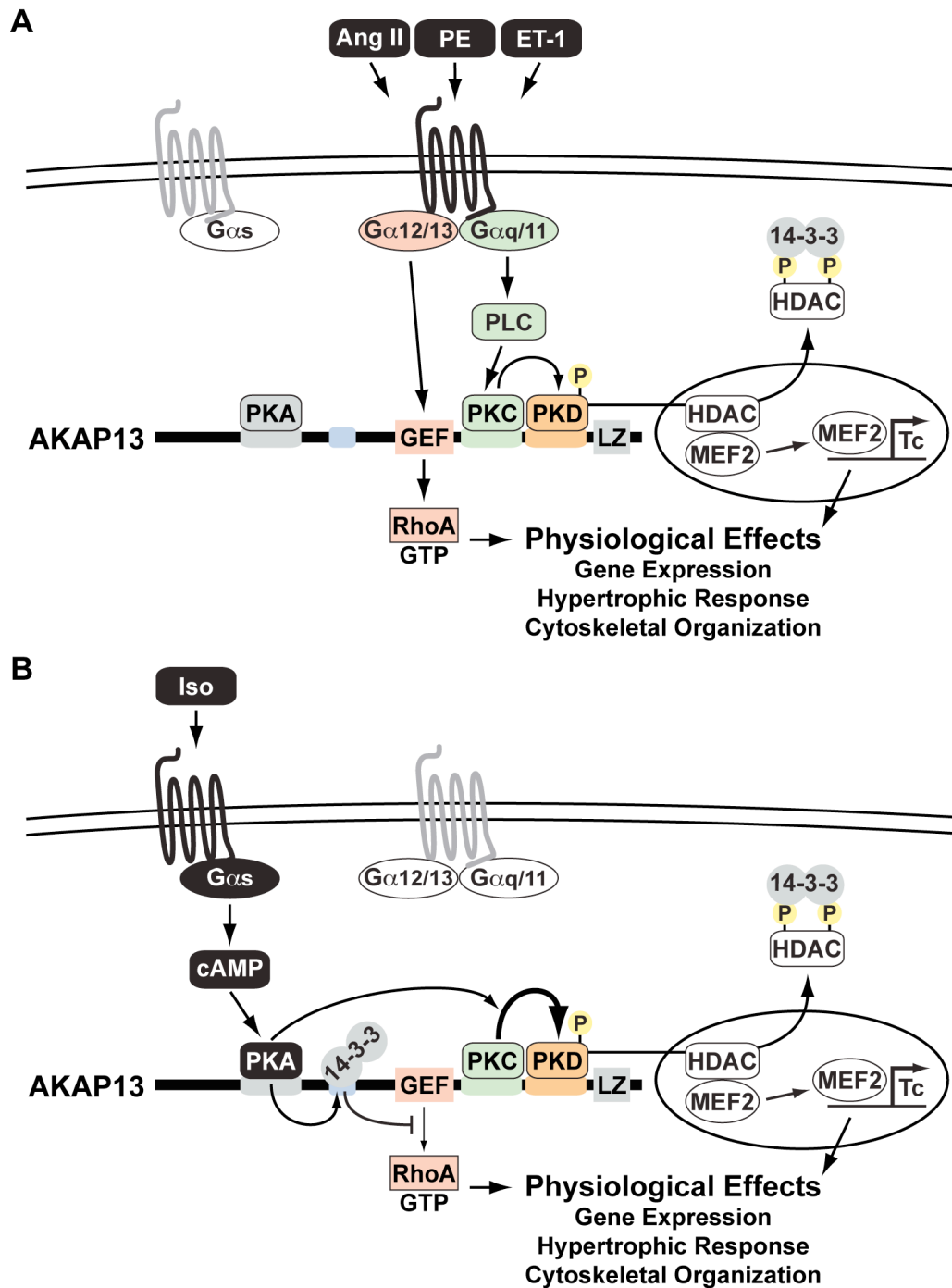
Figure 1.4. Model of AKAP13-mediated signaling. (A) Extracellular signals such as angiotensin II (Ang II), phenylephrine (PE), and endothelin-1 (ET-1) can activate G-protein signaling pathways ($G\alpha_{12/13}$ & $G\alpha_{q/11}$) by binding to GPCRs. The $G\alpha_{12/13}$ pathway stimulates the RhoA-specific guanine nucleotide exchange factor (GEF) domain of AKAP13 to activate RhoA. The $G\alpha_{q/11}$ pathway stimulates PLC activity and leads to the

activation of PKC. PKC initiates a phosphorylation cascade that activates PKD and then PKD phosphorylates class II HDACs. The phosphorylation of HDACs causes them to translocate into the cytoplasm and bind to 14-3-3; this de-represses MEF2 transcriptional activity (Tc) and allows expression of MEF2 responsive genes. Activation of the AKAP13-mediated Rho-GEF and PKC-PKD signaling pathways induce physiological effects including gene expression changes, hypertrophic responses, and cytoskeletal organization in isolated cardiomyocytes. (B) PKA appears to modulate the other two AKAP13-mediated signaling pathways, reducing Rho-GEF and enhancing PKC-PKD signaling. The β-adrenergic ligand isoproterenol (Iso) activates the $G\alpha_s$ pathway to increase cyclic AMP (cAMP) levels that in turn can activate AKAP13-bound PKA in isolated cardiomyocytes. This activated PKA phosphorylates the 14-3-3 binding site of AKAP13 to induce binding. The AKAP13-bound 14-3-3 reduces the Rho-GEF activity of AKAP13. Activated PKA can also phosphorylate the AKAP13-PKD binding domain. This enhances the PKC-mediated activation of PKD. These described AKAP13-mediated signaling events and their physiological consequences were identified in isolated cardiomyocytes, but the physiological function of AKAP13 has not been well characterized *in vivo*. We wanted to delineate the physiological role of AKAP13-mediated signaling during mouse development and *in vivo* physiology. From the experiments dissecting AKAP13-mediated signaling events, it appeared that the Rho-GEF and PKC-PKD pathways regulated the physiological effects controlled by AKAP13. Thus, our experiments focused on identifying the physiological functions controlled by AKAP13, specifically, the Rho-GEF and PKC-PKD binding domains.

Surprisingly, many of the signaling molecules coordinated by AKAP13 are required for cardiac development and differentiation. The three G-protein signaling pathways upstream of AKAP13 ($G\alpha_s$, $G\alpha_{12/13}$, and $G\alpha_{q/11}$) are required for proper cardiovascular development and embryonic survival in mice [14,16,17]. Downstream of the $G\alpha_{q/11}$ pathway, PKD [95] and MEF2c [96] are also required for early mouse development and proper cardiac formation. Additionally, PKC is required for cardiomyocyte differentiation from mouse ES cells [20,21], and class II HDACs inhibit MEF2 transcriptional activity, blocking cardiomyocyte differentiation of an embryonic carcinoma cell line, P19 [97,98]. Downstream of the $G\alpha_{12/13}$ pathway, inhibition of the Rho family GTPases, which includes RhoA, disrupts cardiac morphogenesis and proliferation in mice [23]. Moreover, AKAP13 is required for development as *Akap13*-null mice die during development from cardiovascular defects [65]. Despite the indication that *Akap13*-null mice are embryonic lethal, the phenotype was not initially available to us. Nor was it clear if the lethality was due to cardiac or vascular defects.

Our analysis of AKAP expression during mouse development and ES cell differentiation identified many expressed and regulated AKAP genes. Of the 22 AKAP genes, 12 were either present or regulated during mouse development and eight were regulated during ES cell differentiation. We also found gene-trap events in 15 of the 22 AKAP genes indicating that an amazing 68% of all AKAP genes are expressed in ES cells. Surprisingly, only AKAP13 expression increased in both data sets. We likely identified this up-regulation because of the broad expression pattern of AKAP13 during development. As we will show in

Chapter 4, AKAP13 is expressed in many tissues, including the heart, lung, kidney, gut, muscle, and vasculature during embryonic development. Another possible reason for identifying AKAP13 is that ES cell differentiation by the EB method seems to be biased towards differentiation into mesoderm-derived cell types, especially cardiomyocytes, which express high levels of AKAP13.

We likely missed the up-regulation of additional AKAP genes during development. Mouse development and ES cell differentiation produce many cell types, thus AKAPs with narrow expression patterns in differentiated tissues were likely missed in this analysis. To identify these AKAPs, and other developmentally important genes, future studies should conduct expression analysis during directed differentiation of ES cells into specific cell types and on specific tissues isolated from mouse embryos at various stages of development. We also may have missing up-regulated AKAPs because the microarrays used for these data sets did not probe for several of these genes. Ideally, future studies will use RNA sequencing to identify expressed and regulated genes during differentiation into specific tissue types. This approach will provide much more detailed information on the changes in absolute expression levels and alternative splicing events for all genes, including AKAPs. This information will help guide future studies investigating the role of AKAPs in mediating differentiation into specific cell types.

Several other AKAPs are up-regulated during mouse development, and these could play important roles for general as well as tissue specific development. Wasf1 (WAVE1) was the most highly up-regulated gene during mouse

development. The WASP/WAVE family of proteins regulates actin cytoskeletal dynamics important for cellular processes, such as cell shape changes and motility [99]. Interestingly, WAVE1 is expressed throughout the mouse embryo at E9 and becomes restricted to the central nervous system by E18 [100]. Despite these findings WAVE1 mutant mice have a relatively normal embryonic development but display post-natal lethality, growth defects, and neuronal defects [100,101]. Other WASP/WAVE proteins might compensate for the loss of WAVE1 during early embryonic development. For instance, N-WASP, which is required for neural tube and cardiac formation [102], could have some redundant functions with WAVE1. Another AKAP up-regulated during mouse development is AKAP12 (Gravin). AKAP12 regulates actin cytoskeletal dynamics at least in part through the coordination of PKA, PKC, and Raf signaling to control cell shape changes and decrease cellular chemotaxis and invasion [103]. Moreover, AKAP12 is required for proper extension of the mesoderm during zebrafish gastrulation [104] and is expressed in mouse embryos [105]. It would be interesting to determine if the function of AKAP12 during mesodermal extension is conserved in mammals.

Finally, most of the AKAPs regulated during ES cell differentiation were down-regulated (6 out of 8). As mentioned before, this could be due to the dilution of AKAP expression levels during differentiation. Alternatively, this could indicate that some AKAPs play functional roles in ES biology and maintenance. This is an interesting possibility because several AKAPs are expressed in sperm and oocytes to regulate various aspects of gamete function, maturation and

fertilization [29]. Some of these functions may be maintained during early embryogenesis as the fertilized oocytes (i.e., zygotes) divide and develop into the blastocyst, from which ES cells are derived. Of particular interest is the role pericentrin (Pcnt) might play in mediating ES cell proliferation and self-renewal. Pcnt is an important component of the centrosome and human mutations in this gene lead to Microcephalic osteodysplastic primordial dwarfism type II [106]. Mutant mice also have dramatic growth defects and are embryonic lethal (for review see [57]). Intriguingly, Pcnt is highly expressed in ES cells with over 15 unique exons trapped and is down-regulated over 4.5 fold during differentiation. The competition assay described in Chapter 2 could provide an ideal system to delineate the role of Pcnt and other AKAPs in ES cell maintenance and proliferation.

1.6 Summary of our studies to investigate the role of AKAP13 during cardiovascular development and pathology.

We used several approaches to identify the role of AKAP13 during cardiovascular development and function, and these will be described in detail in the following chapters. Since AKAP13 is highly expressed in ES cell and up-regulated during differentiation, we first investigated its importance in ES cell maintenance and differentiation (see Chapter 2). We used lentiviral mediated RNAi to reduce AKAP13 expression and assessed the effects on ES cell proliferation and expression of an Oct4-GFP reporter construct that marks pluripotent cells. Despite the high level of AKAP13 expression in ES cells, we

found that AKAP13 knockdown did not effect ES cell proliferation or expression of Oct4-GFP. We then used RNAi to knock down AKAP13 expression during differentiation by the EB method and looked for defects in the differentiation of cardiac mesoderm, marked by an Nkx2.5-GFP reporter construct, and functional cardiomyocytes as assessed by the appearance of spontaneously contracting EBs. We found that AKAP13 knockdown did not effect differentiation into Nkx2.5-GFP expressing cells or contracting EBs. We also found that AKAP13 knockdown had no effect on the expression levels of markers for endoderm, endothelial cells, smooth muscle, or cardiac structural genes. These results indicate that AKAP13 is not required for ES cell maintenance or differentiation into multiple cell types, including cardiac and endothelial cells.

As we conducted the ES cell differentiation experiments, we initiated a collaboration with the laboratory of Dr. James Segars at NICHD where the *Akap13*-null mouse was developed. Through this collaboration, we learned more about the phenotype of the *Akap13*-null mice. They die around embryonic day E10.5 and display pericardial edema and a developmental delay [65]. Despite this lethality, the mutant heart appears to have a relatively normal morphology, as does the rest of the embryo. This indicates that differentiation into cardiomyocytes and many other cell types can occur in *Akap13*-null mice. This agrees with our findings that AKAP13 knockdown does not effect ES cell differentiation into cardiac mesoderm and functional cardiomyocytes. This lab suggested that the *Akap13*-null mice have a thin ventricular wall with fewer cardiomyocytes and reduced trabeculation, as well as reduced expression of the

transcription factors Mef2c and Tbx2 [65]. However, it is unclear if this analysis was conducted on properly matched embryos since the mutant embryos appear to be at an earlier developmental stage than the wild-type control embryos. This age discrepancy between the mutant and wild-type embryos could explain the observed cardiac structural and expression defects. This also leaves open the possibility that the cardiac phenotype is a secondary effect and not the cause of lethality. Due to these concerns, we wanted to further investigate the embryonic phenotype of these *Akap13*-null mice and imported them into our mouse facility.

We invested a lot of time and energy in analyzing the imported *Akap13*-null mice; however, we finally determined that the mice we were working with did not contain the proper targeting event to disrupt AKAP13. We are unsure how or when this mix-up occurred, and despite the amount of time spent on these mice, we will not discuss these studies in detail here. Suffice it to say, we were unable to detect decreased AKAP13 expression in the presumed heterozygous mice and never detected homozygous mutant embryos even as early as E6.5 of development. Moreover, we did not detect proper targeting of the AKAP13 gene locus in these mice as determined by Southern blot analysis. From these findings, we concluded that we were not working with the true *Akap13*-null mouse line and decided to focus our efforts on other AKAP13 studies. Further analysis of embryos with the proper targeting event remains to be done.

We decided to focus on two aspects of AKAP13-mediated signaling during embryonic development. The first was to identify the cell types that express AKAP13 and thus may require AKAP13-coordinated signaling during

development. The second was to identify the specific AKAP13 protein domains required for mouse development. To address these questions, we took advantage of the available gene-trap events within the AKAP13 gene. These gene-traps encode a β-galactosidase cassette that can be used to report AKAP13 expression during mouse development and in adult tissue by X-Gal staining. Additionally, there are numerous gene-trap events throughout the AKAP13 gene that can be used to generate a series of AKAP13 truncation mutant mice. We generated mice from three of the 10 unique gene-trap events within AKAP13. These gene-trap mutant mice were then used to determine the expression pattern of AKAP13 during mouse development and in adult tissue and to determine the requirement of specific protein domains for development and cardiac hypertrophy.

We identified AKAP13 expression during mouse embryonic development and in adult tissue by X-Gal staining of AKAP13-gene-trap heterozygous mice (Chapters 3 & 4). Surprisingly, we found that AKAP13 was broadly expressed during mouse development with high levels of expression in cardiac and endothelial cells, as well as expression in the lung, kidney, gut, parts of the brain, and muscle. AKAP13 was also expressed highly in the muscle and endothelial cells of the adult heart, aorta, and pulmonary artery as well as in other vascular tissue.

Since AKAP13 was expressed in endothelial cells, the cardiac outflow tract, and vascular tissue during development and in adult mice, we decided to investigate the function of AKAP13 in human umbilical vein endothelial cells

(HUVECs), a common model for endothelial cell biology and angiogenesis (Chapter 3). Additionally, the *Akap13*-null mouse phenotype of edema could be due to vascular dysfunction, instead of the proposed cardiac phenotype. We were further intrigued by the dramatic similarity of VEGF-induced and AKAP13-coordinated signaling pathways. Specifically, VEGF induces a PKC-PKD-HDAC cascade to activate MEF2 transcriptional activity and in parallel induces RhoA activity. Both of these pathways play important roles during angiogenesis by promoting endothelial cell migration and tube formation. Thus, we hypothesized that AKAP13 coordinates signaling pathways downstream of VEGF to regulate aspects of angiogenesis in HUVECs. To test this, we used RNAi to knock down AKAP13 expression in HUVECs and assessed the ability of these cells to perform processes important for angiogenesis. Contrary to our expectations, AKAP13 knockdown did not affect aspects of angiogenesis, including cell attachment, spreading, and morphology, tube formation, and VEGF-induced wound healing. Moreover, AKAP13-deficient HUVECs had a normal activation of PKD in response to VEGF stimulation. These results indicate that AKAP13 does not regulate aspects of angiogenesis and is not required for VEGF activation of PKD.

As discussed above, AKAP13 integrates multiple upstream signaling pathways to activate a PKC-PKD signaling cascade or the GTPase RhoA. Both of these pathways induce cardiomyocyte hypertrophy *in vitro*, and AKAP13 appears to be required for embryonic development. However, the requirement for the AKAP13-coordinated PKC-PKD and RhoA signaling pathways during mouse

development is unknown. Since the coordination of these pathways appears to be the major function of AKAP13, we hypothesized that AKAP13 Rho-GEF and PKC-PKD binding domain deficient mice would phenocopy the *Akap13*-null mouse (Chapter 4). To determine if these pathways are required for development, we generated a series of AKAP13 mutant mice from gene-trap events that disrupt the PKC and PKD binding domains of AKAP13 or the Rho-GEF as well as the PKC and PKD binding domains. Surprisingly, we found that homozygous mutant mice from both of these mouse lines survive normally and have no obvious phenotypes under normal conditions. These results indicate that the AKAP13 Rho-GEF and PKC-PKD binding domains are not required for mouse development. Furthermore, they suggest that the PKA binding domain of AKAP13 may be sufficient for mouse development and survival. Alternatively, an unidentified region of AKAP13 may be required for mouse development.

This lack of phenotype under normal conditions suggests that AKAP13 may function to regulate stress responses. In agreement with this, the AKAP13 Rho-GEF and PKC-PKD binding domains mediate hypertrophy in isolated cardiomyocytes in response to multiple stimuli including adrenergic, angiotensin II, and endothelin-1 receptor stimulation [63,64]. In addition, PKD is required for a normal cardiac hypertrophic response to adrenergic and angiotensin II receptor stimulation *in vivo* [95]. Thus, we hypothesized that AKAP13 regulates cardiac remodeling in response to β-adrenergic-induced cardiac hypertrophy *in vivo*. To test this, we activated the β-adrenergic receptor by administering isoproterenol to adult mice that lacked the AKAP13 Rho-GEF and PKC-PKD binding domains for

14 days. We measured changes in cardiac structure and function by echocardiograms and further analyzed heart size and morphology after treatment. We found that the AKAP13 mutant mice had the same increase in heart size and structural changes as wild-type mice in response to β-adrenergic-induced hypertrophy. Unexpectedly, these AKAP13 mutant mice did not display the normal increase in ejection fraction or fractional shortening in response to chronic β-adrenergic stimulation. These results indicate that the Rho-GEF and PKC-PKD binding domains of AKAP13 do not regulate cardiac structural remodeling in response to β-adrenergic-induced cardiac hypertrophy. However, these domains are required for the cardiac functional response to chronic β-adrenergic stimulation.

1.7 Materials and Methods

Expression analysis of the AKAP gene family

Publicly available microarray datasets were analyzed by GC-RMA to determine expression profiles during mouse development [52] and ES cell differentiation [53]. Gene expression during mouse development was compared to expression in a blastocyst (GEO series GSE1133). Gene expression during mouse ES cell differentiation was compared to pluripotent mouse ES cells (GSE3749). The largest fold change was reported when greater than an absolute fold change of 1.8. The data set containing mouse developmental time points also included a large number of adult tissues. We considered a gene to be present (P) during

mouse development if its expression was two-fold higher than the minimum

expression across all samples.

Identification of gene-trap events in AKAPs

Gene-trap events within AKAPs were identified from the International Gene Trap

Consortium (IGTC) database (at www.genetrap.org) and the IGTC Sequence

Tag Alignments track on the UCSC Genome Browser [54,55]. The sequence

tags were used to identify uniquely trapped exons and only gene-traps with

sequence aligning to exons were counted (i.e., intron traps were excluded and

duplicate traps effecting the same exon were not counted).

1.8 Acknowledgements

1.9 References

1. Neves SR, Ram PT, Iyengar R (2002) G protein pathways. Science 296: 1636-1639.

2. Malbon CC (2005) G proteins in development. Nat Rev Mol Cell Biol 6: 689-701.

3. Wettschureck N, Moers A, Offermanns S (2004) Mouse models to study G-protein-mediated signaling. Pharmacol Ther 101: 75-89.

4. Takeda S, Kadowaki S, Haga T, Takaesu H, Mitaku S (2002) Identification of G protein-coupled receptor genes from the human genome sequence. FEBS Lett 520: 97-101.

5. Hopkins AL, Groom CR (2002) The druggable genome. Nat Rev Drug Discov 1: 727-730.

6. Insel PA, Tang CM, Hahntow I, Michel MC (2007) Impact of GPCRs in clinical medicine: monogenic diseases, genetic variants and drug targets. Biochim Biophys Acta 1768: 994-1005.

7. Marinissen MJ, Gutkind JS (2001) G-protein-coupled receptors and signaling networks: emerging paradigms. Trends Pharmacol Sci 22: 368-376.

8. Hubbard KB, Hepler JR (2006) Cell signalling diversity of the Gqalpha family of heterotrimeric G proteins. Cell Signal 18: 135-150.

9. Rhee SG (2001) Regulation of phosphoinositide-specific phospholipase C. Annu Rev Biochem 70: 281-312.

10. Dutt P, Nguyen N, Toksoz D (2004) Role of Lbc RhoGEF in Galpha12/13-induced signals to Rho GTPase. Cell Signal 16: 201-209.

11. Seasholtz TM, Majumdar M, Brown JH (1999) Rho as a mediator of G protein-coupled receptor signaling. Mol Pharmacol 55: 949-956.

12. Siehler S (2009) Regulation of RhoGEF proteins by G12/13-coupled receptors. Br J Pharmacol 158: 41-49.

13. Germain-Lee EL, Schwindinger W, Crane JL, Zewdu R, Zweifel LS, et al. (2005) A mouse model of albright hereditary osteodystrophy generated by targeted disruption of exon 1 of the Gnas gene. Endocrinology 146: 4697-4709.

14. Yu S, Yu D, Lee E, Eckhaus M, Lee R, et al. (1998) Variable and tissue-specific hormone resistance in heterotrimeric Gs protein alpha-subunit (Gsalpha) knockout mice is due to tissue-specific imprinting of the gsalpha gene. Proc Natl Acad Sci U S A 95: 8715-8720.

15. Skinner JA, Cattanach BM, Peters J (2002) The imprinted oedematous-small mutation on mouse chromosome 2 identifies new roles for Gnas and Gnasxl in development. Genomics 80: 373-375.

16. Offermanns S, Zhao LP, Gohla A, Sarosi I, Simon MI, et al. (1998) Embryonic cardiomyocyte hypoplasia and craniofacial defects in G alpha q/G alpha 11-mutant mice. Embo J 17: 4304-4312.

17. Offermanns S, Mancino V, Revel JP, Simon MI (1997) Vascular system defects and impaired cell chemokinesis as a result of Galpha13 deficiency. Science 275: 533-536.

18. Amieux PS, Howe DG, Knickerbocker H, Lee DC, Su T, et al. (2002) Increased basal cAMP-dependent protein kinase activity inhibits the formation of mesoderm-derived structures in the developing mouse embryo. J Biol Chem 277: 27294-27304.

19. Yin Z, Jones GN, Towns WH, 2nd, Zhang X, Abel ED, et al. (2008) Heart-specific ablation of Prkar1a causes failure of heart development and myxomagenesis. Circulation 117: 1414-1422.

20. Ventura C, Zinellu E, Maninchedda E, Fadda M, Maioli M (2003) Protein kinase C signaling transduces endorphin-primed cardiogenesis in GTR1 embryonic stem cells. Circ Res 92: 617-622.

21. Ventura C, Zinellu E, Maninchedda E, Maioli M (2003) Dynorphin B is an agonist of nuclear opioid receptors coupling nuclear protein kinase C activation to the transcription of cardiogenic genes in GTR1 embryonic stem cells. Circ Res 92: 623-629.

22. Kaarbo M, Crane DI, Murrell WG (2003) RhoA is highly up-regulated in the process of early heart development of the chick and important for normal embryogenesis. Dev Dyn 227: 35-47.

23. Wei L, Imanaka-Yoshida K, Wang L, Zhan S, Schneider MD, et al. (2002) Inhibition of Rho family GTPases by Rho GDP dissociation inhibitor disrupts cardiac morphogenesis and inhibits cardiomyocyte proliferation. Development 129: 1705-1714.

24. Michel JJ, Scott JD (2002) AKAP mediated signal transduction. Annu Rev Pharmacol Toxicol 42: 235-257.

25. Jarnaess E, Tasken K (2007) Spatiotemporal control of cAMP signalling processes by anchored signalling complexes. Biochem Soc Trans 35: 931-937.

26. Carr DW, Stofko-Hahn RE, Fraser ID, Bishop SM, Acott TS, et al. (1991) Interaction of the regulatory subunit (RII) of cAMP-dependent protein kinase with RII-anchoring proteins occurs through an amphipathic helix binding motif. J Biol Chem 266: 14188-14192.

27. Ruehr ML, Russell MA, Bond M (2004) A-kinase anchoring protein targeting of protein kinase A in the heart. J Mol Cell Cardiol 37: 653-665.

28. Wong W, Scott JD (2004) AKAP signalling complexes: focal points in space and time. Nat Rev Mol Cell Biol 5: 959-970.

29. Carnegie GK, Means CK, Scott JD (2009) A-kinase anchoring proteins: from protein complexes to physiology and disease. IUBMB Life 61: 394-406.

30. Buckingham M, Meilhac S, Zaffran S (2005) Building the mammalian heart from two sources of myocardial cells. Nat Rev Genet 6: 826-835.

31. Garcia-Martinez V, Schoenwolf GC (1993) Primitive-streak origin of the cardiovascular system in avian embryos. Dev Biol 159: 706-719.

32. Tam PP, Parameswaran M, Kinder SJ, Weinberger RP (1997) The allocation of epiblast cells to the embryonic heart and other mesodermal lineages: the role of ingression and tissue movement during gastrulation. Development 124: 1631-1642.

33. Brand T (2003) Heart development: molecular insights into cardiac specification and early morphogenesis. Dev Biol 258: 1-19.

34. Srivastava D (2006) Making or breaking the heart: from lineage determination to morphogenesis. Cell 126: 1037-1048.

35. Srivastava D, Olson EN (2000) A genetic blueprint for cardiac development. Nature 407: 221-226.

36. Rodda SJ, Kavanagh SJ, Rathjen J, Rathjen PD (2002) Embryonic stem cell differentiation and the analysis of mammalian development. Int J Dev Biol 46: 449-458.

37. Boheler KR, Czyz J, Tweedie D, Yang HT, Anisimov SV, et al. (2002) Differentiation of pluripotent embryonic stem cells into cardiomyocytes. Circ Res 91: 189-201.

38. He JQ, Ma Y, Lee Y, Thomson JA, Kamp TJ (2003) Human embryonic stem cells develop into multiple types of cardiac myocytes: action potential characterization. Circ Res 93: 32-39.

39. Kattman SJ, Huber TL, Keller GM (2006) Multipotent flk-1+ cardiovascular progenitor cells give rise to the cardiomyocyte, endothelial, and vascular smooth muscle lineages. Dev Cell 11: 723-732.

40. Murry CE, Keller G (2008) Differentiation of embryonic stem cells to clinically relevant populations: lessons from embryonic development. Cell 132: 661-680.

41. Wu SM, Fujiwara Y, Cibulsky SM, Clapham DE, Lien CL, et al. (2006) Developmental origin of a bipotential myocardial and smooth muscle cell precursor in the mammalian heart. Cell 127: 1137-1150.

42. Tingley WG, Pawlikowska L, Zaroff JG, Kim T, Nguyen T, et al. (2007) Gene-trapped mouse embryonic stem cell-derived cardiac myocytes and human genetics implicate AKAP10 in heart rhythm regulation. Proc Natl Acad Sci U S A 104: 8461-8466.

43. Moretti A, Bellin M, Welling A, Jung CB, Lam JT, et al. (2010) Patient-specific induced pluripotent stem-cell models for long-QT syndrome. N Engl J Med 363: 1397-1409.

44. Itzhaki I, Maizels L, Huber I, Zwi-Dantsis L, Caspi O, et al. (2011) Modelling the long QT syndrome with induced pluripotent stem cells. Nature.

45. Foldes G, Mioulane M, Wright JS, Liu AQ, Novak P, et al. (2010) Modulation of human embryonic stem cell-derived cardiomyocyte growth: A testbed for studying human cardiac hypertrophy? J Mol Cell Cardiol.

46. Doetschman T, Gregg RG, Maeda N, Hooper ML, Melton DW, et al. (1987) Targetted correction of a mutant HPRT gene in mouse embryonic stem cells. Nature 330: 576-578.

47. Thomas KR, Capecchi MR (1987) Site-directed mutagenesis by gene targeting in mouse embryo-derived stem cells. Cell 51: 503-512.

48. Skarnes WC (2000) Gene trapping methods for the identification and functional analysis of cell surface proteins in mice. Methods Enzymol 328: 592-615.

49. Ventura A, Meissner A, Dillon CP, McManus M, Sharp PA, et al. (2004) Cre-lox-regulated conditional RNA interference from transgenes. Proc Natl Acad Sci U S A 101: 10380-10385.

50. Grskovic M, Chaivorapol C, Gaspar-Maia A, Li H, Ramalho-Santos M (2007) Systematic identification of cis-regulatory sequences active in mouse and human embryonic stem cells. PLoS Genet 3: e145.

51. Liu Y, Asakura M, Inoue H, Nakamura T, Sano M, et al. (2007) Sox17 is essential for the specification of cardiac mesoderm in embryonic stem cells. Proc Natl Acad Sci U S A 104: 3859-3864.

52. Su AI, Wiltshire T, Batalov S, Lapp H, Ching KA, et al. (2004) A gene atlas of the mouse and human protein-encoding transcriptomes. Proc Natl Acad Sci U S A 101: 6062-6067.

53. Hailesellasse Sene K, Porter CJ, Palidwor G, Perez-Iratxeta C, Muro EM, et al. (2007) Gene function in early mouse embryonic stem cell differentiation. BMC Genomics 8: 85.

54. Nord AS, Chang PJ, Conklin BR, Cox AV, Harper CA, et al. (2006) The International Gene Trap Consortium Website: a portal to all publicly available gene trap cell lines in mouse. Nucleic Acids Res 34: D642-648.

55. Fujita PA, Rhead B, Zweig AS, Hinrichs AS, Karolchik D, et al. (2010) The UCSC Genome Browser database: update 2011. Nucleic Acids Res [Epub ahead of print].

56. Nord AS, Vranizan K, Tingley W, Zambon AC, Hanspers K, et al. (2007) Modeling insertional mutagenesis using gene length and expression in murine embryonic stem cells. PLoS One 2: e617.

57. Delaval B, Doxsey SJ (2010) Pericentrin in cellular function and disease. J Cell Biol 188: 181-190.

58. Chen L, Marquardt ML, Tester DJ, Sampson KJ, Ackerman MJ, et al. (2007) Mutation of an A-kinase-anchoring protein causes long-QT syndrome. Proc Natl Acad Sci U S A 104: 20990-20995.

59. Neumann SA, Tingley WG, Conklin BR, Shrader CJ, Peet E, et al. (2009) AKAP10 (I646V) functional polymorphism predicts heart rate and heart rate variability in apparently healthy, middle-aged European-Americans. Psychophysiology 46: 466-472.

60. Abrenica B, AlShaaban M, Czubryt MP (2009) The A-kinase anchor protein AKAP121 is a negative regulator of cardiomyocyte hypertrophy. J Mol Cell Cardiol 46: 674-681.

61. Perrino C, Feliciello A, Schiattarella GG, Esposito G, Guerriero R, et al. (2010) AKAP121 downregulation impairs protective cAMP signals, promotes mitochondrial dysfunction, and increases oxidative stress. Cardiovasc Res 88: 101-110.

62. Pare GC, Bauman AL, McHenry M, Michel JJ, Dodge-Kafka KL, et al. (2005) The mAKAP complex participates in the induction of cardiac myocyte hypertrophy by adrenergic receptor signaling. J Cell Sci 118: 5637-5646.

63. Appert-Collin A, Cotecchia S, Nenniger-Tosato M, Pedrazzini T, Diviani D (2007) The A-kinase anchoring protein (AKAP)-Lbc-signaling complex mediates alpha1

adrenergic receptor-induced cardiomyocyte hypertrophy. Proc Natl Acad Sci U S A 104: 10140-10145.

64. Carnegie GK, Soughayer J, Smith FD, Pedroja BS, Zhang F, et al. (2008) AKAP-Lbc mobilizes a cardiac hypertrophy signaling pathway. Mol Cell 32: 169-179.

65. Mayers CM, Wadell J, McLean K, Venere M, Malik M, et al. (2010) The Rho guanine nucleotide exchange factor AKAP13 (BRX) is essential for cardiac development in mice. J Biol Chem 285: 12344-12354.

66. Huang LJ, Wang L, Ma Y, Durick K, Perkins G, et al. (1999) NH2-Terminal targeting motifs direct dual specificity A-kinase-anchoring protein 1 (D-AKAP1) to either mitochondria or endoplasmic reticulum. J Cell Biol 145: 951-959.

67. Schulze DH, Muqhal M, Lederer WJ, Ruknudin AM (2003) Sodium/calcium exchanger (NCX1) macromolecular complex. J Biol Chem 278: 28849-28855.

68. Nichols CB, Rossow CF, Navedo MF, Westenbroek RE, Catterall WA, et al. (2010) Sympathetic stimulation of adult cardiomyocytes requires association of AKAP5 with a subpopulation of L-type calcium channels. Circ Res 107: 747-756.

69. Yang J, Drazba JA, Ferguson DG, Bond M (1998) A-kinase anchoring protein 100 (AKAP100) is localized in multiple subcellular compartments in the adult rat heart. J Cell Biol 142: 511-522.

70. McCartney S, Little BM, Langeberg LK, Scott JD (1995) Cloning and characterization of A-kinase anchor protein 100 (AKAP100). A protein that targets A-kinase to the sarcoplasmic reticulum. J Biol Chem 270: 9327-9333.

71. Kapiloff MS, Schillace RV, Westphal AM, Scott JD (1999) mAKAP: an A-kinase anchoring protein targeted to the nuclear membrane of differentiated myocytes. J Cell Sci 112 (Pt 16): 2725-2736.

72. Mauban JR, O'Donnell M, Warrier S, Manni S, Bond M (2009) AKAP-scaffolding proteins and regulation of cardiac physiology. Physiology (Bethesda) 24: 78-87.

73. Scott JD, Santana LF (2010) A-kinase anchoring proteins: getting to the heart of the matter. Circulation 121: 1264-1271.

74. Fraser ID, Tavalin SJ, Lester LB, Langeberg LK, Westphal AM, et al. (1998) A novel lipid-anchored A-kinase Anchoring Protein facilitates cAMP-responsive membrane events. Embo J 17: 2261-2272.

75. Gray PC, Johnson BD, Westenbroek RE, Hays LG, Yates JR, 3rd, et al. (1998) Primary structure and function of an A kinase anchoring protein associated with calcium channels. Neuron 20: 1017-1026.

76. Hulme JT, Lin TW, Westenbroek RE, Scheuer T, Catterall WA (2003) Beta-adrenergic regulation requires direct anchoring of PKA to cardiac CaV1.2 channels via a leucine zipper interaction with A kinase-anchoring protein 15. Proc Natl Acad Sci U S A 100: 13093-13098.

77. Lygren B, Carlson CR, Santamaria K, Lissandron V, McSorley T, et al. (2007) AKAP complex regulates Ca2+ re-uptake into heart sarcoplasmic reticulum. Embo Reports 8: 1061-1067.

78. Eide T, Coghlan V, Orstavik S, Holsve C, Solberg R, et al. (1998) Molecular cloning, chromosomal localization, and cell cycle-dependent subcellular distribution of the A-kinase anchoring protein, AKAP95. Experimental Cell Research 238: 305-316.

79. Lin JW, Wyszynski M, Madhavan R, Sealock R, Kim JU, et al. (1998) Yotiao, a novel protein of neuromuscular junction and brain that interacts with specific splice variants of NMDA receptor subunit NR1. J Neurosci 18: 2017-2027.

80. Witczak O, Skalhegg BS, Keryer G, Bornens M, Tasken K, et al. (1999) Cloning and characterization of a cDNA encoding an A-kinase anchoring protein located in the centrosome, AKAP450. Embo J 18: 1858-1868.

81. Kurokawa J, Motoike HK, Rao J, Kass RS (2004) Regulatory actions of the A-kinase anchoring protein Yotiao on a heart potassium channel downstream of PKA phosphorylation. Proc Natl Acad Sci U S A 101: 16374-16378.

82. Wang L, Sunahara RK, Krumins A, Perkins G, Crochiere ML, et al. (2001) Cloning and mitochondrial localization of full-length D-AKAP2, a protein kinase A anchoring protein. Proc Natl Acad Sci U S A 98: 3220-3225.

83. Ishikawa K, Nagase T, Suyama M, Miyajima N, Tanaka A, et al. (1998) Prediction of the coding sequences of unidentified human genes. X. The complete sequences of 100 new cDNA clones from brain which can code for large proteins in vitro. DNA Res 5: 169-176.

84. Nauert JB, Klauck TM, Langeberg LK, Scott JD (1997) Gravin, an autoantigen recognized by serum from myasthenia gravis patients, is a kinase scaffold protein. Curr Biol 7: 52-62.

85. Streb JW, Kitchen CM, Gelman IH, Miano JM (2004) Multiple promoters direct expression of three AKAP12 isoforms with distinct subcellular and tissue distribution profiles. J Biol Chem 279: 56014-56023.

86. Rubino D, Driggers P, Arbit D, Kemp L, Miller B, et al. (1998) Characterization of Brx, a novel Dbl family member that modulates estrogen receptor action. Oncogene 16: 2513-2526.

87. Diviani D, Soderling J, Scott JD (2001) AKAP-Lbc anchors protein kinase A and nucleates Galpha 12-selective Rho-mediated stress fiber formation. J Biol Chem 276: 44247-44257.

88. Russell MA, Lund LM, Haber R, McKeegan K, Cianciola N, et al. (2006) The intermediate filament protein, synemin, is an AKAP in the heart. Arch Biochem Biophys 456: 204-215.

89. Benson MA, Tinsley CL, Blake DJ (2004) Myospryn is a novel binding partner for dysbindin in muscle. J Biol Chem 279: 10450-10458.

90. Durham JT, Brand OM, Arnold M, Reynolds JG, Muthukumar L, et al. (2006) Myospryn is a direct transcriptional target for MEF2A that encodes a striated muscle, alpha-actinin-interacting, costamere-localized protein. J Biol Chem 281: 6841-6849.

91. Lacana E, Maceyka M, Milstien S, Spiegel S (2002) Cloning and characterization of a protein kinase A anchoring protein (AKAP)-related protein that interacts with and regulates sphingosine kinase 1 activity. J Biol Chem 277: 32947-32953.

92. Carnegie GK, Smith FD, McConnachie G, Langeberg LK, Scott JD (2004) AKAP-Lbc nucleates a protein kinase D activation scaffold. Mol Cell 15: 889-899.

93. Diviani D, Abuin L, Cotecchia S, Pansier L (2004) Anchoring of both PKA and 14-3-3 inhibits the Rho-GEF activity of the AKAP-Lbc signaling complex. Embo J 23: 2811-2820.

94. Klussmann E, Edemir B, Pepperle B, Tamma G, Henn V, et al. (2001) Ht31: the first protein kinase A anchoring protein to integrate protein kinase A and Rho signaling. FEBS Lett 507: 264-268.

95. Fielitz J, Kim MS, Shelton JM, Qi X, Hill JA, et al. (2008) Requirement of protein kinase D1 for pathological cardiac remodeling. Proc Natl Acad Sci U S A 105: 3059-3063.

96. Lin Q, Schwarz J, Bucana C, Olson EN (1997) Control of mouse cardiac morphogenesis and myogenesis by transcription factor MEF2C. Science 276: 1404-1407.

97. Karamboulas C, Dakubo GD, Liu J, De Repentigny Y, Yutzey K, et al. (2006) Disruption of MEF2 activity in cardiomyoblasts inhibits cardiomyogenesis. J Cell Sci 119: 4315-4321.

98. Karamboulas C, Swedani A, Ward C, Al-Madhoun AS, Wilton S, et al. (2006) HDAC activity regulates entry of mesoderm cells into the cardiac muscle lineage. J Cell Sci 119: 4305-4314.

99. Takenawa T, Suetsugu S (2007) The WASP-WAVE protein network: connecting the membrane to the cytoskeleton. Nat Rev Mol Cell Biol 8: 37-48.

100. Dahl JP, Wang-Dunlop J, Gonzales C, Goad ME, Mark RJ, et al. (2003) Characterization of the WAVE1 knock-out mouse: implications for CNS development. J Neurosci 23: 3343-3352.

101. Soderling SH, Langeberg LK, Soderling JA, Davee SM, Simerly R, et al. (2003) Loss of WAVE-1 causes sensorimotor retardation and reduced learning and memory in mice. Proc Natl Acad Sci U S A 100: 1723-1728.

102. Snapper SB, Takeshima F, Anton I, Liu CH, Thomas SM, et al. (2001) N-WASP deficiency reveals distinct pathways for cell surface projections and microbial actin-based motility. Nat Cell Biol 3: 897-904.

103. Su B, Bu Y, Engelberg D, Gelman IH (2010) SSeCKS/Gravin/AKAP12 inhibits cancer cell invasiveness and chemotaxis by suppressing a protein kinase C-Raf/MEK/ERK pathway. J Biol Chem 285: 4578-4586.

104. Weiser DC, Pyati UJ, Kimelman D (2007) Gravin regulates mesodermal cell behavior changes required for axis elongation during zebrafish gastrulation. Genes Dev 21: 1559-1571.

105. Gelman IH, Tombler E, Vargas J, Jr. (2000) A role for SSeCKS, a major protein kinase C substrate with tumour suppressor activity, in cytoskeletal architecture, formation of migratory processes, and cell migration during embryogenesis. Histochem J 32: 13-26.

106. Willems M, Genevieve D, Borck G, Baumann C, Baujat G, et al. (2010) Molecular analysis of pericentrin gene (PCNT) in a series of 24 Seckel/microcephalic osteodysplastic primordial dwarfism type II (MOPD II) families. J Med Genet 47: 797-802.

Chapter 2

AKAP13 Knockdown Does Not Effect Embryonic Stem Cell Pluripotency or Differentiation

2.1 Abstract

Background: G-protein signaling pathways regulate cardiovascular development as disruption of the G_s, $G_{q/11}$, or $G_{12/13}$ pathways cause embryonic lethality and cardiovascular defects. However, the specific cellular processes controlled by these pathways remain unknown. Scaffolding molecules, such as A-kinase anchoring proteins (AKAPs), organize signaling complexes that integrate G-protein signals into specific cellular processes. In fact, *Akap13*-null mice die during embryonic development and appear to have cardiovascular defects. Interestingly, the AKAP13 complex integrates G_s, $G_{q/11}$, and $G_{12/13}$ signals to induce cardiomyocyte gene expression and cellular growth, and many of the AKAP13-coordinated signaling molecules regulate cardiomyocyte differentiation and cardiovascular development. However, the developmental processes regulated by AKAP13 remain unknown.

Methodology/Principal Findings: To determine if AKAP13 coordinates signaling events required for cardiomyocyte differentiation, we used lentiviral-mediated RNAi to knock down AKAP13 expression in mouse embryonic stem (ES) cells and differentiating embryoid bodies (EBs). We developed a fluorescence-based competition assay to quantify the effect of AKAP13

knockdown on ES cell maintenance and differentiation. We found that ES cell maintenance was normal in AKAP13-deficient cells. Surprisingly, we found that AKAP13 knockdown did not decrease differentiation into Nkx2.5-GFP-positive cardiac mesodermal cells or into functionally beating cardiomyocytes. Additionally, AKAP13 knockdown did not affect the expression of markers for endoderm, endothelial cells, or cardiac structural genes.

Conclusions: These results indicate that AKAP13 is not required for ES cell maintenance or differentiation into functional cardiomyocytes or endothelial cells. This suggests that AKAP13 may regulate other aspects of cardiovascular development, such as morphogenesis, remodeling, or function *in vivo*.

2.2 Introduction

Heart disease is the leading killer of adults in the Western world. In addition, congenital heart malformations are the most common birth defects, occurring in nearly 1% of the population worldwide [1]. Understanding the molecular pathways required for normal heart development will provide insight into the mechanisms of cardiac malformation and new approaches to repair damaged heart tissue.

   G-protein signaling pathways have been extensively studied in the context of adult cardiovascular physiology and disease and this has led to them becoming major drug targets for the treatment of heart disease [2,3]. For example, drugs that target the angiotensin II (ACE inhibitors) and β-adrenergic (β-blockers)

pathways have become common treatments for hypertension and heart failure [4]. Interestingly, disruption of any of the four G-protein signaling pathways (G_s, G_i, $G_{q/11}$, or $G_{12/13}$) in mice results in embryonic lethality, with the G_s, $G_{q/11}$, and $G_{12/13}$ pathways regulating cardiovascular development [5]. The $G_{q/11}$ pathway is of particular interest because the double knockout of the $G\alpha q$ and $G\alpha 11$ genes results in cardiomyocyte hypoplasia and embryonic death [6]. Despite the lethal embryonic phenotypes identified for these ubiquitous signaling molecules, little is known about the functions of specific G-protein pathways during cardiac development.

There are several reasons for the lack of specific developmental functions attributed to G-protein signaling. First, over 800 G-protein coupled receptors (GPCRs) (about 400 non-olfactory GPCRs) signal through the four common G-protein signaling pathways [7]. Many of these GPCRs have overlapping and complementary functions; thus, disrupting a single GPCR often has no functional consequence. Additionally, GPCRs use common second messengers, such as cyclic AMP (cAMP) and calcium to propagate their signaling events. However, these second messengers are promiscuous, and disruption of these common pathways can affect many cellular processes. Finally, the integration of multiple G-protein and other signaling pathways can be required for proper downstream signaling to occur. Thus, disrupting the focal points that coordinate signal integration and downstream specificity should produce specific phenotypes including developmental defects. Scaffolding molecules, such as AKAPs, create signaling focal points by coordinating second messenger signaling specificity and

integrating multiple upstream signaling pathways to control important physiological processes [8]. This makes AKAPs ideal targets for disruption to identify specific G-protein mediated developmental processes.

At least 22 AKAP genes have been identified, and they encode for more than 50 proteins [9,10,11,12,13]. AKAPs are classified by their ability to bind protein kinase A (PKA) [14]. However, they can bind additional signaling proteins such as protein kinases, phosphotases, phosphodiesterases, ion channels, GPCRs, and other signaling molecules and effectors, to create signaling complexes [10,12]. In addition to organizing signaling complexes, AKAPs also localize these complexes to specific subcellular compartments, which aids in target specificity [10]. Moreover, AKAPs regulate aspects of reproduction and development including germ cell function, maturation, and fertilization [15] and zebrafish gastrulation (AKAP12, Gravin) [16]. These properties make AKAPs ideally situated to regulate G-protein-mediated cardiovascular development. In fact, we found that many of the AKAP genes are expressed, and several of them are regulated during mouse embryonic development and ES cell differentiation (Table 1.1; Chapter 1). From the expression and literature analysis conducted in Chapter 1, we identified AKAP13 (AKAP-Lbc) as our top candidate for regulating cardiovascular development.

Multiple factors suggest that AKAP13 might regulate G-protein signaling during cardiovascular developmental. First, AKAP13 was up-regulated in two developmental time courses, mouse embryonic development and mouse ES cell differentiation (Chapter 1) and is highly expressed in the adult heart [17,18].

Second, AKAP13 organizes a signaling complex that mediates cardiomyocyte growth in response to several hypertrophic stimuli, and many of these coordinated signaling molecules are also important for cardiovascular development (Figure 2.1). AKAP13 integrates signaling events from the $G\alpha_s$, $G\alpha_{12/13}$, and $G\alpha_{q/11}$ pathways by binding protein kinase A (PKA), C (PKC), and D (PKD) and encoding for a RhoA-specific guanine nucleotide exchange factor (GEF) domain [18,19,20,21]. In isolated cardiomyocytes, AKAP13 transduces $G\alpha_{q/11}$ signals through a PKC-PKD-class II histone deacetylase (HDAC) signaling cascade to induce myocyte enhancer factor 2 (MEF2) transcriptional activity [19,22,23]. AKAP13 also transduces $G\alpha_{12/13}$ signals through the encoded GEF domain to activate RhoA [24]. The $G\alpha_s$ signals transduced by AKAP13-bound PKA modulate the other two pathways, enhancing the activation of PKD [19] and reducing the activation of RhoA [20]. These AKAP13-mediated signaling processes regulate multiple physiological effects including gene expression changes (i.e., activation of the "fetal" gene program) and increased cell size. Finally, *Akap13*-null mice die early during development and display cardiovascular defects [25]. When we initiated this project, the *Akap13*-null defects were not well described, and it was unclear what aspect of cardiovascular development was affected. However, initial reports suggested that lethality was due to defective cardiomyocyte development.

Interestingly, many of the AKAP13-coordinated signaling molecules are also important for cardiovascular development. In mice, disruption of the G_q pathway [6], PKD [26], or MEF2C [27] all lead to embryonic lethality and cardiac defects.

Similarly, disruption of the $G_{12/13}$ pathway [28,29] or inhibition of Rho family GTPases, which includes RhoA, [30] cause embryonic lethality and cardiovascular defects in mice. Additionally, RhoA signaling is required for cardiac morphogenesis and heart tube fusion in chick embryos [31]. Furthermore, PKC is required for cardiomyocyte differentiation in mouse ES cells, and class II HDACs inhibit MEF2 transcriptional activity, repressing cardiomyocyte differentiation in P19 cells [32,33,34,35,36].

From this information, we hypothesized that AKAP13 is required for proper differentiation into cardiomyocytes. To test this, we used lentiviral-mediated RNA interference (RNAi) to knockdown AKAP13 in ES cells marked with either Oct4-GFP, a reporter for pluripotent ES cells, [37] or Nkx2.5-GFP, a reporter for cardiac mesoderm [38]. We then used flow cytometry to measure the effect of AKAP13 knockdown on pluripotency and proliferation (via Oct4-GFP line) or differentiation into cardiac mesoderm (via Nkx2.5-GFP line) as reported by GFP expression. We also counted the number of beating embryoid bodies to determine the effect of AKAP13 knockdown on the formation of functional cardiomyocytes. Finally, we used real-time quantitative PCR to determine if AKAP13 knockdown effected the expression of endodermal, endothelial, or cardiac marker genes. Despite the high level of AKAP13 expression in ES cells and embryoid bodies, we found that it was not required for ES cell maintenance, differentiation into cardiac mesoderm or functional cardiomyocytes, or expression of differentiation marker genes.
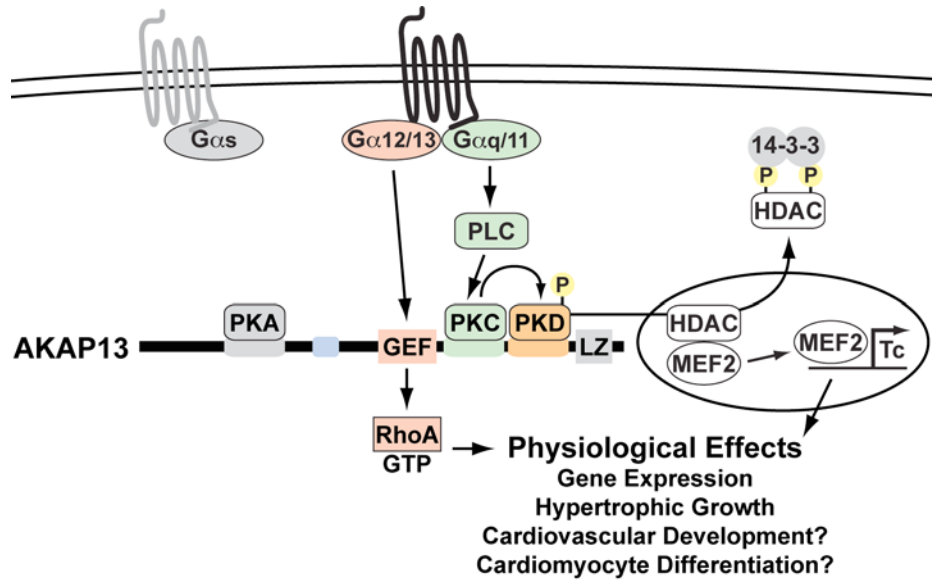
Figure 2.1. Model of AKAP13 signaling during cardiac growth. AKAP13 organizes a signaling complex by binding the protein kinases PKA, PKC, and PKD, and encoding for a RhoA-specific guanine nucleotide exchange factor (GEF) domain. This AKAP13 complex can integrate signals from the $G\alpha_s$, $G\alpha_{12/13}$, and $G\alpha_{q/11}$ pathways. In isolated neonatal ventricular cardiomyocytes, the AKAP13 GEF and PKC-PKD binding domains mediate the induction of gene expression, at least in part through the transcription factor MEF2, and cellular growth (hypertrophic growth). Many of these signaling molecules are also important for cardiovascular development and cardiomyocyte differentiation. Additionally, AKAP13 appears to be required for proper cardiac development and cardiomyocyte formation. Thus, we hypothesized that AKAP13 creates a signaling complex that mediates cardiomyocyte differentiation.

2.3 Results

2.3.1 AKAP13 is highly up-regulated during ES cell differentiation.

From our analysis of AKAP expression during mouse embryonic development and ES cell differentiation (Chapter 1), we identified AKAP13 as the only AKAP up-regulated in both data sets. This suggests that AKAP13 may have an important role in these processes. We also found that AKAP13 has 10 unique exons trapped out of about 40 total exons, indicating that AKAP13 is highly expressed in undifferentiated mouse ES cells. Furthermore, AKAP13 is highly expressed in adult heart tissue [17,18] and appears to be required for proper cardiac development in mice [25]. Thus, we decided to focus our experiments on AKAP13. To verify that AKAP13 was indeed up-regulated during ES cell differentiation, we conducted quantitative PCR for AKAP13 by the Sybr Green method (Figure 2.2). AKAP13 expression was 10–20-fold greater in day 5–13 EBs than in undifferentiated ES cells. Additionally, AKAP13 expression in undifferentiated ES cells was about 40% of that in the adult mouse heart, which expresses very high levels of AKAP13. Finally, the atrial cardiomyocyte cell line, HL-1, expressed AKAP13 at similar levels to day 7 and 13 EBs. These results confirm that AKAP13 is highly expressed in mouse ES cells and this expression is highly increased during differentiation.
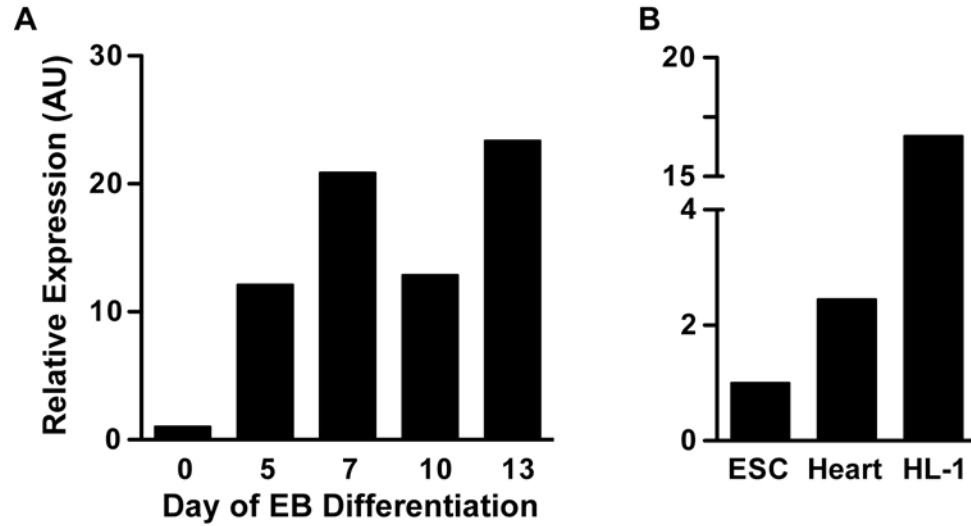
Figure 2.2. AKAP13 expression during ES cell differentiation. (A) Quantitative PCR analysis of undifferentiated mouse ES cell (day 0) and day 5, 7, 10, and 13 differentiated embryoid body RNA for AKAP13. (B) Quantitative PCR of undifferentiated ES cells (ESC), adult mouse heart, and an atrial cardiomyocyte cell line, HL-1, RNA for AKAP13. AKAP13 expression levels in A&B were measured by the Sybr Green method, normalized to cyclophilin, and set relative to undifferentiated ES cell expression levels. Mean values for eight technical replicates are graphed (n=1).

2.3.2 AKAP13 is a large gene that has multiple promoters and undergoes alternative splicing events.

Despite a fair amount of research on the signaling events coordinated by AKAP13 in cell culture and the finding that *Akap13*-null mice have embryonic lethality, the mouse AKAP13 genomic locus is not well annotated. To better annotate the mouse AKAP13 genomic locus, I used the RefSeq gene NM_029332 as the reference exon structure. I then mapped additional exons and splicing events using mouse and human GenBank mRNA and EST sequences as well as the UCSC Genome Browser. The 5' intron-exon and 3' exon-intron boundaries were identified by sequence comparisons of GenBank mRNAs and ESTs to the genomic DNA (Table 2.1). The GenBank sequences used to identify the specific intron-exon junctions are indicated by their accession numbers. Analysis of mRNA and EST splicing events revealed extensive alternative splicing including seven possible alternative initiation exons, five alternative termination exons (or bleeding exons), and four cassette exons. We were able to map the initiation exons for three described AKAP13 transcripts, AKAP-Lbc (Exon 1) [18], Brx (Exon Brx) [17], and Lbc (Exon Lbc) [39], and identified novel candidate initiation exons: A, B, C, and D. We also identified possible alternative termination, or bleeding, exons (indicated by a "b") following exons 4, 6, 11, and 19. Finally, the mRNA and EST splicing data indicated that Exons 9, 10, 12, and 13 are cassette exons.

From this annotation, we determined that the mouse AKAP13 gene spans about 300 kilobases (kb) of chromosome 7qD2 and contains at least 44 exons

(Figure 2.3). This annotation indicates that the AKAP13 gene encodes for many

transcripts through the use of alternative promoters and alternative splicing

events. These promoters likely drive unique expression patterns for the AKAP13

transcripts as several different sized AKAP13 transcripts have been identified

with tissue specific expression patterns [17]. Additionally, the alternative initiation

exons and splicing events likely affect the biological functions of the resulting

protein isoforms by modifying the protein domains contained and the subcellular

localization of the protein isoforms. For example, the PKA-binding domain for

AKAP13 is present in the AKAP-Lbc transcript but not the Brx or Lbc transcripts.

Table 2.1. AKAP13 gene structure, based on RefSeq NM_029332

Exon	5' Intron Sequence	5' Exon Sequence	3' Exon Sequence	3' Intron Sequence	Exon Size	GenBank Accession Number	Alternative Splicing Event
1		GGCGCATGCG	GAGCCGCACG	gtgagagcgc	215	AK157986 AK172125	Initiation Exon
A		GGGGACGCGC	GTCAAGCCGG	gtaaacactg	228	AK006382	Alt Initiation
2	ttggtttcag	TGTCCTGGGT	TCCATTATAT	gtaagtaaat	44	AK157986 AK172125 AK006382	
3	tcttttccag	GGCGATTGTG	ATTGCTCCTG	gtaagtatct	148	AK157986 AK172125 AK006382	
4	ctttctttag	GTCACGACTG	ACTTTGCATG	gtgagaagcc	297	AK157986 AK172125 AK006382	
4b		GTGAGAAGCC	TCTAGTACTG		672	AK006382	Bleeding Exon
5	ccgttcacag	ACGGTGGCCC	TTCTGACTGA	gtgagtgtct	184	AK157986 AK172125	
B		GTCAGTCTCC	GGAGCCCCGC	gtgagtcatg	115	BB654464 CJ056095	Alt Initiation
6	ttgcttgcag	GGAAAATGCA	GCAGCTGATG	gtaagggaaa	193	AK157986 AK172125 BB654464 CJ056095	
6b		GTAAGGGAAA	TTATTTATTC		323	AK157986 AK172125	Bleeding Exon
7	ttcctcctag	AAAACAAACT	TCAGCACCAG	gtaagcaagg	3064	BB654464 CJ056095 AK149507 AY033771	
C		AGACGGCGTT	AGTCCGGAAG	gtcagttgat	608	AK162999 AK172678	Alt Initiation
8	ttcacttcag	AAATGCCAGA	GACCCAGGCG	gtaagcagca	128	AK149507 AY033771 AK162999 AK172678	
Brx		CCTTAACCCG	GTTGCTGAAG	gtaagaaggg	241	AK135576 human mRNAs AK315885 AK309805	Alt Initiation
9	tgtcttccag	ATCAACCGAG	CAGAGCTCAG	gtatgtgtgt	76	AK149507 AY033771 AK162999 AK135576	Cassette Exon
10	tctttttcag	AATGCAGAAG	CTTCCCAAAG	gtactggatg	137	AK149507 AY033771 AK162999 AK135576	Cassette Exon
11	tctgttacag	CCTGAAGAAG	ACCAGCGGAG	gtaagacagg	374	AK149507 AY033771 AK162999 AK172678 AK135576	
11b		GTAAGACAGG	ACTTACTGGT		83	AK162999	Bleeding Exon
12	tcattttcag	TTCAATGCGA	ATAGGAGAAG	gtacagagtt	54	AY033771 human mRNA AB055890	Cassette Exon
13	tcatctccag	TATGAGCTGG	ATATCAGAAG	gtatagtatt	66	AY033771 human mRNA AF406992	Cassette Exon (Missing from NM_029332)

Exon	5' Intron Sequence	5' Exon Sequence	3' Exon Sequence	3' Intron Sequence	Exon Size	GenBank Accession Number	Alternative Splicing Event
14	ctgtgttcag	TTTCAGTCTG	TGATCAGCAG	gtaaggctaa	193	AK149507 AY033771 AK172678 AK135576	
15	aattttgtag	ACATGTTACA	GGATTGGACA	gtgagtatat	109	AK149507 AY033771 AK135576	
Lbc		ATCTAAAACT	GAGTTTTGTA	gtaaataagc	60	human RefSeq NM_144767 human mRNA AF127481	Alt Initiation
16	tgttttctag	GTTCACGGCC	TGACCGAGAG	gtacgaggag	43	AK149507 AY033771 AK135576	
17	ttttttttcag	TATAACAGAA	GAAGAGCAAA	gtaagtacct	133	AK149507 AY033771 AK135576	
D		AGGAAGCAGG	ACATGGGCAG	gtaagagcct	227	AK133803 AK037815	Alt Initiation
18	tctttggcag	GAAAAGGAAA	ACGTGTGCAG	gtaagagaca	175	AY033771 AK135576 AK133803 AK037815	
19	tcctttccag	GCTGTGGTGC	CAAAATGAAG	gtaagatagt	68	AK133803 AK037815	
19b		GTAAGATAGT	CTCAAAAATC		202	AK037815	Bleeding Exon
20	ttctctttag	CAGCCAAAAG	AGAAACAAGT	gtaagtagct	67	AK133803	
21	tcccttgcag	CTTCACAGCC	ACATCACTGG	gtaagtgggg	136	AK133803	
22	ctgtctttag	AGTTGGCAAT	ACTGATGAGG	gtaagaggac	113	AK133803	
23	gtattttgag	GAGTAGGTAC	GTGATTTACG	gtgaggtgct	153	AK133803	
24	cttctcatag	AGTTGATGCA	TGTCAGTCAG	gtgagcagcc	251	AK133803	
25	tctcgagcag	TTCTCAGGTG	CTTTGTGAAG	gtactgacct	126	AK133803	
26	tcccttgcag	AAGAAGATGA	TGTACCAAAG	gtgagtctcc	118	AK133803	
27	ctctcccaag	ACAATGAAGT	AGGCTGAAAG	gtatgactgc	249	AK133803 CF745087	
28	tactttgcag	AGGTTCAAGC	TGCATCCTTG	gtaagctgaa	77	AK133803 CF745087	
29	ctctgtccag	GACCATAAGT	TCAACTCCCT	gtacgtgagc	182	AK133803 CF745087	
30	gttatgtcag	GAATAGAGAT	GAGTTAAAAG	gtaaaatgtt	83	AK133803 CF745087 CF538167	
31	tgccctgcag	AACAGCTTCA	ATAAATGAAG	gtaatttaca	195	CF745087 CF538167 CA752442	
32	tttttttgcag	TGGAAATCCT	GCTTCCAAAG	gtaaaccatc	162	CF745087 CF538167 CA752442	
33	ttttgtttag	GAGGTGAGAA	CCTGAAAAAG	gtatgctctc	71	CF538167 CA752442	
34	tattttgtag	GGTGGAAATG	AAACAGTGAG	gtaagggttc	45	CF538167 CA752442	
35	cctttgctag	CAGGTTGTCC	CATGCTGCAG	gtacatgtgc	51	CF538167 CA752442 BU919116	
36	gccatgacag	GGTGTCGTGC	CCTTTGCCAG	gtacccaaga	450	CF538167 CA752442 BU919116 CB245692	
37	acatgtgcag	GTTTCAAATA	CAGCCTGGTG	gtgagttgtc	331	BU919116 CB245692 CF742755	

Exon	5' Intron Sequence	5' Exon Sequence	3' Exon Sequence	3' Intron Sequence	Exon Size	GenBank Accession Number	Alternative Splicing Event
38	acggttgcag	ACGGCCCTGC	CTTTGAGATC		4032	CB245692 CF742755 AK050038	Termination Exon

Annotation of the AKAP13 genomic locus was conducted using RefSeq gene NM_029332 as a reference to identify the base exons. This RefSeq gene lacked exon 13, so the exons 13–37 in NM_029332 are relabeled to exons 14–38 in this table. Additional GenBank mouse and human mRNA and EST sequences were used to identify alternative exons and verify reference exons as listed. Reference exons are numbered 1–38, alternative initiation exons are labeled with a letter (A, B, C or D) or with Brx or Lbc, and bleeding exons are labeled with a "b" (4b, 6b, 11b, & 19b). Ten-bp sequences upstream and downstream of intron-exon boundaries are given, and the exon size is indicated in bp. Predicted alternative splicing events are indicated.
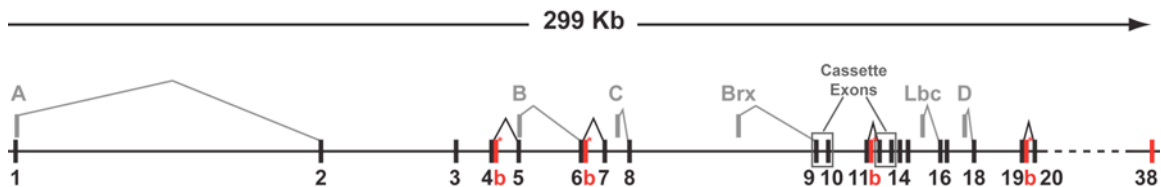
Figure 2.3. AKAP13 genomic organization. The AKAP13 gene spans almost 300 kilobases (Kb) of genomic DNA on mouse chr7qD2 and encodes for at least 44 exons. The exons for the RefSeq gene NM_029332, and exon 13, and the reference splicing events are indicated in black. The locations of the exons are approximately to scale, but the exon sizes are not to scale. Possible alternative initiation exons are in gray above the reference exons with grey lines indicating the predicted splicing events. Possible bleeding exons, predicted to result in transcript termination, are indicated in red with a "b" and "*". Cassette exons are boxed.

To identify the AKAP13 splicing events that occur in mice, we conducted RT-PCR off of total RNA from undifferentiated ES cells, day 10 EBs, adult heart, adult brain, and HL-1 cells. We verified many reference splicing events and several alternative initiation and bleeding exon events (Table 2.2). We verified splicing of the alternative initiation exons Brx into exons 9 & 10 and D into exon 18. We also verified the retention of bleeding exons 4b and 6b. Finally, we verified that cassette exons 12 & 13 could be skipped. These results indicate that many of the alternative splicing events predicted from the gene annotation can occur in mouse tissue. This validation of AKAP13 splicing events is far from comprehensive as only a few tissues were analyzed for a subset of the possible alternative splicing events. Additional analysis of AKAP13 splicing events and full-length AKAP13 clones is needed to better understand the expression patterns of AKAP13 transcripts in mouse tissues and ES cells.

Table 2.2. Validation of AKAP13 splicing events

Exon Junctions Probed		Forward Primer (5'-3')		Reverse Primer (5'-3')	Product Size	Positive Samples
1-2-3-4	MJS135	CCGCCTATTGTCCTTCTCC	MJS175	GGTGTCTGAATGCCAGTGC	516	ESC
3-4b	MJS181	TGCTTGCTGAAGAGGACAAA	MJS185	CTGCTTCCAACAACTCCACA	733	ESC, D10 EB, HL-1
4-5	MJS139	GCACTGGCATTCAGACACC	MJS140	TGTAACAGGAACCATGTCAACC	146	Heart
5-6b	MJS143	AGCATCCACAACAAGGAAGG	MJS144	GCAAGATTCACTGGGTGAGG	339	Heart, ESC, D10 EB
6-7	MJS145	GTGAACCCCATGGAGACAGC	MJS146	TACACTGGGCACACAAGACG	146	Heart, Brain
Brx-9-10	MJS186	TCTCCAAGGTGGACAGGACT	MJS187	GCCTTCTTTTGAGGCACACT	173	ESC, D10 EB
11-14	MJS147	GGGGACCTGGGAAGAACG	MJS148	GGATGGCTTATTTCCAACACC	98	Heart
11-12-13-14	MJS147	GGGGACCTGGGAAGAACG	MJS148	GGATGGCTTATTTCCAACACC	218	Heart
13-14	MJS154	GGTGTCCCTCTGGTGTGC	MJS153	GACGAGGATGGCTTATTTCC	112	Heart
15-16-17	MJS155	TGTACATCAGCCATTTCTTCTCC	MJS156	TGTTATACTCTCGGTCAGGTTGG	123	Heart
17-18	MJS158	AGGTTAGTCGCACCTTCAGC	MJS159	CCGTTAAGAGTCTTTTTATCTTTTTCC	142	Heart, Brain
D-18	MJS160	CCCGAAGTTCCTCTCATAACC	MJS159	CCGTTAAGAGTCTTTTTATCTTTTTCC	134	Heart, Brain, D10 EB
18-19	MJS161	GCAGCCAGTGCATGAAGC	MJS162	CAGGAGGCTAGATTTTCTCTGC	100	Heart
24-25-26-27	MJS177	AGGGGATGTGCTTGTCAGTC	MJS178	GCCTTCCTGTTGTGCTCTTC	509	ESC, D10 EB, HL-1
37-38	MJS163	CAAGCCAAAGGAAAAGAAGG	MJS164	CGTCCAGTGTAAGAGACTTGTGC	197	Heart, Brain, ESC, D10 EB, HL-1

AKAP13 splicing events were validated by RT-PCR off of total RNA from mouse ES cells (ESC), day 10 EBs (D10 EB), HL-1 cells, or adult mouse heart or brain. The exon-exon junctions probed, the primer pairs used, and PCR product sizes (in base pairs) are indicated. The cell or tissue sample(s) that gave the proper PCR product size is indicated. This analysis is not comprehensive, as all junctions were not probed for all cell and tissue samples. Additionally, only a subset of all possible splicing events was analyzed.

2.3.3 pSicoR-EF1α-mCh(-Puro) lentiviral constructs drive strong levels of mCherry expression in ES cells and differentiated EBs.

To establish a method for assaying gene function during ES cell differentiation, we modified an existing lentiviral-RNAi construct to strongly express the fluorescent molecule mCherry in ES cells and during EB differentiation. To do this, we replaced the CMV promoter in the pSicoR-mCherry lentiviral construct [37,40] with an EF1α promoter to create pSicoR-EF1α-mCh (Figure 2.4A), to drive stronger mCherry expression in ES and differentiated cells [41]. We also wanted a method to select for a pure population of lentiviral-RNAi transduced ES cells. For this, we cloned a T2A ribosomal skip motif [42,43], followed by the puromycin-resistance gene in-frame with mCherry to create the antibiotic selectable pSicoR-EF1α-mCh-Puro lentivirus (Figure 2.4B). The pSicoR-EF1α-mCh lentiviral construct transduced ES cells with around 50% efficiency, and mCherry fluorescence was readily detected by fluorescent microscopy (Figure 2.4C). The pSicoR-EF1α-mCh-Puro lentivirus had similar transduction efficiency and fluorescent intensity; additionally, stable ES cell clones and pools of transduced ES cells could be selected for by puromycin treatment (data not shown).

To determine if pSicoR-EF1α-mCh drives continuous expression during ES cell differentiation, we differentiated transduced ES cells and measured fluorescence by flow cytometry. Lentivirus-transduced ES cells were isolated by fluorescent activated cell sorting (FACS) for mCherry expression. These mCherry positive ES cells were differentiated by hanging drop into EBs and the percent of

mCherry positive cells was determined by flow cytometry on day 0 (ESC), 5, 7, and 12 of differentiation (Figure 2.4D). Over 90% of the cells at day 12 of differentiation expressed mCherry when normalized to mCherry expression in ES cells (the mCherry sorted cell sample is graphed in red). Additionally, the mCherry fluorescent intensity was maintained during differentiation and the mCherry-positive cells could be distinguished from mCherry-negative cells (black histogram). These results indicate that the pSicoR-EF1α-mCh and pSicoR-EF1α-mCh-Puro lentiviral constructs can drive strong, detectable levels of mCherry expression in ES cells as well as differentiating cells. Thus, mCherry expression can be used to identify the lentivirus-transduced cells. Additionally, lentivirus-transduced cells can be isolated by antibiotic selection.

A. pSicoR-EF1α-mCh shRNA Lentiviral Construct

B. pSicoR-EF1α-mCh-Puro shRNA Lentiviral Construct

C. pSicoR-EF1α-mCh Infected ESCs

D. Differentiation of FAC Sorted pSicoR-EF1α-mCh Infected ESCs
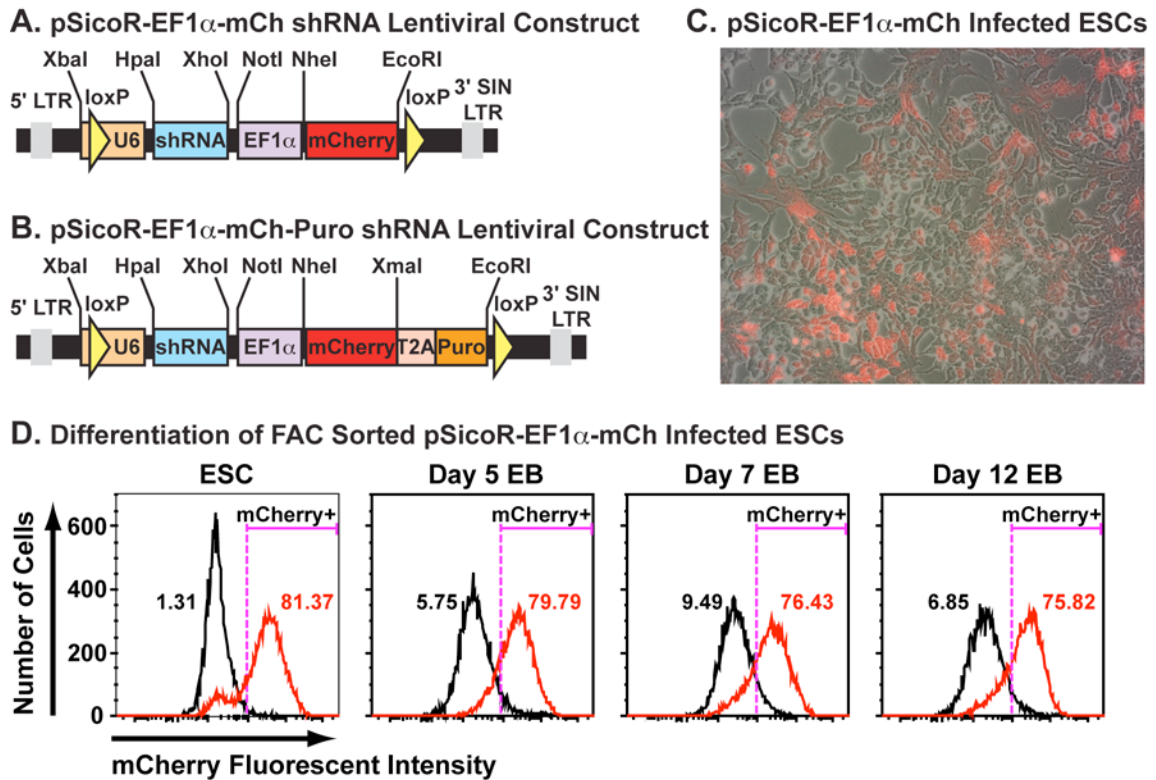
Figure 2.4. pSicoR-EF1α-mCh(-Puro) lentiviral constructs drive strong levels of mCherry expression in ES cells and differentiated EBs. (A) The CMV promoter for pSicoR-mCherry was replaced with the EF1α promoter to create pSicoR-EF1α-mCh. (B) A T2A, ribosomal skip motif, followed by the puromycin resistance gene (Puro) was cloned in-frame with mCherry to create pSicoR-EF1α-mCh-Puro. The T2A motif allows mCherry and Puro to be expressed as separate polypeptides from a single mRNA molecule expressed under the control of the EF1α promoter. The common pSicoR lentiviral backbone contains a U6 promoter to express short hairpin RNAs cloned into the HpaI-XhoI restriction sites [40]. (A&B) Unique restriction enzyme sites are indicated. (C) Around 50% of ES cells could be transduced with concentrated pSicoR-EF1α-mCh lentivirus and mCherry fluorescence was detected by fluorescent microscopy. (D) mCherry-positive cells were isolated from pSicoR-EF1α-mCh transduced ES cells by FACS. The isolated mCherry-positive cells were differentiated using the EB method and mCherry fluorescence was measured by flow cytometry at day 0 (ESC), 5, 7, and 12 of EB formation. Histograms of mCherry fluorescent intensity are shown for untransduced cells (black) and mCherry-sorted cells (red). The percent of mCherry-positive cells for the given gating cutoff is given. mCherry expression is stable during the differentiation time course.

2.3.4 A lentiviral-mediated RNAi competition assay was developed to study gene function during ES cell differentiation.

To determine gene function during ES cell differentiation, we expanded on a lentiviral-mediated RNAi competition assay developed to study the role of genes in undifferentiated ES cells [37,44]. The differentiation efficiency of ES cells into specific cell types, including cardiomyocytes, can vary from day to day and between different cell lines. This makes it difficult to quantitatively compare the differentiation potentials in wild-type and mutant cell lines in a high-throughput manner. A co-culture of both lentiviral-RNAi transduced and wild-type cells differentiated together, in competition, can control for this variability. This competition assay ensures that the RNAi and wild-type cells are treated identically, and it provides an internal control, wild-type cells, for differentiation. A similar assay has been used to study the role of genes in maintaining ES cell pluripotency and proliferation [37,44]; however, this approach has not been used during ES cell differentiation.

A lentiviral-RNAi competition assay can be used to assess gene function in maintaining ES cell pluripotency and proliferation (schematic of this assay is shown in Figure 2.5A). This assay uses an Oct4-GFP reporter ES cell line, Oct4-GiP [45], to label pluripotent ES cells [37]. These GFP-labeled ES cells are infected with pSicoR-EF1α-mCh lentivirus, which results in mCherry expression in the infected, and shRNA producing, cells. The effect of gene knockdown on ES cell pluripotency and proliferation can then be followed during ES cell propagation by flow cytometry. There are several outcomes that could result from

62

gene knockdown: no effect, blocked pluripotency, or inhibited proliferation. If a gene knockdown does not effect ES cell pluripotency or differentiation, the proportion of infected cells expressing mCherry (and the shRNA) will be maintained over time (Figure 2.5A-2). However, if gene knockdown disrupts ES cell pluripotency, the infected cells will lose GFP but will maintain mCherry expression (Figure 2.5A-1); if knockdown inhibits proliferation, all the infected, red, cells will be lost (Figure 2.5A-3).

A similar lentiviral-RNAi competition assay could be used to analyze gene function during ES cell differentiation (schematic is shown in Figure 2.5B). In this assay, a tissue-specific (ts) promoter is used to drive expression of GFP (ts-GFP ESCs). These ts-GFP ES cells are infected with the pSicoR-EF1α-mCh lentiviral construct, and the infected cells become mCherry positive and produce the shRNA to knockdown gene expression. The pool of infected and uninfected cells is then differentiated and flow cytometry is conducted to measure GFP and mCherry fluorescence. The effect of knockdown on differentiation into the tissue type of interested, marked by the ts-GFP, is assessed by comparing the ratios of infected GFP-positive cells (yellow, I+) versus infected GFP-negative cells (red, I-) to uninfected GFP-positive cells (green, U+) versus uninfected GFP-negative cells (grey, U-) at different time points. Some of the possible results from this include:

1) $\dfrac{I+}{I} = \dfrac{U+}{U}$ RNAi knockdown does not effect differentiation (Figure 2.5B-2),

2) $\dfrac{I+}{I} < \dfrac{U+}{U}$ RNAi blocks differentiation (Figure 2.5B-1), or

3) $\dfrac{I+}{I} > \dfrac{U+}{U}$ RNAi promotes differentiation (Figure 2.5B-3).

In other words, if the lentivirus-infected, shRNA-producing, ES cells differentiate into the GFP-expressing cells as efficiently as uninfected cells do, the gene does not effect differentiation. Alternatively, if the differentiation efficiency of the lentivirus-infected, mCherry-positive cells into GFP-expressing cells is different, then the gene functions during differentiation into the specific cell type. In this competition assay, the uninfected cells provide an internal control for differentiation efficiency (U+/U-). Finally, the gene knockdown might inhibit proliferation or general differentiation. In this case, all infected cells could be lost during differentiation (similar to Figure 2.5A-3).
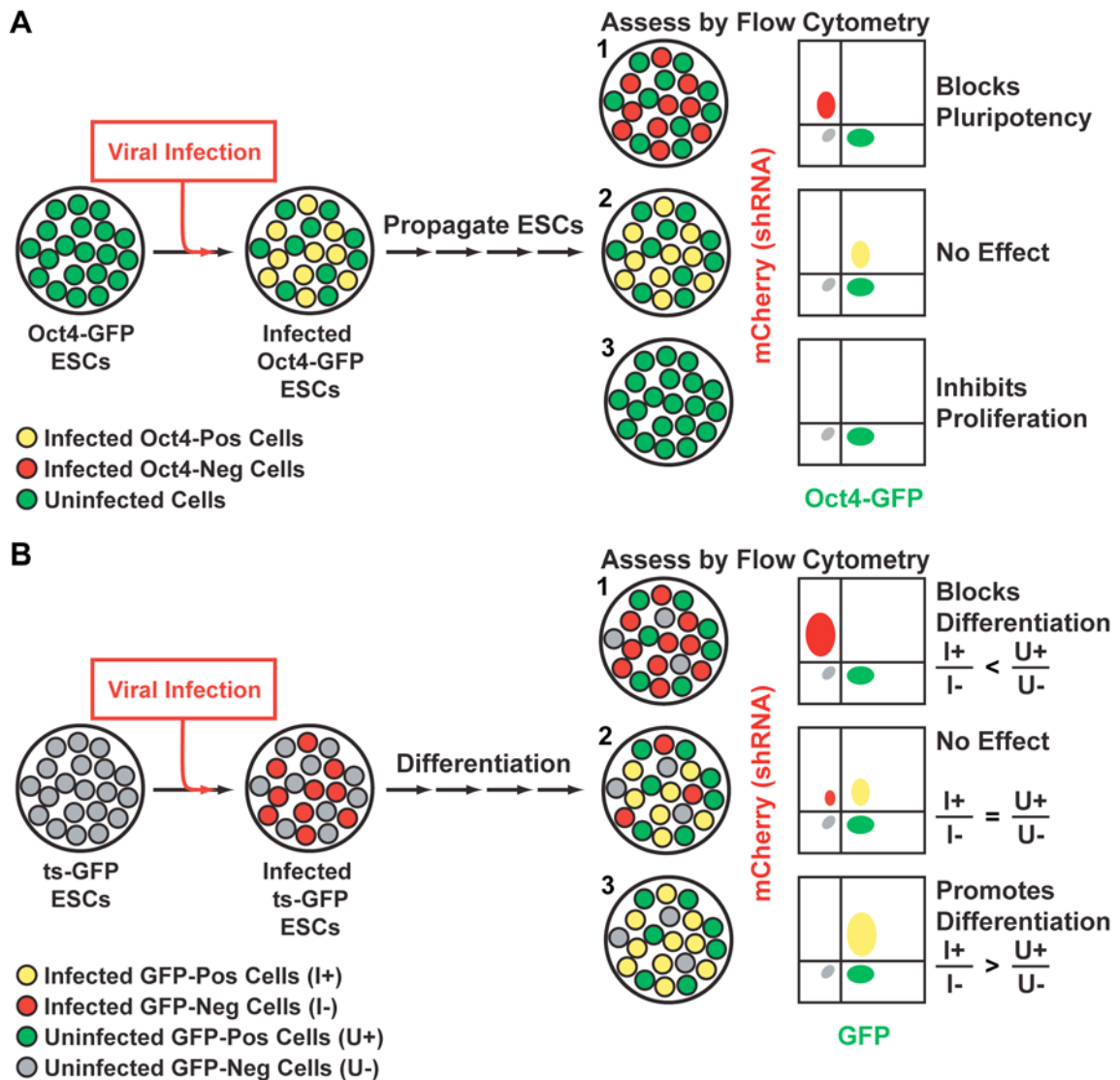
Figure 2.5. Schematic of lentiviral-mediated RNAi competition assay.

(A) Model of the ES cell competition assay. Oct4-GFP labeled cells (green) are infected with a lentiviral construct that expresses mCherry and an shRNA to knockdown gene expression. Some of the Oct4-GFP ES cells will become virally infected (yellow). This pool of infected and uninfected cells is propagated and assessed by flow cytometry. (A-1) If gene knockdown blocks pluripotency, infected GFP-positive cells (yellow) would lose GFP expression (become red only). (A-2) If gene knockdown causes no effect, the ratio of infected (yellow) and uninfected (green) GFP-positive cells would remain constant over time. (A-3) If gene knockdown inhibited proliferation, the infected (yellow and red) cells would be lost. (B) Model of the differentiation competition assay. Undifferentiated ES cells that contain a tissue-specific GFP (ts-GFP) reporter (grey) are

infected with a lentiviral construct that expresses mCherry and an shRNA to knockdown gene expression. Some of the ES cells will become virally infected (red). This pool of infected and uninfected cells is differentiated, and mCherry and GFP fluorescence is measured by flow cytometry. (B-1) If gene knockdown blocks differentiation, the infected cells will not become GFP positive as efficiently as the uninfected cells. (B-2) If gene knockdown has no effect on differentiation, both the infected and uninfected cells will become GFP positive to the same extent. (B-3) If gene knockdown promotes differentiation, the infected cells will become GFP positive more efficiently than uninfected cells.

2.3.5 AKAP13 is not required for ES cell proliferation, pluripotency, or cardiac mesoderm differentiation.

To determine if AKAP13 is required for ES cell maintenance or differentiation into cardiac cells, we designed shRNAs to knockdown AKAP13 expression and conducted the ES cell and differentiation competition assays described above. We selected RNAi target sequences and designed the shRNAs with Psicoligomaker 1.5 and cloned the shRNAs into the pSicoR-EF1α-mCh lentiviral construct. We verified that the AKAP13i-1 shRNA knocked down AKAP13 expression in HL-1 cells by 73%, compared to uninfected cells.

To determine if AKAP13 regulates ES cell maintenance, we infected Oct4-GiP [45] ES cells with empty pSicoR-EF1α-mCh lentivirus or lentivirus expressing the shRNAs GFPi, Oct4i, and AKAP13i-1. These pools of infected and uninfected Oct4-GFP ES cells were passaged every other day for 12 days and GFP, and mCherry fluorescence was measured at each passage (Figure 2.6). Representative flow cytometry plots show that 60–65% of the ES cells were infected with pSicoR-EF1α-mCh lentivirus on day 2 (Figure 2.6A). The GFPi shRNA knocked down GFP expression in infected cells, decreasing the percentage of mCherry–GFP double-positive cells and increasing the percentage of mCherry-positive–GFP-negative cells. The Oct4i shRNA targets the Oct4 gene, Pou5f1, which is required for ES cell maintenance. Thus, as expected, the Oct4i shRNA led to the loss of all infected, mCherry-positive cells by day 6. However, the percentage of GFP–mCherry double-positive cells remained constant for the AKAP13i-1 shRNA. The control shRNA constructs, GFPi and

Oct4i, both gave the expected decreases in GFP and mCherry fluorescence, respectively. These results indicate that this ES cell competition assay is functioning as expected. Furthermore, AKAP13 does not regulate ES cell maintenance.

We then quantified the percent of mCherry-positive, lentivirus-shRNA-infected cells at each passage to determine the effect of the shRNAs on ES cell proliferation (Figure 2.6B). Since each lentiviral transduction gave a different percentage of infected cells, we normalized each series to the day 2 values. There was a slight decrease in the percent of mCherry-positive cells over time for the empty lentivirus sample. The GFPi and AKAP13i-1 shRNAs decreased the percent of mCherry positive cells in a similar manner, and this decrease was only slightly larger than that for the empty lentivirus. Finally, the Oct4i shRNA dramatically decreased the percent of mCherry-positive cells by day 4 and, mCherry cells were completely lost by day 8. These results indicate that the lentivirus-infected cells are at a slight disadvantage in the competition assay compared to the uninfected cells. Thus, lentivirus-infected cells expressing a control shRNA are required for comparison with the experimental shRNA. In this experiment, the GFPi and AKAP13i-1 shRNAs had the same curve for mCherry positive cells. This indicates that AKAP13 is not required for ES cell proliferation.

Finally, to determine if AKAP13 was required for ES cell differentiation into cardiac mesoderm, we infected Nkx2.5-GFP ES cells [38] with empty pSicoR-EF1α-mCh lentivirus or lentivirus expressing the AKAP13i-1 shRNA. We then differentiated the pool of cells by the hanging-drop method [46,47]. Differentiation

into Nkx2.5-GFP-positive cells was measured at day 5 of EB differentiation by flow cytometry (Figure 2.6C). In uninfected Nkx2.5-GFP cells (No Virus), around 25% of undifferentiated ES cells were GFP positive and this to about 60% on day 5 of EB differentiation. Both the empty (no shRNA) and AKAP13i-1 lentiviral samples also had about 60% GFP-positive cells on day 5 of differentiation when infected and uninfected cells were combined. Moreover, when analyzed separately, 64% of the "no shRNA" infected cells became GFP positive, while 59% of the uninfected cells became GFP positive. Similarly, 63% of the AKAP13i-1 shRNA-infected cells became GFP positive, while 51% of the uninfected cells became GFP positive. These results show that the AKAP13i-1 shRNA did not effect differentiation into Nkx2.5-GFP-positive cells. Furthermore, they indicate that AKAP13 is not required for ES cell differentiation into cardiac mesoderm.
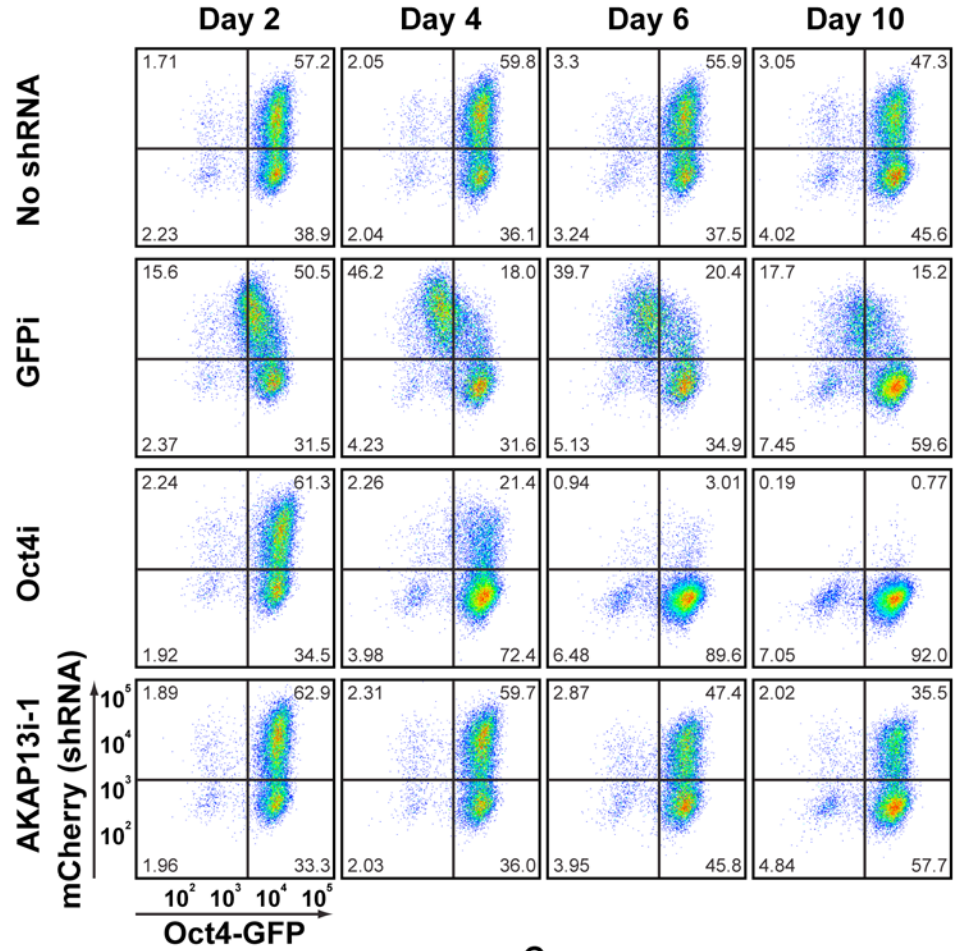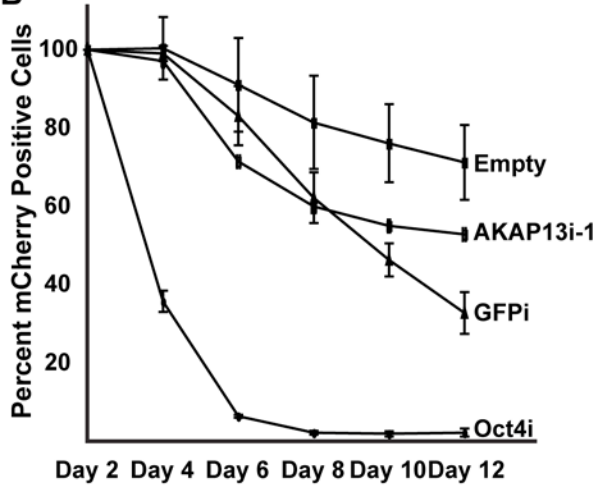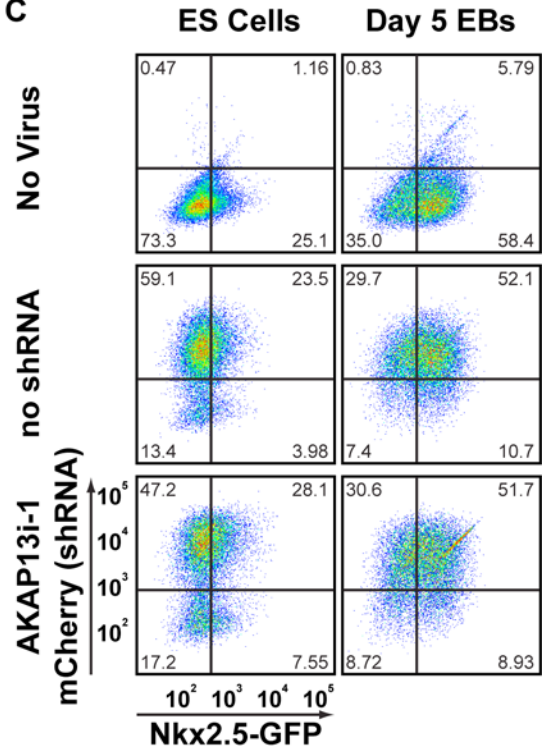
Figure 2.6. AKAP13 is not required for ES cell proliferation, pluripotency, or cardiac mesoderm differentiation. (A) Representative flow cytometry plots for mCherry and GFP fluorescence are shown for empty, GFPi, Oct4i, and AKAP13i-1 pSicoR-EF1α-mCh lentiviral infected Oct4-GFP ES cells on days 2, 4, 6, and 10 of propagation. The percent of cells in each quadrant is indicated. (B) Quantification of cellular proliferation for empty, GFPi, Oct4i, and AKAP13i-1 shRNA-lentiviral infected Oct4-GFP ES cells propagated for six passages. The percent of mCherry positive cells at each passage was normalized to day 2 values for that sample. Means and std deviations are graphed (n=4). (C) Representative flow cytometry plots for mCherry and GFP fluorescence are shown for no virus (FACSed mCherry-negative pSicoR-EF1α-mCh no shRNA), empty (mCherry-positive pSicoR-EF1α-mCh no shRNA), and AKAP13i-1 (mCherry-positive pSicoR-EF1α-mCh AKAP13i-1) infected Nkx2.5-GFP ES cells and cells from day 5 EBs. The percent of cells in each quadrant is indicated (n=1).

2.3.6 AKAP13 is not required for ES cell differentiation into functional cardiomyocytes.

We next wanted to determine if AKAP13 is required for ES cell differentiation into functional cardiomyocytes. To do this, mouse E14 ES cells were infected with pSicoR-EF1α-mCh-Puro lentiviral constructs expressing shRNAs, infected cells were selected for, and these pools of infected cells were differentiated into embryoid bodies. Multiple shRNAs were used to knock down AKAP13 (AKAP13i-1 & AKAP13i-3) expression, and an shRNA against Sox17 (Sox17i) was used as a control to disrupt functional cardiomyocyte formation [48]. We also used multiple negative-control shRNAs targeting GFP (GFPi), luciferase (Luci) and a scrambled version of AKAP13i-3 (AKAP13i-3m). To verify that AKAP13 and Sox17 expression was decreased by their respective shRNAs, we conducted quantitative PCR with TaqMan probes on ES cells and day-5 differentiated EBs (Figure 2.7A). The two AKAP13 shRNAs, AKAP13i-1 and AKAP13i-3, reduced expression by 70–80% in ES cells and 40–50% in day 5 EBs as compared to uninfected E14 cells (No Virus). The negative-control shRNAs, GFPi, Luci, and AKAP13i-3m, did not reduce AKAP13 expression levels. Likewise, the Sox17i shRNA reduced Sox17 expression by 87% compared to E14 cells with no virus at day 5 of differentiation. Expression of Sox17 is only shown for day 5 EBs because Sox17 expression was not detected in ES cells.

To determine if AKAP13 knockdown effected ES cell differentiation into functional cardiomyocytes, we counted the number of spontaneously contracting EBs on day 10 of differentiation (Figure 2.7B). E14 cells without virus produced

beating areas in 93% of EBs. The negative-control shRNAs produced beating

EBs to a similar extent as no virus (72–87%), and the Sox17i shRNA, positive

control, dramatically reduced the percent of beating EBs to 11%. We found that

both AKAP13-specific shRNAs produced beating EBs at the same percent as the

negative controls (83–86%). These results indicate that AKAP13 is not required

for the differentiation of functional cardiomyocytes from ES cells.

Finally, to determine if AKAP13 knockdown affected ES cell differentiation

into other cell types, we conducted quantitative PCR for tissue-specific markers

on day 5 and 7 of EB differentiation (Figure 2.7C). For this analysis, the three

negative control samples, GFPi, Luci, and AKAP13i-3m, were combined into the

control group. Likewise, both AKAP13 samples, AKAP13i-1 and -3, were

combined; the Sox17 control sample remained in its own group. AKAP13

knockdown did not effect expression of markers for endoderm (AFP), endothelial

cells (PECAM1), cardiac mesoderm (Nkx2.5), smooth muscle (Acta2) or the

second heart field (Hand2). In agreement with the formation of functional

cardiomyocytes, AKAP13 knockdown did not effect expression of the

cardiomyocyte structural genes cTnT or Myh7. As expected, Sox17 knockdown

decreased expression of the cardiomyocyte structural genes cTnT and Myh7 in

day 5 and 7 EBs. Sox17 knockdown also decrease expression of the endodermal

marker AFP at day 5 and 7 of EB differentiation. Additionally, Sox17 knockdown

decreased Nkx2.5 expression in day 5 EBs and Acta2 expression in day 7 EBs.

These results show that AKAP13 is not required normal expression of

differentiation markers for endoderm, endothelial cells, and cardiomyocytes. This

suggests that AKAP13 does not mediate ES cell differentiation into endoderm, endothelium, or functional cardiomyocytes. These results also confirm that Sox17 is required for differentiation into functional cardiomyocytes.

While conducting the above experiments, we noticed that antibiotic treatment tended to decrease the efficiency of ES cell differentiation into beating EBs. To determine if puromycin treatment decreases ES cell differentiation into functional cardiomyocytes, we treated ES cells previously selected for the pSicoR-EF1α-mCh-Puro lentivirus with or without puromycin and differentiated the cells via the hanging drop method. We then determined the number of beating EBs on day 10 of differentiation (Figure 2.8). Indeed, puromycin treatment decreased the percent of beating EBs by 15–30%. However, the number of EBs formed was not different. These results indicate that antibiotic treatment, including puromycin selection, reduces the efficiency of ES cell differentiation into functional cardiomyocytes.
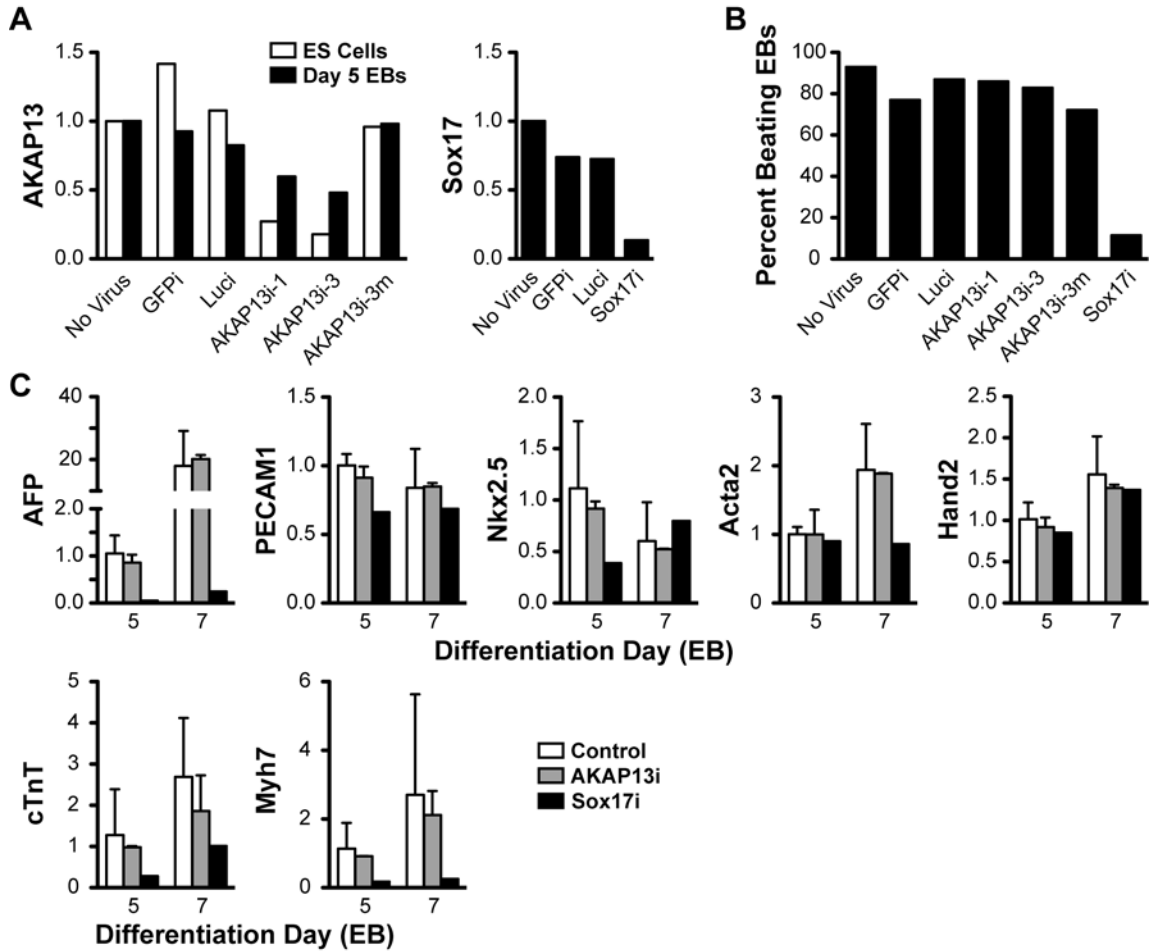
Figure 2.7. AKAP13 is not required for ES cell differentiation into functional cardiomyocytes. (A) ES cells were infected with the pSicoR-EF1α-mCh-Puro lentivirus expressing the indicated shRNAs, and infected ES cells were selected for with puromycin. Quantitative PCR was conducted on ES cell and day 5 EB total RNA with AKAP13 and Sox17 TaqMan probes. Expression levels were normalized to Ubb and β-actin and are relative to the No Virus ES or Day 5 EB sample. The mean of technical triplicates is shown. (B) The percent of beating EBs were determined on day 10 of EB differentiation. Total number of EBs assessed: No virus, 43; GFPi, 48; Luci, 46; AKAP13i-1, 43; AKAP13i-3, 47; AKAP13i-3m, 43; Sox17i, 44. (C) Quantitative PCR was conducted on day 5 and 7 of EB differentiation for marker genes with TaqMan probes. Expression levels were normalized to Ubb and β-actin. The values for the control samples, GFPi, Luci, and AKAP13i-3m, were averaged to create the Control group; similarly, AKAP13i samples -1 and -3 were averaged into a single group. Expression levels are relative to the day 5 Control group values.
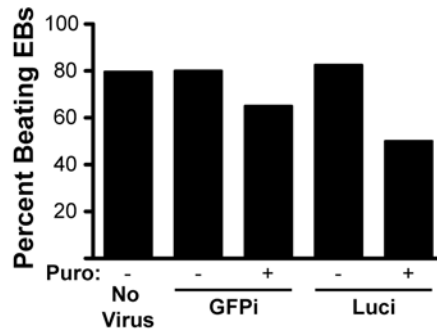
Figure 2.8. Puromycin treatment decreased ES cell differentiation into functional cardiomyocytes. ES cells previously selected for the pSicoR-EF1α-mCh-Puro lentivirus were cultured with or without puromycin before differentiation. The percent of beating EBs was determined on day 10 of differentiation. Total number of EBs assessed: No Virus n=59; GFPi n=60; GFPi + Puro n=63; Luci n=63; Luci + Puro n=64.

2.4 Discussion

Our study investigated the role of AKAP13 in maintaining ES cell proliferation, pluripotency, and differentiation into cardiomyocytes. This study demonstrates that, despite a large increase in AKAP13 expression during mouse ES cell differentiation, it is not required for ES cell maintenance or differentiation into functional cardiomyocytes. Additionally, we developed a lentiviral-mediated RNAi competition assay that can be used to test gene function during differentiation into any cell type of interest that can be labeled with a tissue-specific GFP marker. We identified AKAP13 as being up-regulated during both mouse embryonic development and ES cell differentiation and highly expressed in heart tissue and ES cells (Chapter 1 and Figure 2.2). However knockdown of AKAP13 with shRNAs did not effect expression of an Oct4-GFP marker for pluripotency or the proliferation of infected cells. Additionally, AKAP13 knockdown ES cells had normal differentiation into Nkx2.5-GFP marked cardiac mesodermal cells and functional cardiomyocytes, as determined by the percent of beating EBs. Finally, AKAP13 deficient EBs expressed normal levels of tissue-specific markers for endoderm, endothelium, and cardiac cells as well as cardiac structural genes.

The lentiviral-mediated RNAi competition assay developed in this study could be used to identify genes required for differentiation into any specific cell type. To make this assay functional during ES cell differentiation, we needed to replace the original CMV-driven mCherry fluorescent reporter [37] because this gave weak expression in ES cells and the fluorescent expression was lost during differentiation. We chose to use the ubiquitous EF1α promoter to drive higher

levels of mCherry expression in ES cells and differentiated cell types [41]. We easily detected EF1α-driven mCherry expression by fluorescent microscopy and flow cytometry in ES cells, and this expression was stable during differentiation. This competition assay also requires a method for identifying specific cell types. In our assay, we used an ES cell line that expresses a tissue-specific fluorescent reporter, GFP driven by Nkx2.5 [38]. Similarly, any other ES cell line that contains a tissue specific promoter driving a fluorescent marker could be used. This approach is useful for identifying genes required for differentiation into a specific cell type. However, it is limited because it requires ES cell lines that contain the tissue specific reporter. One way to expand the scope of differentiated cells analyzed would be to use an ES cell line that contains multiple tissue specific promoters driving complementary fluorescent reporter molecules. This would allow several cell types to be analyzed from a single RNAi experiment. An alternative approach would be to use antibodies against cell-type specific surface molecules in combination with the lentiviral-mediated RNAi construct. As new cell-type specific surface molecules are identified, this approach could become very useful because it would allow for the identification of many differentiated cell types from a single RNAi experiment.

There are several limitations with this lentiviral-mediated RNAi competition assay. One limitation is that the mCherry fluorescent reporter is cytoplasmically expressed, and this makes it impossible to identify individual mCherry-positive cells within the three-dimensional EB. Thus, the EBs need to be broken up into individual cells and analyzed by flow cytometry. For the competition assay to be

useful as a high-throughput assay, individual cells expressing the lentiviral fluorescent marker, mCherry, need to be easily identified. This could be done by targeting the fluorescent reporter to the nucleus through the use of a nuclear localization sequence [49] or by fusion to the histone H2B [50]. This would greatly improve the detection of individual cells and allow the transduced EBs to be analyzed by high-content microscopy.

Another issue with the competition assay is that it only identifies cell-autonomous functions. Wild-type cells are present during the competitive differentiation, and they could express sufficient levels of the target gene to maintain normal differentiation through non-cell-autonomous mechanisms. To address this issue, we created a lentiviral-RNAi construct with antibiotic resistance, pSicoR-EF1α-mCh-Puro, to select for a pure population of lentivirus-infected ES cells. This approach was validated by knocking down Sox17, which disrupted the formation of beating EBs and decreased the expression of cardiac structural genes as expected [48]. Even with this selection for lentiviral infection, we noticed that some mCherry fluorescence was lost during ES cell maintenance and differentiation. Additionally, AKAP13 knockdown was less efficient in day 5 EBs than it was in ES cells. This silencing may be due to chromatin remodeling that blocks lentiviral expression of both the mCherry fluorescence and shRNA. However, we did obtain very efficient knockdown of Sox17 in EBs, so it is possible that the EF1α promoter alone was silenced. It is unclear if the silencing of mCherry expression occurs in random cells or specific cell types. We have noticed that the EF1α promoter is silenced during differentiation in other settings

79

as well. Thus, the EF1α promoter may not be ideal for driving ubiquitous expression. The CAG promoter is likely a better alternative to EF1α as it would likely drive higher levels of mCherry expression more stably [51].

We initially identified AKAP13 as a prime candidate for regulating cardiomyocyte differentiation: it was up-regulated during mouse development and ES cell differentiation, was highly expressed in the adult heart, and coordinated a hypertrophic signaling pathway to activate MEF2 transcriptional activity in cardiomyocytes. Additionally, many of the signaling molecules in the AKAP13 coordinated pathway have important roles during cardiac development and differentiation. We also had insight that an *Akap13*-null mice die during development and have an underdeveloped heart (cardiac hypoplasia) with fewer cardiomyocytes [52]. Given this initial evidence that AKAP13 might regulate PKC signaling and MEF2 transcriptional activity during cardiomyocyte development, we were surprised that AKAP13 knockdown did not decrease differentiation into cardiomyocytes or the formation of beating EBs. While these experiments were being conducted, more information on the *Akap13*-null mouse phenotype became available [25]. From these figures, we noticed that the *Akap13*-null mice appear to form hearts with relatively normal structure and cardiomyocyte number, but they fail to develop past day E9.5 of embryonic development. The comparisons between wild-type and *Akap13*-null embryonic hearts made in the publication do not appear to be from somite matched embryos. Thus, the suggested decrease in cardiomyocytes, and ventricular wall thickness, in the *Akap13*-null embryos could be due to the difference in developmental stage

between these embryos. This reinterpretation of the *Akap13*-null embryonic

phenotype along with our ES cell differentiation results indicate that AKAP13 is

not required for differentiation into functional cardiomyocytes. Furthermore, our

results suggest that cardiomyocytes form properly and are able to contract in the

Akap13-null embryonic heart. This suggests that other developmental processes

are defective in the *Akap13*-null embryos.

There are several possible alternative explanations for the lethal *Akap13*-null

phenotype. One possibility is that vascular cells do not properly differentiate. Our

results indicate, however, that the expression of the endothelial (vascular) marker

PECAM1 is unaffected by AKAP13 knockdown. This suggests that endothelial

cells also differentiate normally in the absence of AKAP13. Another possibility is

that the embryonic death is due to morphological, structural, or functional

defects. The ES cell differentiation model is powerful for identifying defects in

cell-type differentiation, proliferation, and gene expression. However, this system

is not designed to identify morphological or structural defects, which are best

studied in the developing embryos. Additionally, identifying functional defects in

ES cell-derived EBs can be difficult since the EBs contain many cell types, and it

is unclear what cells may have defective functions. To manage this cellular

heterogeneity, future studies could use specific ES cell-derived tissue types to

study AKAP13 functions.

The AKAP13 gene locus is very large and complex with multiple alternative

initiation, termination, and cassette exons. Our annotation of the AKAP13 gene

identified multiple exons not included in the mouse RefSeq gene. We validated

splicing for some of these exons, but many remain to be thoroughly tested. We looked for exon-exon splicing in a small number of tissue and cell samples, and we verified the use of at least three alternative initiation exons in ES cells, EBs, and/or heart tissue. However, a survey of many more tissue types is needed to better understand the expression patterns of these alternative exons and the resulting AKAP13 transcripts. The increase in deep sequencing will likely bring a better understanding of the exons expressed and splicing events used in specific tissue types. In addition, analysis of the regulatory elements that drive the expression of specific transcripts through the use of alternative initiation exons is needed. Finally, none of the full-length transcripts for mouse AKAP13 have been cloned. Cloned transcripts are essential for understanding the signaling properties of and functional roles for these transcripts.

Our analysis of AKAP expression during mouse development and ES cell differentiation identified many expressed and regulated AKAP genes. Surprisingly, only AKAP13 expression was increased in both data sets. However, we noticed that several AKAPs including AKAP1, 9, and Pericentrin were down-regulated in both data sets. This down regulation could indicate that these AKAPs are important for ES cell maintenance or proliferation. In fact Pericentrin might be important in controlling stem cell self-renewal [53]. Thus, it would be interesting to determine if any of these AKAPs are required for ES cell maintenance or proliferation. The lentiviral-mediated RNAi competition assays described in this study could be used to test for these functions. Furthermore,

future studies could use a similar competition assay to screen all AKAP family members for defects in differentiation.

In summary, we found that despite a large increase in AKAP13 expression during mouse ES cell differentiation, it is not required for ES cell maintenance or differentiation into functional cardiomyocytes. These results agree with the *Akap13*-null mouse that is able to form the heart and produce cardiomyocytes but fails to develop past embryonic day E9.5. This indicates that AKAP13 is not required for cardiomyocyte differentiation but suggests that it is required for other developmental processes *in vivo*, possibly morphogenesis, maturation, or function. These results also suggest that additional AKAPs may compensate for the loss of AKAP13 during cardiomyocyte differentiation. In this study, we developed a lentiviral-mediated RNAi competition assay that can be used to identify genes required for differentiation into any GFP-marked cell type. This assay should be an ideal system for studying the requirement of any gene for differentiation into any detectable cell type. Moreover, the modifications discussed above should allow this method to be used in high-throughput screening assays.

2.5 Materials and Methods

AKAP13 expression analysis

Mouse β-MHC-GFP ES cells (a transgenic E14 cell line) were differentiated by the hanging drop method as described [46,47]. Total RNA was collected from ES cells and EBs at days 5, 7, 10, and 13 of differentiation, adult mouse heart tissue,

and HL-1 cells with Trizol (Invitrogen). Adult mouse heart tissue was homogenized using a 4.5-mm Tissue Tearor (Research Products International) in Trizol. RNA was cleaned with RNeasy columns (Qiagen), and cDNA synthesized with SuperScript III RT-PCR kit and random hexamers (Invitrogen) as described by the manufacturer. Expression was assessed using Sybr Green primers for AKAP13 (forward = 5'-TGAAGAGCACAACAGGAAGG-3'; reverse = 5'-GTCCAAGGATGCAAACACG-3') and Cyclophilin [54] (forward = 5'-TGGAAGAGCACCAAGACAGACA-3'; reverse = 5'-TGCCGGAGTCGACAATGAT-3'). AKAP13 primers were designed using Primer3 [55]. Real-time quantitative PCR (qPCR) was conducted using the Sybr Green method (Applied Biosystems) on an Applied Biosystems 7900HT real-time thermocycler. Samples were assayed in technical triplicates and AKAP13 expression levels were normalized to cyclophilin. Relative expression was calculated against mouse ES cell samples. This expression analysis was conducted on one set of samples.

Annotation of AKAP13 gene structure

The 300-kb genomic region of mouse AKAP13 (chr7qD2) was annotated with Vector NTI (Invitrogen) with available mouse and human GenBank mRNAs and ESTs and the UCSC Genome Browser. The RefSeq gene NM_029332 was used as the reference exon structure, and additional mRNA and EST sequences were aligned to the genomic sequence to annotate the AKAP13 exons. Exon 13 was not contained in NM_029332, and the subsequent exons were relabeled as 14-

38. Sequences are reported for the 5' intron-exon and 3' exon-intron junctions. Sequences for ten bp upstream and downstream of the 5'-splice acceptor (intron-exon) and 3'-splice donor (exon-intron) are given. The size of each exon is listed as are the GenBank accession numbers used to verify the exons. Finally, any alternative splicing events identified are indicated.

AKAP13 splicing validation

AKAP13 splicing events identified by annotating the genomic locus were verified by RT-PCR. Total RNA from mouse adult heart, brain, E14 ES cells, and day 10 EBs was extracted with Trizol. RT-PCR was conducted with SuperScript III One-Step RT-PCR kit (Invitrogen) using 25ng of total RNA. Additionally, cDNA was synthesized from E14 ES cells, day 10 EBs, and HL-1 cells (atrial cardiomyocyte cell line) [56] with SuperScript III RT-PCR kit and random hexamers, an oligo dT primer, or gene specific primers. PCR was then conduced using the synthesized cDNA as the template. Exon-exon junctions that produced PCR products, the primers used, PCR product size, and tissue sample that gave the PCR product are listed in Table 2.2. All primers were designed with Primer3 [55].

Modification of pSicoR-mCherry to pSicoR-EF1α-mCh and pSicoR-EF1α-mCh-T2A-Puro

The CMV promoter that drives mCherry in pSicoR-mCherry [37,40] was exchanged for the EF1α promoter to create pSicoR-EF1α-mCh [57]. The CMV promoter was removed from the pSicoR-mCherry plasmid by enzymatic digestion

with NotI and NheI (New England Biolabs; NEB). The linearized plasmid backbone was gel extracted and treated with CIP (NEB) to dephosphorylate the overhanging plasmid ends. The EF1α promoter was PCR amplified with PfuTurbo (Stratagene) to add NotI and NheI restriction sites with forward primer MJS103 (5'- ATAAGAATGCGGCCGC-GGATCTGCGATCGCTCCGGT-3') and reverse primer MJS104 (5'- CTAGGCTAGC-GTAGGCGCCGGTCACAGCTT-3'). The sequences preceding the hyphens in MJS103 & MJS104 added the restriction sites while those following the hyphens are specific for the EF1α promoter. The PCR product was digested with NotI and NheI restriction enzymes and the NotI-EF1α-NheI fragment was cleaned up with a PCR cleanup kit (Qiagen). The linearized pSicoR-mCherry and NotI-EF1α-NheI DNA were ligated using T4 DNA ligase (NEB). Properly annealed pSicoR-EF1α-mCh plasmids were sequence verified.

A T2A-Puro cassette was then added to pSicoR-EF1α-mCh to create pSicoR-EF1α-mCh-T2A-Puro so that lentivirally infected cells could be selected for by puromycin treatment as described [58]. In brief, the pSicoR-EF1α-mCh plasmid was linearized by BsrGI and EcoRI digest (NEB). A T2A-Puro cassette was PCR amplified with PfuTurbo (Stratagene) to add BsrGI and EcoRI restriction sites with forward primer MJS173 (5'- GAGCTGTACAAG-CCCCGGGAGGGCAGAG-3') and reverse primer MJS174 (5'- CCGGAATTCTTA-GGCACCGGGCTTGCGG-3'). The sequences preceding the hyphens in MJS173 & MJS174 added the restriction sites while those following the hyphens are specific for the T2A-Puro cassette. The T2A-Puro cassette was digested with

BsrGI and EcoRI restriction enzymes (NEB) and ligated into the linearized

pSicoR-EF1α-mCh plasmid as described above. Properly annealed pSicoR-

EF1α-mCh-T2A-Puro plasmids were sequence verified.

RNAi of AKAP13 in embryonic stem cells

RNAi target sequences were selected from overlapping predictions by the

program pSICOLIGOMAKER 1.5 (http://web.mit.edu/jacks-

lab/protocols/pSico.html) and the Broad Institute mouse hairpin library

(http://www.broadinstitute.org/rnai/trc/lib) as described [58]. The 19-mer target

sequences were designed into short-hairpin RNAs (shRNAs) with the program

pSICOLIGOMAKER 1.5. The shRNA sequences were split into two sense oligos

(of 23 and 32 bp) and two antisense oligos (of 28 and 31 bp). These four

overlapping oligos were phosphorylated, annealed together, and ligated into HpaI

and XhoI (NEB) double digested pSicoR-EF1α-mCh plasmids using standard

protocols. The AKAP13 RNAi target sequences are: AKAP13i-1:

GAATAGAGATGAAGATGAA, AKAP13i-2: GGATTCTCTTCTGTGAGAA, and

AKAP13i-4: GAAGAAAGATGTGGTCAAA. Published AKAP13 RNAi target

sequences were also used: AKAP13i-3: GCAAGTCGATCATGAGAAT and

AKAP13i-3m: GCATGTCGATCATGCGATT [24]. RNAi target sequences for

GFPi: ACAGCCACAACGTCTATAT, Oct4i: GAACCTGGCTAAGCTTCCA [37],

Sox17i: GCAGGTGAAGCGCATGAAG, and Luciferase (Luci):

CTTACGCTGAGTACTTCGA [48] were from published literature.

Lentivirus was packaged in HEK293 cells cotransfected with a pSicoR-EF1α-mCh plasmid (3 μg) and 1 μg of each of the packaging plasmids: pVSV-G (Clontech), pRSV-Rev [59], and pMDL-g/pRRE [59] with FuGENE6 (Roche). Viral supernatant was collected from the transfected HEK293 cells at 48 hours and filtered through a 45-μm filter. Viral particles were concentrated with a Beckman L8-70M Ultracentrifuge in a SW41 rotor spun at 25k rpm for 90 minutes at 4°C. The supernatant was removed form the viral particles, and the viral particles were resuspended in 100 μl of PBS.

Validation of gene knockdown

HL-1 cells (532k cells) were infected with 200 μl of unconcentrated viral containing supernatant in a 6-well plate. Positive and negative mCherry-expressing HL-1 cells were isolated by FACS 4 days after infection. Cells were homogenized in Trizol (Invitrogen) and total RNA collected. cDNA was synthesized with SuperScriptIII RT-PCR kit and random hexamers (Invitrogen). Real-time quantitative PCR (qPCR) was conducted using the Sybr Green method (Applied Biosystems) on an Applied Biosystems 7900HT real-time thermocycler. Samples were assayed in technical triplicates (n=1) and AKAP13 expression levels were normalized to cyclophilin. Relative expression was calculated against mCherry-negative sorted cell samples.

Lentiviral-mediated RNAi competition assay

Mouse Oct4-GiP [45] ES cells (150k cells in 1 mL of LIF medium) were infected with 30 μl of fresh, concentrated, lentivirus on Day 0. Cells were incubated with viral particles on a rotator for 3–6 hours at 37°C, plated onto gelatinized 12-well plates, and cultured in ES cell medium with LIF. ES cells were analyzed with a BD Biosciences LSR II flow cytometer for Oct4-GFP and lentiviral-mCherry expression every other day. During flow cytometry, cells were gated for single cells and live cells. The percent of mCherry-positive cells during propagation were normalizing to Day 2 mCherry-positive cells. The ES cell competition assay was conduced in quadruplicate.

Mouse Nkx2.5-GFP [38] ES cells (200k cells in 1mL of LIF media) were infected with 30μl of fresh, concentrated, pSicoR-EF1α-mCh lentivirus containing no shRNA or AKAP13i-1 shRNA . Cells were incubated with viral particles on a rotator for 4 hours at 37°C, plated onto gelatinized 6-well plates, and cultured in ES cell medium containing LIF. Four days after lentiviral infection, infected (mCherry-positive) and uninfected (mCherry-negative) Nkx2.5-GFP ES cells were isolated by FACS. These sorted cells were differentiated by the hanging drop method and analyzed by flow cytometry for GFP and mCherry expression at day 0 (ES Cells) and day 5 (Day 5 EBs). The sorted cell populations used were: No Virus = pSicoR-EF1α-mCh no shRNA mCherry negative, no shRNA = pSicoR-EF1α-mCh no shRNA mCherry positive, and AKAP13i-1 = pSicoR-EF1α-mCh AKAP13i-1 shRNA mCherry positive. This differentiation experiment was conducted once following this specific protocol. However, multiple differentiation experiments using AKAP13-deficient ES cells obtained from puromycin selection

(for pSicoR-EF1α-mCh-Puro) for clonal cell lines and pools of infected cells also had no effect on differentiation into Nkx2.5-GFP positive cells.

AKAP13 RNAi with pSicoR-EF1α-mCh-Puro during ES cell differentiation

Mouse ES cells were infected with fresh, concentrated, lentivirus as described above. Infected cells were selected with 2 μg/mL puromycin (InvivoGen). ES cells were differentiated using the hanging drop method [46,47] and plated onto gelatinized wells at day 5 of differentiation. The number of spontaneously contracting, beating, EBs out of total EBs were determined on day 10 of differentiation. Total number of EBs assessed: No virus, 43; GFPi, 48; Luci, 46; AKAP13i-1, 43; AKAP13i-3, 47; AKAP13i-3m, 43; Sox17i, 44.

Gene expression analysis was performed on total RNA isolated from ES cells, day 5, and day 7 EBs. Samples were homogenized in Trizol (Invitrogen), and cDNA was synthesized from DNase Turbo (Ambion) treated RNA with SuperScriptIII RT-PCR kit and random hexamers (Invitrogen). Real-time qPCR was conducted using TaqMan probe sets (Applied Biosystems) on an Applied Biosystems 7900HT real-time thermocycler. TaqMan probe sets: AKAP13 E24-25 (Mm01320086_m1), Sox17 (Mm00488363_m1), AFP (Mm00431715_m1), PECAM1 (Mm00476702_m1), Nkx2.5 (Mm00657783_m1), Acta2 (Mm00725412_s1), Hand2 (Mm00439247_m1), cTnT/Tnnt2 (Mm00441922_m1), Myh7 (Mm00600555_m1), Ubb (Mm01622233_g1), and β-actin (Mm00607939_s1). Samples were assayed in technical triplicates and average expression levels were determined from Ubb and β-actin normalized values.

Relative expression was calculated against the no virus ES cell and Day 5 EB

samples for AKAP13 and Sox17 expression (Figure 2.6A) or an average of day 5

EB expression for GFPi, Luci, and AKAP13i-3m samples (Control in Figure

2.6C). AKAP13i values were determined by averaging AKAP13i-1 and AKAP13i-

3 expression levels.

Effect of antibiotic treatment on ES cell differentiation

Mouse ES cell lines (E14 p34, GFPi p32, & Luci p32) previously selected for

lentiviral integration were thawed and cultured in LIF media without puromycin for

7–8 days. ES cells were then cultured in LIF media alone or LIF media with

puromycin for 4–5 days. ES cells were differentiated in 20% FBS medium without

puromycin by the hanging drop method and transferred to gelatinized 96-well

plates on day 5 of differentiation. The numbers of spontaneously contracting EBs

were counted on day 10 of differentiation. Total number of EBs assessed: No

Virus n=59; GFPi n=60; GFPi + Puro n=63; Luci n=63; Luci + Puro n=64.

2.6 Acknowledgements

2.7 References

1. Hoffman JI, Kaplan S (2002) The incidence of congenital heart disease. J Am Coll Cardiol 39: 1890-1900.
2. Kang M, Chung KY, Walker JW (2007) G-protein coupled receptor signaling in myocardium: not for the faint of heart. Physiology (Bethesda) 22: 174-184.
3. Salazar NC, Chen J, Rockman HA (2007) Cardiac GPCRs: GPCR signaling in healthy and failing hearts. Biochim Biophys Acta 1768: 1006-1018.
4. Insel PA, Tang CM, Hahntow I, Michel MC (2007) Impact of GPCRs in clinical medicine: monogenic diseases, genetic variants and drug targets. Biochim Biophys Acta 1768: 994-1005.
5. Wettschureck N, Moers A, Offermanns S (2004) Mouse models to study G-protein-mediated signaling. Pharmacol Ther 101: 75-89.
6. Offermanns S, Zhao LP, Gohla A, Sarosi I, Simon MI, et al. (1998) Embryonic cardiomyocyte hypoplasia and craniofacial defects in G alpha q/G alpha 11-mutant mice. Embo J 17: 4304-4312.
7. Takeda S, Kadowaki S, Haga T, Takaesu H, Mitaku S (2002) Identification of G protein-coupled receptor genes from the human genome sequence. FEBS Lett 520: 97-101.
8. Michel JJ, Scott JD (2002) AKAP mediated signal transduction. Annu Rev Pharmacol Toxicol 42: 235-257.
9. Langeberg LK, Scott JD (2005) A-kinase-anchoring proteins. J Cell Sci 118: 3217-3220.
10. Wong W, Scott JD (2004) AKAP signalling complexes: focal points in space and time. Nat Rev Mol Cell Biol 5: 959-970.
11. Kapiloff MS (2002) Contributions of protein kinase A anchoring proteins to compartmentation of cAMP signaling in the heart. Mol Pharmacol 62: 193-199.
12. Ruehr ML, Russell MA, Bond M (2004) A-kinase anchoring protein targeting of protein kinase A in the heart. J Mol Cell Cardiol 37: 653-665.

13. Mauban JR, O'Donnell M, Warrier S, Manni S, Bond M (2009) AKAP-scaffolding proteins and regulation of cardiac physiology. Physiology (Bethesda) 24: 78-87.

14. Carr DW, Stofko-Hahn RE, Fraser ID, Bishop SM, Acott TS, et al. (1991) Interaction of the regulatory subunit (RII) of cAMP-dependent protein kinase with RII-anchoring proteins occurs through an amphipathic helix binding motif. J Biol Chem 266: 14188-14192.

15. Carnegie GK, Means CK, Scott JD (2009) A-kinase anchoring proteins: from protein complexes to physiology and disease. IUBMB Life 61: 394-406.

16. Weiser DC, Pyati UJ, Kimelman D (2007) Gravin regulates mesodermal cell behavior changes required for axis elongation during zebrafish gastrulation. Genes Dev 21: 1559-1571.

17. Rubino D, Driggers P, Arbit D, Kemp L, Miller B, et al. (1998) Characterization of Brx, a novel Dbl family member that modulates estrogen receptor action. Oncogene 16: 2513-2526.

18. Diviani D, Soderling J, Scott JD (2001) AKAP-Lbc anchors protein kinase A and nucleates Galpha 12-selective Rho-mediated stress fiber formation. J Biol Chem 276: 44247-44257.

19. Carnegie GK, Smith FD, McConnachie G, Langeberg LK, Scott JD (2004) AKAP-Lbc nucleates a protein kinase D activation scaffold. Mol Cell 15: 889-899.

20. Diviani D, Abuin L, Cotecchia S, Pansier L (2004) Anchoring of both PKA and 14-3-3 inhibits the Rho-GEF activity of the AKAP-Lbc signaling complex. Embo J 23: 2811-2820.

21. Klussmann E, Edemir B, Pepperle B, Tamma G, Henn V, et al. (2001) Ht31: the first protein kinase A anchoring protein to integrate protein kinase A and Rho signaling. FEBS Lett 507: 264-268.

22. Vega RB, Harrison BC, Meadows E, Roberts CR, Papst PJ, et al. (2004) Protein kinases C and D mediate agonist-dependent cardiac hypertrophy through nuclear export of histone deacetylase 5. Mol Cell Biol 24: 8374-8385.

23. Carnegie GK, Soughayer J, Smith FD, Pedroja BS, Zhang F, et al. (2008) AKAP-Lbc mobilizes a cardiac hypertrophy signaling pathway. Mol Cell 32: 169-179.

24. Appert-Collin A, Cotecchia S, Nenniger-Tosato M, Pedrazzini T, Diviani D (2007) The A-kinase anchoring protein (AKAP)-Lbc-signaling complex mediates alpha1 adrenergic receptor-induced cardiomyocyte hypertrophy. Proc Natl Acad Sci U S A 104: 10140-10145.

25. Mayers CM, Wadell J, McLean K, Venere M, Malik M, et al. (2010) The Rho guanine nucleotide exchange factor AKAP13 (BRX) is essential for cardiac development in mice. J Biol Chem 285: 12344-12354.

26. Fielitz J, Kim MS, Shelton JM, Qi X, Hill JA, et al. (2008) Requirement of protein kinase D1 for pathological cardiac remodeling. Proc Natl Acad Sci U S A 105: 3059-3063.

27. Lin Q, Schwarz J, Bucana C, Olson EN (1997) Control of mouse cardiac morphogenesis and myogenesis by transcription factor MEF2C. Science 276: 1404-1407.

28. Offermanns S (2001) In vivo functions of heterotrimeric G-proteins: studies in Galpha-deficient mice. Oncogene 20: 1635-1642.

29. Offermanns S, Mancino V, Revel JP, Simon MI (1997) Vascular system defects and impaired cell chemokinesis as a result of Galpha13 deficiency. Science 275: 533-536.

30. Wei L, Imanaka-Yoshida K, Wang L, Zhan S, Schneider MD, et al. (2002) Inhibition of Rho family GTPases by Rho GDP dissociation inhibitor disrupts cardiac morphogenesis and inhibits cardiomyocyte proliferation. Development 129: 1705-1714.

31. Kaarbo M, Crane DI, Murrell WG (2003) RhoA is highly up-regulated in the process of early heart development of the chick and important for normal embryogenesis. Dev Dyn 227: 35-47.

32. Wettschureck N, Offermanns S (2005) Mammalian G proteins and their cell type specific functions. Physiol Rev 85: 1159-1204.

33. Ventura C, Zinellu E, Maninchedda E, Maioli M (2003) Dynorphin B is an agonist of nuclear opioid receptors coupling nuclear protein kinase C activation to the transcription of cardiogenic genes in GTR1 embryonic stem cells. Circ Res 92: 623-629.

34. Ventura C, Zinellu E, Maninchedda E, Fadda M, Maioli M (2003) Protein kinase C signaling transduces endorphin-primed cardiogenesis in GTR1 embryonic stem cells. Circ Res 92: 617-622.

35. Karamboulas C, Dakubo GD, Liu J, De Repentigny Y, Yutzey K, et al. (2006) Disruption of MEF2 activity in cardiomyoblasts inhibits cardiomyogenesis. J Cell Sci 119: 4315-4321.

36. Karamboulas C, Swedani A, Ward C, Al-Madhoun AS, Wilton S, et al. (2006) HDAC activity regulates entry of mesoderm cells into the cardiac muscle lineage. J Cell Sci 119: 4305-4314.

37. Grskovic M, Chaivorapol C, Gaspar-Maia A, Li H, Ramalho-Santos M (2007) Systematic identification of cis-regulatory sequences active in mouse and human embryonic stem cells. PLoS Genet 3: e145.

38. Hsiao EC, Yoshinaga Y, Nguyen TD, Musone SL, Kim JE, et al. (2008) Marking embryonic stem cells with a 2A self-cleaving peptide: a NKX2-5 emerald GFP BAC reporter. PLoS One 3: e2532.

39. Sterpetti P, Hack AA, Bashar MP, Park B, Cheng SD, et al. (1999) Activation of the Lbc Rho exchange factor proto-oncogene by truncation of an extended C terminus that regulates transformation and targeting. Mol Cell Biol 19: 1334-1345.

40. Ventura A, Meissner A, Dillon CP, McManus M, Sharp PA, et al. (2004) Cre-lox-regulated conditional RNA interference from transgenes. Proc Natl Acad Sci U S A 101: 10380-10385.

41. Wang R, Liang J, Jiang H, Qin LJ, Yang HT (2008) Promoter-dependent EGFP expression during embryonic stem cell propagation and differentiation. Stem Cells Dev 17: 279-289.

42. Donnelly ML, Luke G, Mehrotra A, Li X, Hughes LE, et al. (2001) Analysis of the aphthovirus 2A/2B polyprotein 'cleavage' mechanism indicates not a proteolytic reaction, but a novel translational effect: a putative ribosomal 'skip'. J Gen Virol 82: 1013-1025.

43. Osborn MJ, Panoskaltsis-Mortari A, McElmurry RT, Bell SK, Vignali DA, et al. (2005) A picornaviral 2A-like sequence-based tricistronic vector allowing for high-level therapeutic gene expression coupled to a dual-reporter system. Mol Ther 12: 569-574.

44. Gaspar-Maia A, Alajem A, Polesso F, Sridharan R, Mason MJ, et al. (2009) Chd1 regulates open chromatin and pluripotency of embryonic stem cells. Nature 460: 863-868.

45. Ying QL, Nichols J, Evans EP, Smith AG (2002) Changing potency by spontaneous fusion. Nature 416: 545-548.

46. Boheler KR, Czyz J, Tweedie D, Yang HT, Anisimov SV, et al. (2002) Differentiation of pluripotent embryonic stem cells into cardiomyocytes. Circ Res 91: 189-201.

47. Tingley WG, Pawlikowska L, Zaroff JG, Kim T, Nguyen T, et al. (2007) Gene-trapped mouse embryonic stem cell-derived cardiac myocytes and human genetics implicate AKAP10 in heart rhythm regulation. Proc Natl Acad Sci U S A 104: 8461-8466.

48. Liu Y, Asakura M, Inoue H, Nakamura T, Sano M, et al. (2007) Sox17 is essential for the specification of cardiac mesoderm in embryonic stem cells. Proc Natl Acad Sci U S A 104: 3859-3864.

49. Kodiha M, Tran D, Morogan A, Qian C, Stochaj U (2009) Dissecting the signaling events that impact classical nuclear import and target nuclear transport factors. PLoS One 4: e8420.

50. Hadjantonakis AK, Papaioannou VE (2004) Dynamic in vivo imaging and cell tracking using a histone fluorescent protein fusion in mice. BMC Biotechnol 4: 33.

51. Alexopoulou AN, Couchman JR, Whiteford JR (2008) The CMV early enhancer/chicken beta actin (CAG) promoter can be used to drive transgene expression during the differentiation of murine embryonic stem cells into vascular progenitors. BMC Cell Biol 9: 2.

52. Wadell JL, McLean, K., Driggers, P., Sarber, K., Jackson, R., Moorman, A., Westphal, H., Segars, J. Elucidation of the role of AKAP-Brx, an activator of RhoA, in murine cardiac morphogenesis.; 2006; Santa Fe, New Mexico. pp. 75.

53. Delaval B, Doxsey SJ (2010) Pericentrin in cellular function and disease. J Cell Biol 188: 181-190.

54. Levin MC, Monetti M, Watt MJ, Sajan MP, Stevens RD, et al. (2007) Increased lipid accumulation and insulin resistance in transgenic mice expressing DGAT2 in glycolytic (type II) muscle. Am J Physiol Endocrinol Metab 293: E1772-1781.

55. Rozen S, Skaletsky H (2000) Primer3 on the WWW for general users and for biologist programmers. Methods Mol Biol 132: 365-386.

56. Claycomb WC, Lanson NA, Jr., Stallworth BS, Egeland DB, Delcarpio JB, et al. (1998) HL-1 cells: a cardiac muscle cell line that contracts and retains phenotypic characteristics of the adult cardiomyocyte. Proc Natl Acad Sci U S A 95: 2979-2984.

57. Herker E, Harris C, Hernandez C, Carpentier A, Kaehlcke K, et al. (2010) Efficient hepatitis C virus particle formation requires diacylglycerol acyltransferase-1. Nat Med 16: 1295-1298.

58. Salomonis N, Schlieve CR, Pereira L, Wahlquist C, Colas A, et al. (2010) Alternative splicing regulates mouse embryonic stem cell pluripotency and differentiation. Proc Natl Acad Sci U S A 107: 10514-10519.

59. Dull T, Zufferey R, Kelly M, Mandel RJ, Nguyen M, et al. (1998) A third-generation lentivirus vector with a conditional packaging system. J Virol 72: 8463-8471.

Chapter 3

A-Kinase Anchoring Protein 13 Is Not Required for Angiogenic Processes in Human Umbilical Vein Endothelial Cells

3.1 Abstract

Background: Vascular endothelial growth factor (VEGF) regulates many aspects of angiogenesis by activating multiple downstream signaling molecules, including protein kinase D (PKD) and the small GTPase RhoA. VEGF induces expression of MEF2 responsive genes, cell migration, and tube formation through a protein kinase C (PKC), PKD, and histone deacetylase signaling cascade. VEGF activation of RhoA is also required for endothelial cell migration and tube formation. Interestingly, the scaffolding molecule A-kinase anchoring protein 13 (AKAP13) coordinates these two signaling cascades in cardiomyocytes and is expressed in endothelial cells. Additionally, *Akap13*-null mouse embryos die during embryonic development and display edema, which could be caused by vascular defects. However, it is unclear if AKAP13 coordinates the PKD and RhoA signaling cascades downstream of VEGF to regulate angiogenic processes.

Methodology/Principal Findings: To determine if AKAP13 coordinates PKD and RhoA signaling events during angiogenic processes, we knocked down AKAP13 expression in human umbilical vein endothelial cells (HUVECs) by RNAi. Surprisingly, we found that AKAP13-deficient HUVECs maintained normal

cell size and shape, tube formation, and VEGF-induced wound healing. Additionally, these HUVECs had normal levels of PKD phosphorylation in response to VEGF stimulation. Finally, we found that the AKAP13 RhoA-specific guanine nucleotide exchange factor (Rho-GEF) and PKC-PKD binding domains were not required for mouse developmental angiogenesis or basal vascular function.

Conclusions: These results suggest that AKAP13 does not coordinate endothelial cell angiogenesis or VEGF-induced signaling. However, the roles of AKAP13 in mediating endothelial cell responses to stresses remain unknown.

3.2 Introduction

Endothelial cells play important roles in development, physiology, and pathology of the cardiovascular system. The formation of blood vessels during embryonic development by vasculogenesis and angiogenesis requires proper endothelial cell interaction with the extracellular matrix, migration, and formation of vascular tubes. Vasculogenesis and angiogenesis are also important during wound healing and tissue regeneration and can be hijacked to promote tumor growth [1,2,3].

Vascular endothelial growth factor (VEGF) appears to be a master regulator of these physiological and pathological processes [4,5]. For example, VEGF and both the VEGF receptors, Flt-1 (VEGFR-1) and Flk-1 (VEGFR-2), are required for proper blood vessel formation and embryo survival during mouse

development [6,7,8,9]. VEGF activates multiple intracellular signaling molecules, including protein kinase D (PKD) [10] and the small GTPase RhoA [11] in endothelial cells (Figure 3.1 A). Furthermore, disruption of either the PKD or RhoA signaling cascades reduces VEGF-mediated angiogenesis *in vitro* and *in vivo* [11,12,13,14].

Similar to VEGF, PKD is required for mouse embryonic development [15], and PKD mediates VEGF-induced endothelial cell proliferation, migration, and tube formation [10,14,16]. VEGF activates PKD through a signaling cascade that contains the receptor, VEFGR-2, phospholipase Cγ (PLCγ), and protein kinase C (PKC) [10]. Activated PKD then phosphorylates class II histone deacetylase 5 (HDAC5) and 7 (HDAC7) causing their association with the chaperone protein 14-3-3 and relocation out of the nucleus into the cytoplasm [12,17]. This decrease in nuclear class II HDACs is required for VEGF-induced endothelial cell migration and tube formation, as well as the induced expression of myocyte enhancer factor-2 (MEF2)-responsive genes [12,17].

The Rho family of small GTPases also regulates multiple aspects of angiogenesis and vascular barrier integrity by regulating cytoskeletal changes [18,19]. RhoA, one member of this family, is required for embryonic development [20] and regulates multiple aspects of angiogenesis including barrier function, interaction with the extracellular matrix, migration, proliferation, and morphogenesis [19]. Moreover, RhoA signaling is required for normal VEGF-induced endothelial cell migration and tube formation through Rho-associated kinases (ROCK) [11,13,21]. Thus, it appears that PKD and RhoA have

complementary functions during angiogenesis, possibly by regulating gene expression and the cytoskeleton, respectively.

Despite the requirement for PKD and RhoA signaling in propagating VEGF-induced angiogenesis, little is known about the molecules that regulate and control these signaling cascades. It is also unclear if the PKD and RhoA pathways interact during angiogenesis. Proper control of these signaling pathways is essential for downstream specificity. Scaffolding molecules, such as A-kinase anchoring proteins (AKAPs), provide this needed specificity by organizing multi-protein signaling complexes at specific locations within the cell [22]. The diverse AKAP family is defined by the ability to bind protein kinase A (PKA); however, these scaffolds also bind many other signaling molecules, including PKC and PKD [22,23]. Furthermore, the signaling complexes organized by AKAPs regulate a wide variety of processes, including development, fertility, learning and memory, and cardiac physiology [23]. Additionally, AKAPs can regulate cytoskeletal organization at least in part by regulating the activity of small GTPases [24,25]. Finally, AKAPs are important in regulating endothelial cell migration and barrier function in response to specific stimuli [26,27]. This suggests that AKAPs could regulate VEGF-induced angiogenesis.

The signaling molecules used by VEGF during angiogenesis could be organized into a signaling complex by AKAP13. AKAP13 binds PKC, PKD, and the chaperone protein 14-3-3 [28,29] and coordinates a PKC-PKD-HDAC signaling cascade to regulate MEF2 gene expression and hypertrophy in cardiomyocytes (Figure 3.1 B) [30]. This AKAP13 coordinated signaling pathway

is strikingly similar to the cascade induced by VEGF in endothelial cell. AKAP13 also functions as a Rho-specific guanine nucleotide exchange factor (Rho-GEF) to activate RhoA [31,32], which can then induce stress fiber formation in fibroblasts [31] and hypertrophy in cardiomyocytes [33]. Finally, *Akap13*-null mice die during embryonic development and exhibit hemorrhaging, which could be due to vascular defects [34]. Thus, AKAP13 could coordinate the VEGF-induced PKC-PKD and Rho signaling pathways during angiogenesis.

In this study, we hypothesized that AKAP13 coordinates PKD and RhoA signaling pathways downstream of VEGF to regulate endothelial cell processes important for angiogenesis. To test this hypothesis, we used RNA interference (RNAi) to knockdown AKAP13 expression in HUVECs. We then assessed these AKAP13-deficient HUVECs for the ability to attach to several extracellular matrices, "heal" a scratched wound, spread on matrices, and form tubes. We also assessed these cells for their ability to activate PKD in response to VEGF treatment.
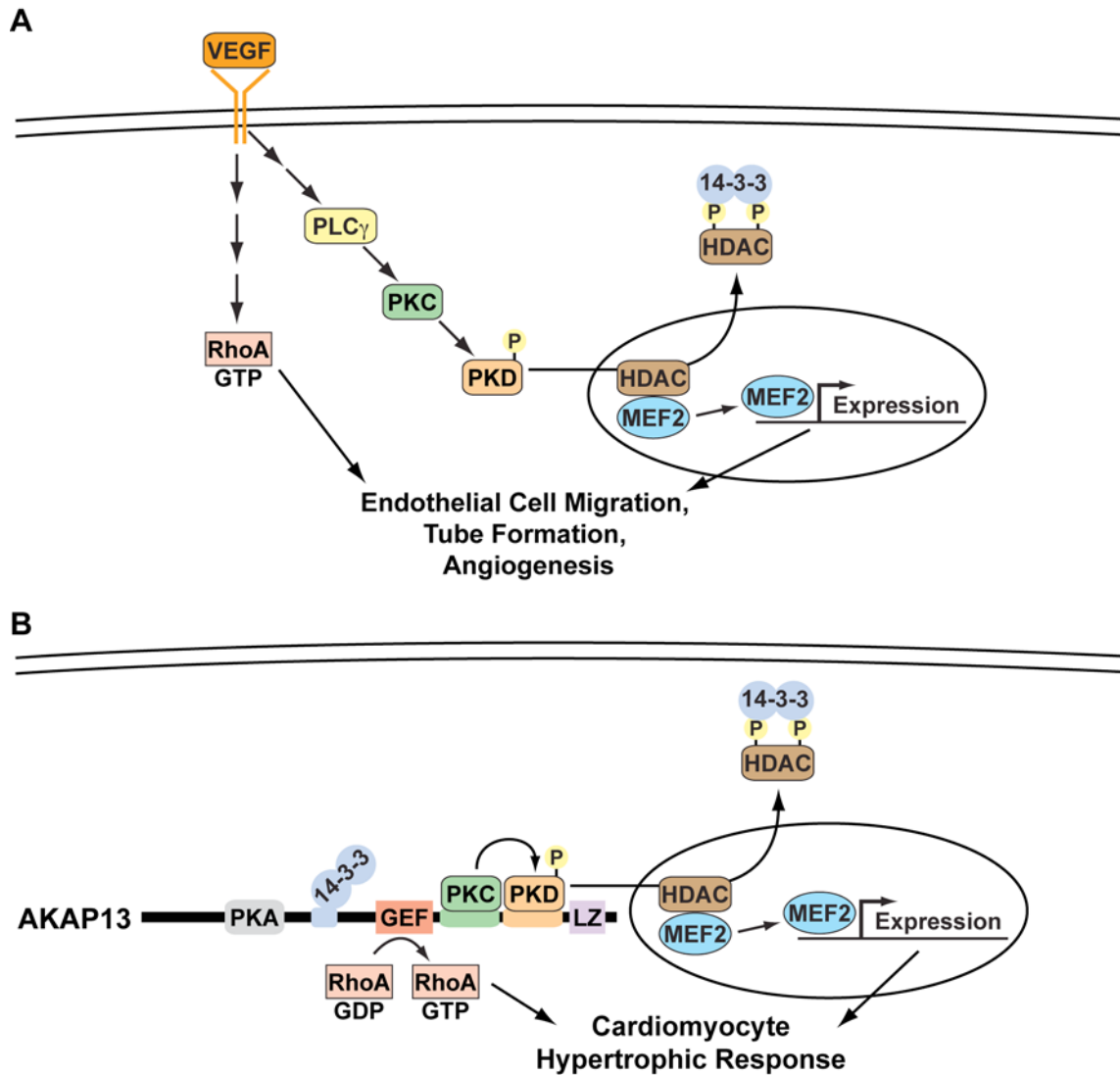
Figure 3.1. Models of VEGF-induced angiogenesis and AKAP13-coordinated signaling pathways. (A) VEGF signals through a PLC-PKC-PKD-HDAC-MEF2 signaling cascade and RhoA to induce endothelial cell migration, tube formation, and angiogenesis. (B) AKAP13 organizes the same signaling molecules into a complex in cardiomyocytes to regulate hypertrophy. AKAP13 binds PKA, PKC, PKD, and 14-3-3 to regulate HDAC localization and MEF2 transcriptional activity and functions as a RhoA-specific GEF. P = phosphorylation event; LZ = leucine zipper.

3.3 Results

3.3.1 AKAP13 is expressed in endothelial cells of embryonic and adult mice.

To determine if AKAP13 is expressed in endothelial cell types of the mouse, we conducted X-Gal staining on three AKAP13 gene-trap mouse lines derived in our lab (see Chapter 4). The gene-trap construct uses a strong splice acceptor to fuse endogenous AKAP13 mRNA with the trapping cassette [35]. This gene-trap event creates a fusion protein that contains the amino-terminus of AKAP13 fused to the βGeo cassette (β-galactosidase and neomyocin resistance). Thus, the gene-trap mouse lines report the expression pattern of AKAP13 because the endogenous AKAP13 promoters drive expression of the fusion protein. All three AKAP13 gene-trap mouse lines generated had strong X-Gal staining throughout the embryonic heart, including the endocardium, trabeculea, aorta and pulmonary artery (Figure 3.2 A), as well as in peripheral vasculature, umbilical cords, and yolk sac (not shown). In the adult heart, the atrial-ventricular and aortic valves, as well as the aorta and pulmonary artery, were X-Gal positive (Figure 3.2 B). Finally, the vasculature surrounding the adult brain clearly showed X-Gal staining (Figure 3.2 C). These results show that AKAP13 is expressed in endothelial cells of the developing heart and vasculature of mouse embryos. They also show that AKAP13 is expressed in endothelial cells of the adult mouse heart and vasculature.
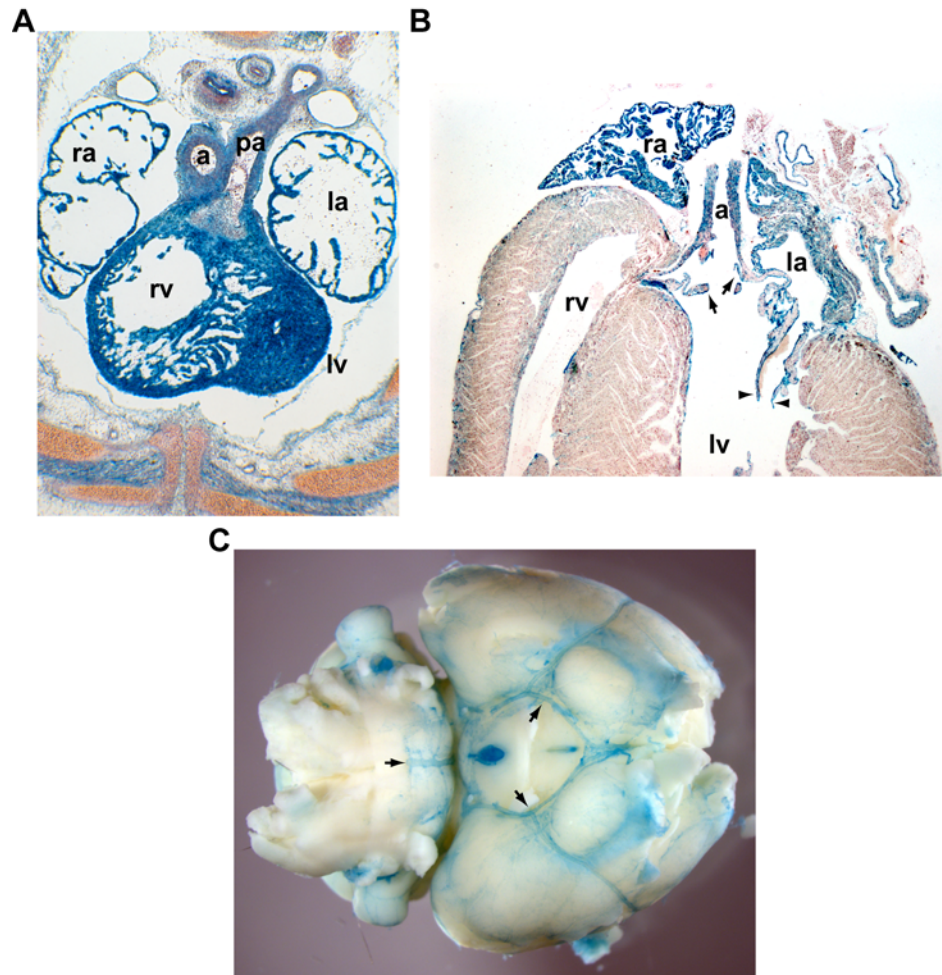
Figure 3.2. AKAP13 is expressed in mouse embryonic and adult endothelial cells.
(A) A transverse section of an E14.5 mouse (CSJ306) showing a four-chamber view of
the heart stained with X-Gal (in blue). X-Gal staining was evident in the myocardial and
endocardial layers of all four chambers of the heart: right atrium (ra), right ventricle (rv),
left atrium (la), and left ventricle (lv). Additionally, the aorta (a) and pulmonary artery (pa)
stained positive. All three gene-trap mouse lines gave the same staining pattern; a
representative image is shown. (B) An adult mouse heart (CSJ288) was stained with X-
Gal in whole mount and sectioned. The leaflets of the aortic (arrows) and atrial-
ventricular (arrowheads) valves were X-Gal positive. The aorta (a) was also positive, as
were the right and left atria (ra and la, respectively). Unlike the adult hearts from CSJ288
mice, hearts from both the AG0213 and CSJ306 mice had ventricular myocardial
staining (see chapter 4). (C) A view of the base of a whole-mount X-Gal-stained adult
brain (AG0213). The vasculature surrounding the brain stained positive (arrows) and the
same staining pattern was seen in all three mouse lines.

3.3.2 AKAP13 can be efficiently knocked down in HUVECs with RNAi.

Despite the expression of AKAP13 in endothelial cells, nothing is known about its function in these cells. Since AKAP13 binds multiple protein kinases (PKA, PKC & PKD) and encodes for a Rho-GEF domain, it could regulate endothelial cell physiology, such as angiogenesis, migration, or cytoskeletal organization [10,11,14,18]. To determine if AKAP13 is important for regulating endothelial cell physiology, we knocked down AKAP13 expression in HUVECs using small interfering RNAs (siRNAs). Silencer siRNAs 1475 & 1569 (from Ambion) knocked down AKAP13 mRNA expression in HUVEC cells to 30% and 33% of control levels, respectively (Figure 3.3). This shows that both siRNAs knock down AKAP13 expression to the same level in HUVECs.
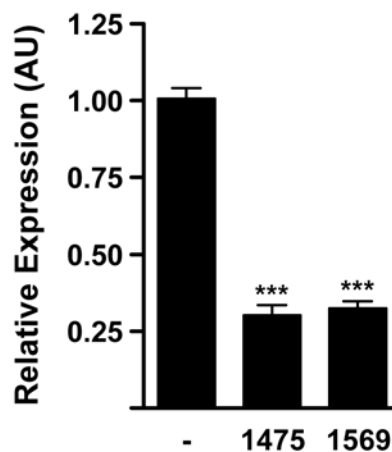
Figure 3.3. siRNA knocked down AKAP13 expression in HUVECs. Quantitative PCR using TaqMan probe sets showed that siRNAs targeting AKAP13 (1475 and 1569) efficiently decreased expression as compared to a negative control, siRNA #1 (-). Means and standard deviations are graphed (n=2). One-way ANOVA and Tukey's multiple comparision tests were conducted (Prism 5; GraphPad). ***, $p < 0.001$.

3.3.3 AKAP13 is not required for HUVEC attachment or wound healing.

Many cellular processes are necessary for angiogenesis, including the attachment and detachment of cells to extracellular matrix, cell-cell adhesion, proliferation, migration, and cytoskeletal organization. Both RhoA and PKD are required for VEGF-induced angiogenesis [11,14], and AKAP13 coordinates signaling pathways to activate both molecules [28,32]. In addition, RhoA signaling is required for normal levels of VEGF-induced wound healing in human microvascular endothelial cells [21]; however, the upstream Rho-GEFs involved are unknown. Thus, we investigated the role of AKAP13 in mediating aspects of endothelial cell angiogenesis and wound healing in AKAP13 knockdown HUVECs.

To assess the ability of AKAP13-deficient HUVECs to attach to various extracellular matrices, we plated them onto tissue-culture wells coated with Matrigel, fibronectin, or gelatin, and counted the number of cells attached after 15, 30, and 60 minutes. AKAP13-deficient HUVECs had normal numbers of cells attached to these extracellular matrices at all time points (Figure 3.4). These results show that AKAP13 is not required for HUVEC attachment to multiple extracellular matrices.

To determine if AKAP13-mediated signaling regulates VEGF-induced proliferation and migration, we used a scratch, wound healing, assay. In this assay, serum-starved HUVEC monolayers were scratched to create a wound, treated with VEGF, and assessed for wound closure. AKAP13 siRNA did not affect HUVEC proliferation and migration into the wound as the scratches closed

normally (Figure 3.5). This result shows that AKAP13-mediated RhoA signaling is

not required for VEGF-induced wound healing in HUVECs.
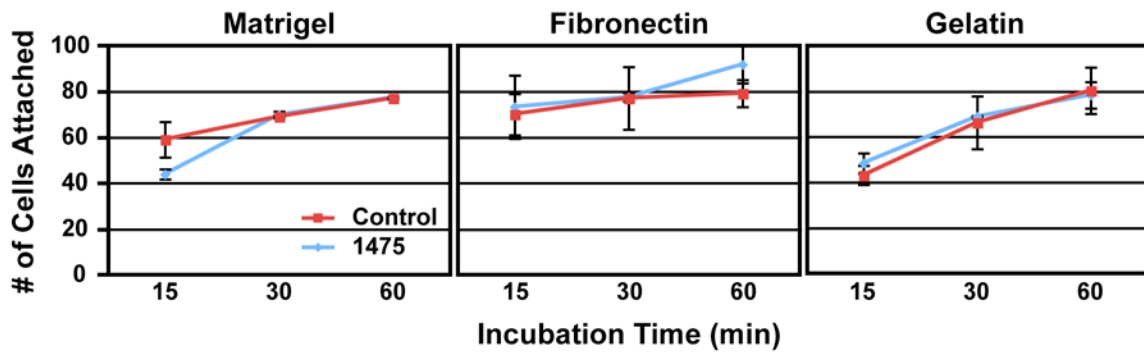
Figure 3.4. AKAP13 is not required for HUVEC attachment to extracellular matrices. HUVECs, transfected with negative control (Control) or AKAP13 (1475) siRNA, were plated onto tissue-culture wells coated with Matrigel, fibronectin, or gelatin. The number of cells attached to each extracellular matrix was counted at 15, 30, and 60 minutes. HUVECs transfected with AKAP13 siRNA 1475 attached to the matrices in the same manner as the Control siRNA. Means and standard deviations are graphed (n=2).
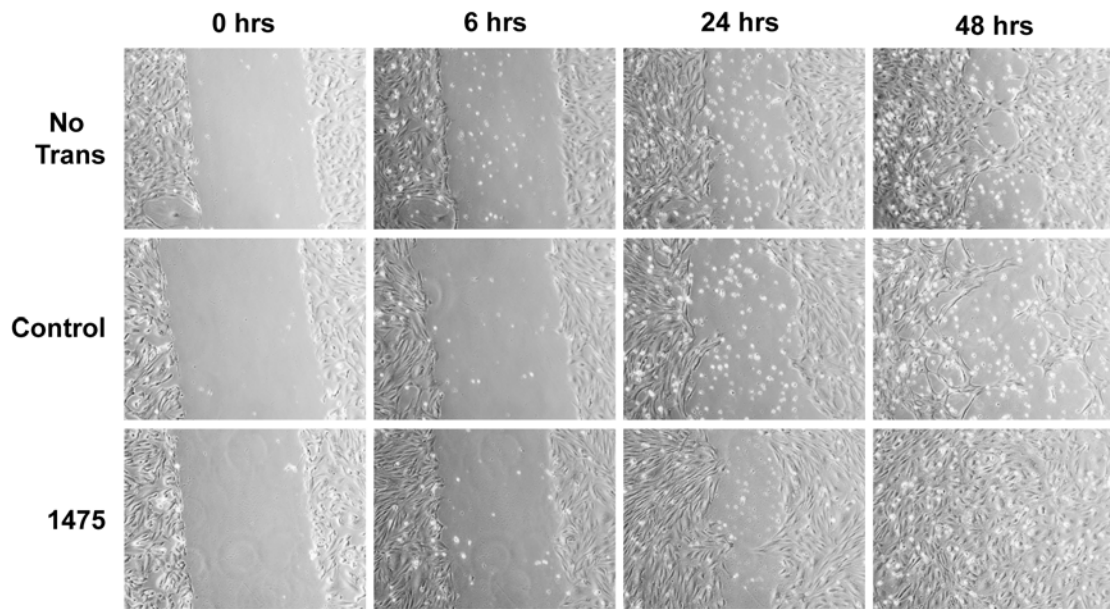
Figure 3.5. AKAP13 is not required for HUVEC wound healing. Representative images of scratched HUVEC monolayers cultured in VEGF-containing medium at 0, 6, 24, and 48 hours post-scratch. HUVECs transfected with the AKAP13 siRNA 1475 closed the scratch similarly to the no transfection (No Trans) and negative control (Control) samples (n=2).

3.3.4 AKAP13 is not required for HUVEC spreading or tube formation.

To determine if AKAP13-mediated RhoA signaling regulates basal cell spreading in endothelial cells, AKAP13-deficient HUVECs were cultured on fibronectin or Matrigel and stained with phalloidin to mark actin. RhoA activation causes cytoskeletal rearrangements that lead to endothelial cell contraction [18]. Thus, we expected that AKAP13 knockdown would lead to larger cellular areas. Despite equal levels of AKAP13 knockdown, only the 1475 siRNA, but not the 1569 siRNA, increased the cellular area of HUVECs attached to fibronectin and Matrigel by 34% and 26%, respectively, compared to a control siRNA (Figure 3.6). Additionally, the 1475 siRNA-transfected cells (Figure 3.6 B) appeared to be less polarized as fewer cells displayed the elongated cell shape seen in the control cells (Figure 3.6 A). In contrast, the second AKAP13 siRNA, 1569, did not change cellular area on these matrices, and the cell shape remained normal (Figure 3.6 C & D). These results indicate that the 1475 siRNA has off-target effects that change cell size and shape, since the second AKAP13 siRNA, 1569, did not reproduce these phenotypes. Thus, the 1569 siRNA results show that AKAP13 does not regulate basal HUVEC cell spreading or shape.
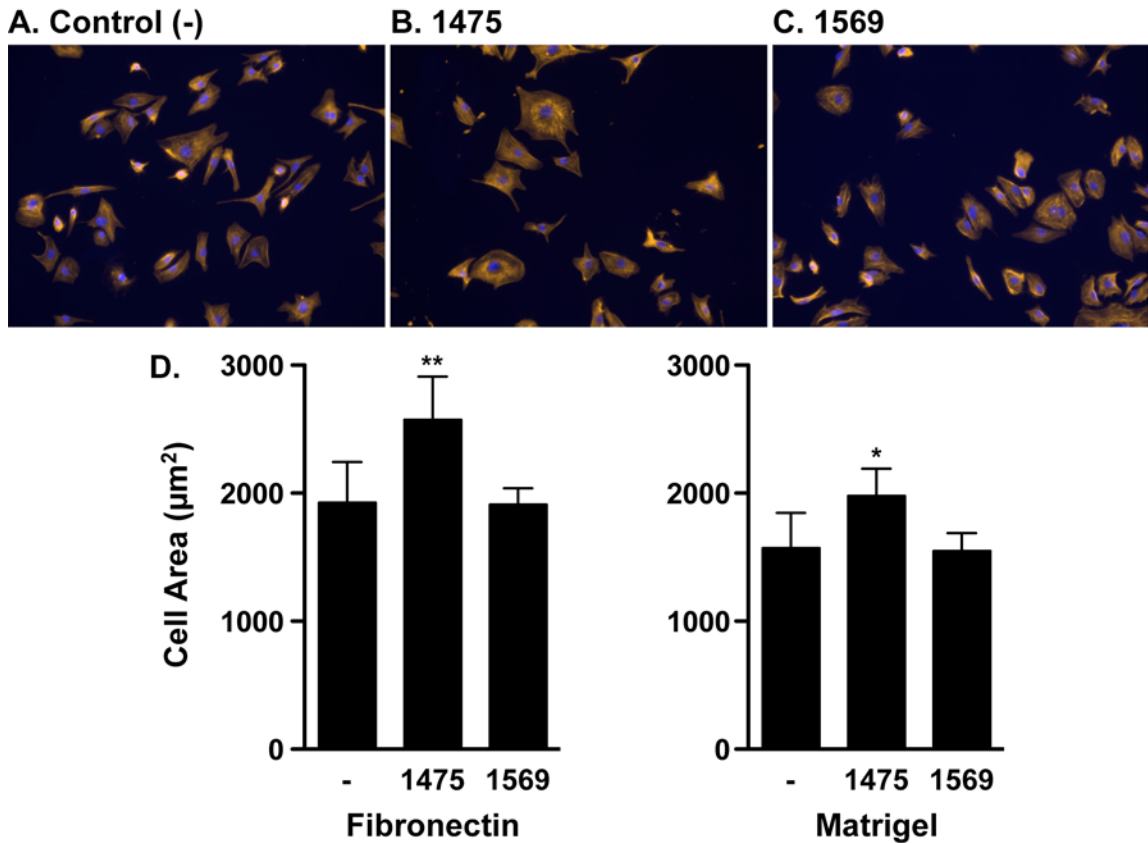
Figure 3.6. AKAP13 is not required for normal HUVEC cell spreading or shape. (A–C) Representative images of HUVECs plated onto fibronectin and stained with rhodamine-phalloidin to mark actin (orange) and DAPI to mark nuclei (blue). (D) Cell area (in square micrometers) was quantified for HUVECs transfected with a negative control siRNA (-) or AKAP13 siRNAs 1475 or 1569. The 1475 siRNA increases cell area on both fibronectin and Matrigel; however, 1569 does not. Means and standard deviations are graphed (-, n=10; 1475, n=8; 1569, n=4). *, $p < 0.05$; **, $p < 0.01$.

We then asked if AKAP13 was required for proper tube formation. To address this, we plated AKAP13-deficient onto a thick layer of Matrigel and monitored the tube formation process by microscopy. Tube formation was slightly delayed by the 1475 siRNA as compared to the control siRNA sample (Figure 3.7). At 24 hours, these tubes lacked cellular bodies at the nodes and appeared to have clumps of cells attached to the tubes. Again, the second AKAP13 siRNA, 1569, did not confirm this phenotype; the tubes that formed from the 1569 siRNA sample were indistinguishable from the control. Similar to the cell spreading results, these results indicate that the 1475 siRNA has off-target effects on HUVEC tube formation. Thus, the 1569 results show that AKAP13 is not necessary for HUVEC tube formation.
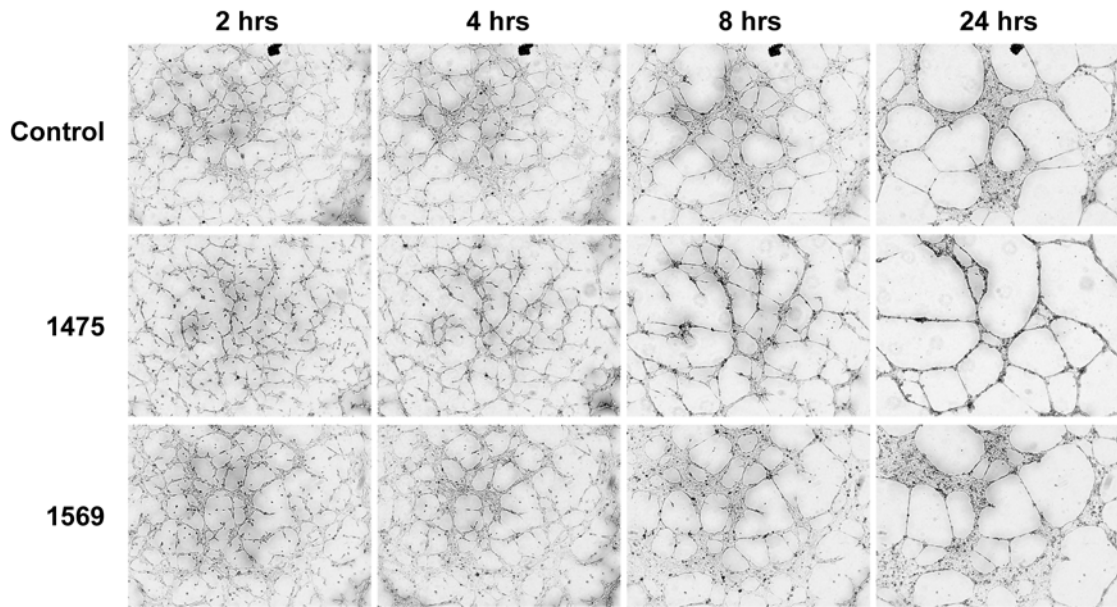
Figure 3.7. AKAP13 is not required for HUVEC tube formation. HUVECs were transfected with a negative control siRNA (Control) or siRNAs against AKAP13 (1475 & 1569). 48-hours post-transfection, these cells were resuspended, counted, and plated onto a thick layer of Matrigel. Tube formation was monitored by microscopy at 2, 4, 8, and 24 hours post-plating. Tube formation was identical in the Control and 1569 siRNA samples. Representative images are shown (control and 1475, n=4; 1569, n=2).

3.3.5 AKAP13 does not coordinate VEGF activation of PKD in HUVECs.

The experiments and results described above indicate that AKAP13 is not required for angiogenic processes or VEGF-induced wound healing in HUVECs. However, they did not directly test whether AKAP13 mediates VEGF activation of PKD. To determine if VEGF signals through AKAP13 to activate PKD, we conducted a VEGF signaling assay in AKAP13-deficient HUVECs. Control and 1475 siRNA-transfected HUVECs were serum starved overnight and stimulated with a vehicle control (0), 5, or 20 ng/mL of VEGF-165 or the positive control, phorbol 12-myristate 13-acetate (PMA; 100 nM) for 15 minutes. Total and phosphorylated PKD was then measured by western blotting. The phosphorylation of PKD in response to VEGF stimulation was unaffected by AKAP13 siRNA (Figure 3.8). PKD was not phosphorylated in HUVECs treated with vehicle control (0) at either the PKC phosphorylation site (S744/748) [36] or the autophosphorylation site (S916) [37]. VEGF treatment increased phosphorylation at both of these sites in a dose-dependent manner, and the extent of phosphorylation was equivalent in control and AKAP13-deficient HUVECs. Similarly, PMA treatment increased PKD phosphorylation to similar levels in both control and AKAP13-deficient HUVECs. Finally, total PKD and α-actin expression was equivalent in all samples. These results show that AKAP13 does not coordinate VEGF-induced phosphorylation of PKD in HUVECs. Furthermore, they suggest that VEGF does not signal through AKAP13 to activate PKD.
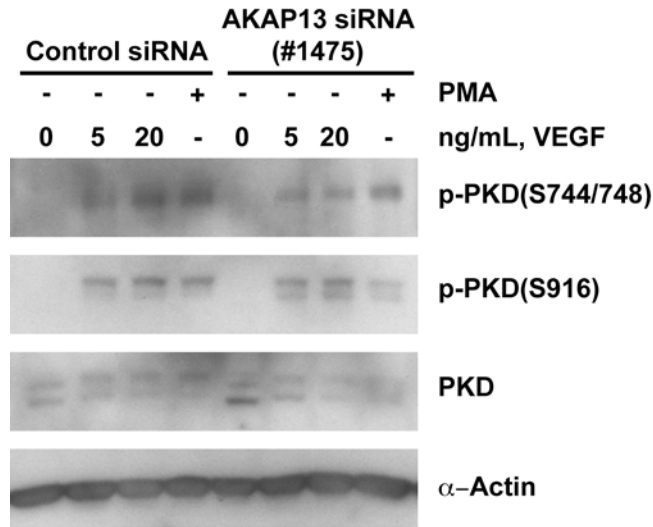
Figure 3.8. AKAP13 does not coordinate VEGF activation of PKD in HUVECs.
HUVECs were transfected with negative control (Control siRNA) or AKAP13 (#1475)
siRNA. Cells were serum starved over night and treated with vehicle control (0), 5 or 20
ng/mL VEGF-165, or 100 nM PMA (positive control) for 15 minutes. Total cell lysates
were probed for phospho-PKD (p-PKD) at S744/748 and S916, total PKD, and α-Actin.
VEGF-165 and PMA increased p-PKD to the same extent in Control and 1475 siRNA
HUVECs. Total PKD and α-Actin blots show that equivalent amounts of protein
were loaded into each lane.

3.4 Discussion

In this study, we investigated the role of AKAP13 in coordinating PKD and RhoA signaling pathways downstream of VEGF to regulate endothelial cell processes important for angiogenesis. Our results show that AKAP13 is not required for processes important for angiogenesis, including basal HUVEC physiology, tube formation, or VEGF-induced wound healing and PKD activation. We found that AKAP13 is strongly expressed in endothelial cells of the developing and adult mouse cardiovascular system, as well as in HUVECs. However, knockdown of AKAP13 in HUVECs did not affect the ability of these cells to attach to various extracellular matrices, proliferate and migrate into a scratched cell monolayer, or maintain normal cell size and shape. Additionally, AKAP13-deficient HUVECs formed tubes and activated PKD in response to VEGF stimulation normally.

Contrary to our expectations that AKAP13 coordinates PKD and RhoA activity to mediate aspects of developmental angiogenesis, we found that AKAP13 is not required for these processes *in vitro* or *in vivo*. *Akap13*-null mice die during embryonic development around E9.5 and display pericardial edema [34]. However, it is unclear if the cause of death is due to cardiac or vascular defects since AKAP13 is expressed in both tissues. Given the edema phenotype, the vasculature of these developing embryos might be defective. In agreement with this, RhoA [11] and PKD [14] signaling events are required for angiogenesis. Since AKAP13 can coordinate both of these signaling pathways, we expected that AKAP13 knockdown would disrupt angiogenesis. However, our results show that AKAP13 is not required for multiple angiogenic processes or tube formation

in HUVECs. Furthermore, mutant mice that lack the Rho-GEF and PKC-PKD

binding domains of AKAP13 develop normally and are viable (see Chapter 4).

These results indicate that AKAP13 does not regulate developmental

angiogenesis or basal vascular function. However, AKAP13 might function during

pathological or regenerative angiogenesis, and it would be interesting to test for

AKAP13 function in these models.

We also found that AKAP13 was not required for VEGF-induced closure of a

scratched wound or activation of PKD. The VEGF-induced wound healing assay

was used as a surrogate for proliferation and migration. This disproves our

hypothesis that AKAP13 regulates RhoA and PKD signaling events downstream

of VEGF. This finding was surprising because AKAP13 coordinates signaling

pathways in cardiomyocytes that are very similar to those activated by VEGF in

endothelial cells (Figure 3.1). Thus, AKAP13 was a prime candidate for

regulating PKD and RhoA signaling pathways in endothelial cells as well. Since

VEGF-induced proliferation and migration were resistant to AKAP13 knockdown,

other Rho-GEFs must activate RhoA to induce these processes. One of the Rho-

GEFs that mediate VEGF signaling is the synectin-binding guanine exchange

factor, Syx. Syx regulates angiogenesis in zebrafish and mice [38,39] and was

required for VEGF-induced migration and tube formation in rat fat-pad endothelial

cells [39]. Other Rho-GEFs likely have similar and redundant functions in

endothelial cells, since the Syx mutant mice survive normally and display a

specific, but not complete, decrease in secondary artery and capillary numbers.

Further investigation is needed to identify the additional Rho-GEFs that regulate

developmental angiogenesis. It also is unclear if scaffolding molecules are required to mediate VEGF-induced PKD activation. A more complete assessment of the AKAPs and other signaling scaffolds expressed in endothelial cell is required to identify potential proteins that could regulate this process. Finally, it is unclear if VEGF-induced migration requires the interaction of RhoA and PKD signaling pathways or if these pathways regulate independent processes.

The lack of an *in vitro* angiogenesis or motility phenotype or an obvious *in vivo* developmental defect indicates that AKAP13 is not required for normal vascular development. Additionally, AKAP13 mutant mice that lacked the Rho-GEF and PKC-PKD binding domains did not display vascular leak or hemorrhaging (see Chapter 4), indicating that AKAP13 does not regulate endothelial cell-cell junctions or barrier function under normal conditions. These results suggest that AKAP13 might function in regulating endothelial cell responses to extracellular signals and stresses.

One of the most intriguing roles AKAP13 might play in endothelial cell signaling and stress responses is in regulating cell-cell junctions and vascular permeability. Rho GTPases dynamically regulate endothelial cell barrier formation and permeability, and RhoA signaling can strengthen or disrupt endothelial barriers depending on the signaling context [18]. Thrombin is a well-known inducer of endothelial permeability through the activation of RhoA signaling [40], which mediates endothelial cell contraction and disruption of cell-cell junctions [41]. The thrombin receptor, protease-activated receptor-1 (PAR1),

couples to the G-protein pathways $G\alpha_{12/13}$ and $G\alpha_{q/11}$ to activate Rho-GEFs and calcium signaling which interact to coordinate the multiple processes required for endothelial permeability [42]. Interestingly, AKAP13 is a convergence point for $G\alpha_{12/13}$ [31,33] and $G\alpha_{q/11}$ [28] signaling in cardiomyocytes, and it could organize this interaction in endothelial cells as well. It would be interesting to determine if the AKAP13 Rho-GEF and PKC-PKD deficient mice have reduced vascular permeability in response to thrombin treatment. AKAP13 might also function to regulate crosstalk between RhoA [21] and PKC-PKD [14] signaling during VEGF-induced endothelial permeability. Thus, it would also be interesting to determine the level of VEGF-induced vascular permeability in AKAP13 mutant mice.

We identified AKAP13 expression in the vasculature of the mouse and focused this study on the roles of AKAP13 in endothelial cell biology. Given the vascular expression, it is intriguing to consider the broader roles AKAP13 might play in mediating signaling events that regulate vascular biology and disease. The signaling molecules endothelin-1 (ET-1) and angiotensin II (Ang II) regulate physiological vasoconstriction and inflammation, as well as pathological endothelial dysfunction and vascular disease [43,44,45]. The signaling pathways induced by ET-1 and Ang II are transduced by AKAP13 in isolated cardiomyocytes to activate hypertrophic gene expression [30,33]. Thus, these signaling pathways could also be transduced by AKAP13 in endothelial and vascular smooth muscle cells. Future experiments should focus on the role of AKAP13 in coordinating ET-1 and Ang II signaling in these cell types. In addition, the mutant AKAP13 mice described in Chapter 4 could be used to delineate the

role of AKAP13 in regulating vasoconstriction and endothelial dysfunction *in vivo*. These studies might be confounded because of the high level of AKAP13 expression throughout the cardiovascular system and additional tissues; thus, tissue specific disruption of AKAP13 may be required.

In conclusion, we found that AKAP13 is not required for processes important for angiogenesis, including basal HUVEC physiology, tube formation, or VEGF-induced wound healing and PKD activation. We also found that mice lacking the Rho-GEF and PKC-PKD binding domains of AKAP13 have normal survival (see Chapter 4). These findings suggest that other scaffolding molecules regulate endothelial cell physiology and developmental angiogenesis under normal conditions possibly in redundancy to AKAP13. They also suggest that other Rho-GEFs and scaffolding molecules coordinate VEGF-induced RhoA and PKD activation. Finally, the role of AKAP13 in coordinating endothelial cell responses to specific signaling events remains unknown. The HUVEC system described here and the mouse models described in Chapter 4 are ideal systems to investigate the possible functions of AKAP13 in mediating endothelial cell and vascular responses to stresses, including thrombin, VEGF, ET-I, and Ang II.

3.5 Materials and Methods

X-Gal staining of gene-trap embryos and adult tissue

To identify AKAP13 expression patterns during development and in adult tissue, cryosectioned E14.5 embryos and whole adult organs were stained with X-Gal. E14.5 embryos were bisected and fixed in 4% paraformaldehyde (PFA; Sigma) and 0.2% glutaraldehyde (Sigma) in PBS (Mediatech) for 1 hour at 4°C. The embryos were sucrose protected and frozen in Tissue-Tek OCT (Sakura Finetek). Cryostat sections were stained with X-Gal (Fermentas, AllStar Scientific, and Invitrogen), mounted, and imaged with an upright Leica DM4000B microscope with a QImaging Retiga EXi Fast 1394 camera and Image-Pro Plus software.

Adult organs were obtained from euthanized 17–18-week-old mice. Euthanized mice were perfused with 10 mM KCl (Sigma), then PBS, and finally 4% PFA. Heart and brain samples were bisected, and organs were fixed in 4% PFA for 1 hour at 4°C. Organs were permeabilized in 2 mM $MgCl_2$ (Sigma), 0.01% sodium deoxycholate (Sigma), and 0.02% Nonidet P-40 Substitute (Fluka) in PBS at 4°C overnight. Samples were stained in 5 mM potassium ferricyanide (Sigma), 5 mM potassium ferrocyanide (Sigma), 2 mM $MgCl_2$, 0.01% sodium deoxycholate, and 0.02% Nonidet P-40 Substitute, and 1 mg/mL X-Gal in PBS at 37°C. Organs were post-fixed in 4% PFA at 4°C overnight. The heart sample was embedded in paraffin, sectioned, counter stained with neutral red, and imaged using an upright Leica DM4000B microscope with a QImaging Retiga EXi Fast 1394 camera and Image-Pro Plus software. The brain sample was imaged using

121

a Leica MZ FLIII dissecting microscope with an AxioCam (Carl Zeiss) camera and Openlab 4.0.4 software.

HUVEC culture

HUVECs were purchased from ScienCell and cultured following the manufacturer's protocols with slight modifications. In brief, cells were seeded onto 0.1% gelatin (Sigma) coated tissue culture plates and cultured in complete ECM medium: endothelial cell medium (ECM; ScienCell Cat. #1001) supplemented with 5% FBS (Cat. #0025), endothelial cell growth supplement (ECGS; Cat. #1052; containing 10 μg/mL BSA, 10 μg/mL apo-transferrin, 5 μg/mL insulin, 10 ng/mL EGF, 2 ng/mL FGF-2, 2 ng/mL VEGF, 2 ng/mL IGF-I, 1 μg/mL hydrocortisone, and 10^{-7} M retinoic acid), and penicillin/streptomycin (P/S: Cat. #0503). Cells were detached from culture plates with TrypLE (Gibco) and passaged at a 1:10 dilution every 3–4 days.

Transfection of HUVECs with Stealth RNAi

The day before transfection, HUVECs were seeded into gelatinized 6-well plates at 3 x 10^5 cells per well and cultured in complete ECM. RNAi Max transfection reagent (Invitrogen) was used to transfect HUVECs with Silencer siRNAs (Ambion) that target AKAP13: siRNA IDs 1475 (5'-GGA GAA GGA GAA AGA UUC Utt-3') and 1569 (5'-GGA GAA AGA UUC UAA AGA Ctt-3') or Silencer Negative Control #1 siRNA (Ambion; Cat. #AM4611) as reported [46]. In brief, 5 μL of RNAi Max and 64 pmol of Silencer siRNA were mixed with OptiMEM I

Reduced Serum Medium (Invitrogen) for a total volume of 2.5 mL, and this was added to the previously seeded HUVECs (at about 90% confluency). HUVECs were incubated in the Silencer siRNA-OptiMEM medium for 6–8 hours at 37°C and subsequently fed with complete ECM. All assays were conducted 48 hours post-transfection of Silencer siRNAs.

Quantitative PCR analysis

Gene expression analysis was preformed on total RNA isolated from HUVEC cultures. Samples were homogenized in Trizol (Invitrogen), and cDNA was synthesized from DNase Turbo (Ambion) treated RNA with SuperScript III RT-PCR kit and random hexamers (Invitrogen) as described by the manufacturers. Expression was assessed using TaqMan probesets (Applied Biosystems) for AKAP13 (Hs00180747_m1), β-Actin (Hs00963193_m1), GAPDH (Hs99999905_m1), and TATA-binding protein (TBP; Hs00427620_m1).

Reactions were run on an Applied Biosystems 7900HT real-time thermocycler. Samples were assayed in technical quadruplicates and average AKAP13 expression levels were determined from β-Actin, GAPDH, and TBP normalized values. Relative expression was calculated against HUVECs transfected with negative control #1 siRNA. Means ± standard deviations were reported for two transfections of each siRNA. One-way ANOVA and Tukey's multiple comparison tests were conducted to determine significant differences (Prism 5; GraphPad).

Cell-attachment assay

The ability and kinetics of HUVEC attachment to extracellular matrices was measured by plating cells onto 6-well tissue-culture plates coated with various extracellular matrices, and the number of attached cells were measured at 15, 30, and 60 minutes. Six-well tissue-culture plates were coated with Matrigel (BD Biosciences) diluted 1 to 100 in basal ECM (containing no FBS or growth factors), 5 μg/ml fibronectin (R&D Systems) diluted in PBS, or 0.1% gelatin and incubated at room temperature for 1 hour. Excess extracellular matrix was removed, and the wells were washed with basal ECM. Cells were seeded at 7 x 10^4 cells per well and incubated at 37°C for 15, 30, or 60 minutes in complete ECM. At the desired time points, non-adherent cells were washed off the plate using PBS and cells were fixed using 4% PFA in PBS at room temperature for 10 minutes. Cells were then permeabilized with 0.1% Triton X-100 (Sigma) in PBS at room temperature for 10 minutes and blocked with 1% normal goat serum (Sigma) and 1% BSA (Sigma) in PBS at room temperature for 15 minutes. Vectashield Hard Set with DAPI (Vector Laboratories) was added to the cells and a square cover slip was overlaid onto the cells. Images of DAPI-positive adherent cells were obtained using an inverted Axiovert 200M microscope, AxioCam (Carl Zeiss) camera, and AxioVision Software for multiple fields of view per well. The number of DAPI-positive adherent cells was quantified using Velocity 5.3. Means ± standard deviations were reported for two transfections of each siRNA. Student t-tests were performed for each time point comparison and no significant differences were identified (Excel).

Wound healing / Scratch assay

The ability of HUVECs to migrate into a wound in the presence of VEGF was monitored over time. HUVECs (at 1 day post-transfection with siRNA) were serum starved with 0.1% FBS in basal ECM overnight. The cell monolayer was then "scratched" using P200 pipet tips to create denuded areas and washed with PBS to remove non-adhered cells. Four scratches were made per well. Basal ECM supplemented with 0.1% FBS was added to the cells and the scratches were imaged for the 0 time point. Cells were then fed with basal ECM supplemented with 0.1% FBS and 50 ng/mL of VEGF-165 (R&D Systems). The scratches were imaged after 6, 24, and 48 hours of culture using an inverted Axiovert 200M microscope, AxioCam (Carl Zeiss) camera, and AxioVision Software. Two siRNA transfections were conducted and representative images are shown.

Cell-spreading assay

The extent of HUVEC spreading and organization was measured by plating cells onto cover slips coated with 1:100 Matrigel or 5 μg/ml fibronectin (as described above) in 12-well tissue-culture plates. HUVECs were seeded at 4 x 10^4 cells per well and incubated at 37°C for 2 hours in complete ECM. Cells were then fixed and permeabilized as described above and blocked with 1% BSA in PBS. The actin cytoskeleton of the cells was stained with rhodamine-phalloidin (Invitrogen), according to manufacturer's recommendations, and the cover slips were mounted using Vectashield Hard Set with DAPI. Images were obtained using an

inverted Axiovert 200M microscope, AxioCam (Carl Zeiss) camera, and

AxioVision Software for multiple fields of view per cover slip. Technical triplicates

were done per siRNA transfection and extracellular matrix. Cellular area was

quantified using Velocity 5.3. In brief, the total area of rhodamine-phalloidin

fluorescent staining minus any fluorescent area on the edge of the field of view

was determined. The number of DAPI-positive nuclei was then counted within the

rhodamine-positive area. Finally, cellular area was calculated by dividing the total

area of rhodamine fluorescence by the number of nuclei. Means ± standard

deviations were reported for multiple independent transfections of each siRNA

(negative control #1 siRNA, n=10; AKAP13 siRNA #1475, n=8; and AKAP13

siRNA #1569, n=4). One-way ANOVA and Tukey's multiple comparison tests

were conducted to determine significant differences (Prism 5; GraphPad).

Tube formation assay

To assess the ability of HUVECs to form capillary-like tubes, cells were seeded

onto a thick layer of Matrigel in complete ECM and imaged at several time points

after seeding. The tube formation assay was conduced in 48-well tissue culture

plates. A thick layer of Matrigel (150 μL per well) was allowed to set for 1 hour at

room temperature. HUVECs (4 x 10^4 cells in 0.5 mL complete ECM) were

seeded onto the Matrigel and incubated at 37°C. Bright field images were

obtained at 2, 4, 8, and 24 hours post-seeding using an inverted Axiovert 200M

microscope, AxioCam (Carl Zeiss) camera, and AxioVision Software. Technical

triplicate wells were analyzed per siRNA transfection (negative control #1, n=4;

AKAP13 siRNA #1475, n=4; and AKAP13 siRNA #1569, n=2). Representative images are shown.

VEGF signaling assay

VEGF-induced phosphorylation of PKD was observed by western blotting of total cell lysis from negative control #1 and 1475 siRNA-transfected HUVECs. HUVECs (at one day post-transfection with siRNA) were serum starved with 0.1% FBS in basal ECM overnight. Cells were stimulated with vehicle (appropriate volume of 0.1% BSA in PBS), 5 ng/mL and 20 ng/mL of VEGF-165 (in 0.1% BSA-PBS; R&D Systems), and 100 nM PMA (Sigma) in 0.1% FBS-basal ECM for 15 minutes at 37°C. Cells were then washed with PBS and lysed with protein lysis buffer: 50 mM Tris-HCl (Mediatech), 150 mM NaCl (Teknova), 5 mM EDTA (Teknova), 5 mM EGTA (Sigma), 1% Triton-X 100 (Sigma), 1% DOC (Sigma), and 0.1% SDS (Teknova), supplemented with Complete Protease Inhibitor (Roche) and Phosphatase Inhibitor Cocktail A & B (Santa Cruz Biotech). Cellular DNA was sheared by running the lysis buffer through a 25-gauge needle, and the sheared lysis was incubated on ice for 30 minutes. Cell debris was pelleted by centrifugation, and the supernatant harvested for western blot analysis. Protein levels were quantified using Bio-Rad D_C Protein Assay (Bio-Rad).

Western blots were conducted with 15 μg of total cell protein mixed with 4x Tris-Glycine sample buffer and 10x Reducing Agent (Invitrogen) and boiled at 100°C for 5 minutes. Protein samples were run on an 8% Tris-Glycine gel

(Invitrogen) in 1x Tris-Glycine running buffer (Invitrogen) at 30 volts (constant) for 30 minutes, then 125 volts (constant) for 2 hours. Protein was transferred to a PVDF membrane (Invitrogen) in Tris-Glycine transfer buffer (Invitrogen) containing 20% methanol (Sigma) at 100 volts (constant) and 4°C for 2 hours. PVDF membranes were blocked with 5% BSA in TBS-T, then probed with 1:1000 rabbit phospho-PKD (S744/748) (Cell Sig Tech; #2054), phospho-PKD(S916) (Cell Sig Tech; #2051), and pan-PKD (Cell Sig Tech; #2052) for 24 hours at 4°C. Membranes were then incubated with 1:5000 dilution of donkey anti-rabbit IgG-HRP (Amersham Biosci; NA934V) secondary antibody for 2 hours at room temperature. Membranes were also probed using 1:5000 mouse α-Actin (Cal Biochem; Ab-1, JLA20) overnight at 4°C, then 1:10,000 goat anti-mouse IgG-HRP (Jackson Immuno Research Labs) secondary antibody for 2 hours at room temperature. Protein blots were detected with West Pico Substrate (Thermo) and exposed to Kodak Biomax Light film.

3.6 Acknowledgments

staining. I would also like to thank E. LaDow for discussions in designing and troubleshooting the PKD western blotting protocol and for providing PMA. Finally, I thank the member of my thesis committee: B. R. Conklin, D. Srivastava, and M. von Zastrow, as well as members of the B. R. Conklin lab: J. Ng, E. Hsiao, T. D. Nguyen, S. Baba, J. Dunham, F. Kreitzer, E. Hua, M. Sears, and M. Scott for valuable discussions planning these experiments and interpreting the results.

3.7 References

1. Ricci-Vitiani L, Pallini R, Biffoni M, Todaro M, Invernici G, et al. (2010) Tumour vascularization via endothelial differentiation of glioblastoma stem-like cells. Nature 468: 824-828.
2. Wang R, Chadalavada K, Wilshire J, Kowalik U, Hovinga KE, et al. (2010) Glioblastoma stem-like cells give rise to tumour endothelium. Nature 468: 829-833.
3. Carmeliet P (2003) Angiogenesis in health and disease. Nat Med 9: 653-660.
4. Ferrara N, Gerber HP, LeCouter J (2003) The biology of VEGF and its receptors. Nat Med 9: 669-676.
5. Munoz-Chapuli R, Quesada AR, Angel Medina M (2004) Angiogenesis and signal transduction in endothelial cells. Cell Mol Life Sci 61: 2224-2243.
6. Carmeliet P, Ferreira V, Breier G, Pollefeyt S, Kieckens L, et al. (1996) Abnormal blood vessel development and lethality in embryos lacking a single VEGF allele. Nature 380: 435-439.
7. Ferrara N, Carver-Moore K, Chen H, Dowd M, Lu L, et al. (1996) Heterozygous embryonic lethality induced by targeted inactivation of the VEGF gene. Nature 380: 439-442.
8. Fong GH, Rossant J, Gertsenstein M, Breitman ML (1995) Role of the Flt-1 receptor tyrosine kinase in regulating the assembly of vascular endothelium. Nature 376: 66-70.
9. Shalaby F, Rossant J, Yamaguchi TP, Gertsenstein M, Wu XF, et al. (1995) Failure of blood-island formation and vasculogenesis in Flk-1-deficient mice. Nature 376: 62-66.

10. Wong C, Jin ZG (2005) Protein kinase C-dependent protein kinase D activation modulates ERK signal pathway and endothelial cell proliferation by vascular endothelial growth factor. J Biol Chem 280: 33262-33269.

11. Bryan BA, Dennstedt E, Mitchell DC, Walshe TE, Noma K, et al. (2010) RhoA/ROCK signaling is essential for multiple aspects of VEGF-mediated angiogenesis. Faseb J 24: 3186-3195.

12. Ha CH, Wang W, Jhun BS, Wong C, Hausser A, et al. (2008) Protein kinase D-dependent phosphorylation and nuclear export of histone deacetylase 5 mediates vascular endothelial growth factor-induced gene expression and angiogenesis. J Biol Chem 283: 14590-14599.

13. Hoang MV, Whelan MC, Senger DR (2004) Rho activity critically and selectively regulates endothelial cell organization during angiogenesis. Proc Natl Acad Sci U S A 101: 1874-1879.

14. Qin L, Zeng H, Zhao D (2006) Requirement of protein kinase D tyrosine phosphorylation for VEGF-A165-induced angiogenesis through its interaction and regulation of phospholipase Cgamma phosphorylation. J Biol Chem 281: 32550-32558.

15. Fielitz J, Kim MS, Shelton JM, Qi X, Hill JA, et al. (2008) Requirement of protein kinase D1 for pathological cardiac remodeling. Proc Natl Acad Sci U S A 105: 3059-3063.

16. Evans IM, Bagherzadeh A, Charles M, Raynham T, Ireson C, et al. (2010) Characterization of the biological effects of a novel protein kinase D inhibitor in endothelial cells. Biochem J 429: 565-572.

17. Ha CH, Jhun BS, Kao HY, Jin ZG (2008) VEGF stimulates HDAC7 phosphorylation and cytoplasmic accumulation modulating matrix metalloproteinase expression and angiogenesis. Arterioscler Thromb Vasc Biol 28: 1782-1788.

18. Beckers CM, van Hinsbergh VW, van Nieuw Amerongen GP (2010) Driving Rho GTPase activity in endothelial cells regulates barrier integrity. Thromb Haemost 103: 40-55.

19. Bryan BA, D'Amore PA (2007) What tangled webs they weave: Rho-GTPase control of angiogenesis. Cell Mol Life Sci 64: 2053-2065.

20. Wang L, Zheng Y (2007) Cell type-specific functions of Rho GTPases revealed by gene targeting in mice. Trends Cell Biol 17: 58-64.

21. van Nieuw Amerongen GP, Koolwijk P, Versteilen A, van Hinsbergh VW (2003) Involvement of RhoA/Rho kinase signaling in VEGF-induced endothelial cell migration and angiogenesis in vitro. Arterioscler Thromb Vasc Biol 23: 211-217.

22. Wong W, Scott JD (2004) AKAP signalling complexes: focal points in space and time. Nat Rev Mol Cell Biol 5: 959-970.

23. Carnegie GK, Means CK, Scott JD (2009) A-kinase anchoring proteins: from protein complexes to physiology and disease. IUBMB Life 61: 394-406.

24. Diviani D, Baisamy L, Appert-Collin A (2006) AKAP-Lbc: a molecular scaffold for the integration of cyclic AMP and Rho transduction pathways. Eur J Cell Biol 85: 603-610.

25. Diviani D, Scott JD (2001) AKAP signaling complexes at the cytoskeleton. J Cell Sci 114: 1431-1437.

26. Sehrawat S, Ernandez T, Cullere X, Takahashi M, Ono Y, et al. (2010) AKAP9 regulation of microtubule dynamics promotes Epac1 induced endothelial barrier properties. Blood.

27. Zhang D, Ouyang J, Wang N, Zhang Y, Bie J, et al. (2010) Promotion of PDGF-induced endothelial cell migration by phosphorylated VASP depends on PKA anchoring via AKAP. Mol Cell Biochem 335: 1-11.

28. Carnegie GK, Smith FD, McConnachie G, Langeberg LK, Scott JD (2004) AKAP-Lbc nucleates a protein kinase D activation scaffold. Mol Cell 15: 889-899.

29. Diviani D, Abuin L, Cotecchia S, Pansier L (2004) Anchoring of both PKA and 14-3-3 inhibits the Rho-GEF activity of the AKAP-Lbc signaling complex. Embo J 23: 2811-2820.

30. Carnegie GK, Soughayer J, Smith FD, Pedroja BS, Zhang F, et al. (2008) AKAP-Lbc mobilizes a cardiac hypertrophy signaling pathway. Mol Cell 32: 169-179.

31. Diviani D, Soderling J, Scott JD (2001) AKAP-Lbc anchors protein kinase A and nucleates Galpha 12-selective Rho-mediated stress fiber formation. J Biol Chem 276: 44247-44257.

32. Dutt P, Nguyen N, Toksoz D (2004) Role of Lbc RhoGEF in Galpha12/13-induced signals to Rho GTPase. Cell Signal 16: 201-209.

33. Appert-Collin A, Cotecchia S, Nenniger-Tosato M, Pedrazzini T, Diviani D (2007) The A-kinase anchoring protein (AKAP)-Lbc-signaling complex mediates alpha1 adrenergic receptor-induced cardiomyocyte hypertrophy. Proc Natl Acad Sci U S A 104: 10140-10145.

34. Mayers CM, Wadell J, McLean K, Venere M, Malik M, et al. (2010) The Rho guanine nucleotide exchange factor AKAP13 (BRX) is essential for cardiac development in mice. J Biol Chem 285: 12344-12354.

35. Skarnes WC (2000) Gene trapping methods for the identification and functional analysis of cell surface proteins in mice. Methods Enzymol 328: 592-615.

36. Waldron RT, Rey O, Iglesias T, Tugal T, Cantrell D, et al. (2001) Activation loop Ser744 and Ser748 in protein kinase D are transphosphorylated in vivo. J Biol Chem 276: 32606-32615.

37. Matthews SA, Rozengurt E, Cantrell D (1999) Characterization of serine 916 as an in vivo autophosphorylation site for protein kinase D/Protein kinase Cmu. J Biol Chem 274: 26543-26549.

38. Ernkvist M, Luna Persson N, Audebert S, Lecine P, Sinha I, et al. (2009) The Amot/Patj/Syx signaling complex spatially controls RhoA GTPase activity in migrating endothelial cells. Blood 113: 244-253.

39. Garnaas MK, Moodie KL, Liu ML, Samant GV, Li K, et al. (2008) Syx, a RhoA guanine exchange factor, is essential for angiogenesis in Vivo. Circ Res 103: 710-716.

40. Klarenbach SW, Chipiuk A, Nelson RC, Hollenberg MD, Murray AG (2003) Differential actions of PAR2 and PAR1 in stimulating human endothelial cell exocytosis and permeability: the role of Rho-GTPases. Circ Res 92: 272-278.

41. Wojciak-Stothard B, Potempa S, Eichholtz T, Ridley AJ (2001) Rho and Rac but not Cdc42 regulate endothelial cell permeability. J Cell Sci 114: 1343-1355.

42. Gavard J, Gutkind JS (2008) Protein kinase C-related kinase and ROCK are required for thrombin-induced endothelial cell permeability downstream from Galpha12/13 and Galpha11/q. J Biol Chem 283: 29888-29896.

43. Bohm F, Pernow J (2007) The importance of endothelin-1 for vascular dysfunction in cardiovascular disease. Cardiovasc Res 76: 8-18.

44. Higuchi S, Ohtsu H, Suzuki H, Shirai H, Frank GD, et al. (2007) Angiotensin II signal transduction through the AT1 receptor: novel insights into mechanisms and pathophysiology. Clin Sci (Lond) 112: 417-428.

45. Mehta PK, Griendling KK (2007) Angiotensin II cell signaling: physiological and pathological effects in the cardiovascular system. Am J Physiol Cell Physiol 292: C82-97.

46. Shibolet O, Giallourakis C, Rosenberg I, Mueller T, Xavier RJ, et al. (2007) AKAP13, a RhoA GTPase-specific guanine exchange factor, is a novel regulator of TLR2 signaling. J Biol Chem 282: 35308-35317.

Chapter 4

AKAP13 Rho-GEF and PKC-PKD Binding Domain-Deficient Mice Develop Normally Yet Fail to Induce a Functional Cardiac Response to β-Adrenergic Stimulation

Matthew J. Spindler[1,2], Yu Huang[1], Edward C. Hsiao[1,3], Nathan Salomonis[1], Mark J. Scott[1], Deepak Srivastava[1,4,5], Bruce R. Conklin[1,2,6,7]

[1]Gladstone Institute of Cardiovascular Disease, San Francisco, CA, [2]Pharmaceutical Sciences and Pharmacogenomics Graduate Program, Department of Bioengineering and Therapeutic Sciences, University of California, San Francisco, CA, [3]Division of Endocrinology and Metabolism, Department of Medicine, University of California, San Francisco, CA, [4]Department of Pediatrics, University of California, San Francisco, CA, [5]Department of Biochemistry and Biophysics, University of California, San Francisco, CA, [6]Department of Medicine, University of California, San Francisco, CA, [7]Department of Cellular and Molecular Pharmacology, University of California, San Francisco, CA

Author Contributions

Conceived and designed the experiments: MJSpindler DS BRC. Performed the experiments: MJSpindler YH ECH NS MJScott. Analyzed the data: MJSpindler YH DS BRC. Wrote the paper: MJSpindler BRC.

4.1 Abstract

Background: A-kinase anchoring proteins (AKAPs) are scaffolding molecules that coordinate and integrate G-protein signaling events to regulate development, physiology, and disease. One family member, AKAP13, encodes for multiple protein isoforms that contain binding sites for protein kinase A, C (PKC), and D (PKD) and an active Rho-guanine nucleotide exchange factor (Rho-GEF)

domain. In mice, AKAP13 is required for development as null embryos die by E10.5 with cardiovascular phenotypes. Additionally, the AKAP13 Rho-GEF and PKC-PKD binding domains mediate cardiomyocyte hypertrophy in cell culture. However, the requirements for the Rho-GEF and PKC-PKD binding domains during development and cardiac hypertrophy are unknown.

Methodology/Principal Findings: To determine if these AKAP13 protein domains are required for development, we used gene-trap events to create mutant mice that lacked the Rho-GEF and/or the protein kinase C–PKD binding domains. Surprisingly, heterozygous matings produced mutant mice at Mendelian ratios that had normal viability and fertility. The adult mutant mice also had normal cardiac structure and electrocardiograms. To determine the role of these domains during β-adrenergic-induced cardiac hypertrophy, we stressed the mice with isoproterenol. We found that heart size increased normally in mice lacking the Rho-GEF and PKC-PKD binding domains. However, the mutant hearts failed to develop the expected increase in ejection fraction and fractional shortening.

Conclusions: These results suggest the Rho-GEF and PKC-PKD binding domains of AKAP13 are not required for mouse development, normal cardiac architecture, or β-adrenergic-induced cardiac hypertrophy. However, the domains are necessary for a proper cardiac functional response to β-adrenergic stimulation.

135

4.2 Introduction

A-kinase anchoring proteins (AKAPs) organize multi-protein signaling complexes to control a wide range of signaling events, including those important for development [1,2], fertility [3,4], learning and memory [5,6,7], and cardiac structure and physiology [8,9,10,11]. The diverse AKAP family members all bind protein kinase A (PKA) as well as a wide variety of other signaling proteins, such as protein kinase C (PKC) and D (PKD), to create unique signaling complexes [12,13]. Many of these signaling proteins are activated by common intracellular second messengers (e.g., cyclic AMP (cAMP) and calcium), which activate PKA and PKC, respectively. If the activated signaling proteins are left uncontrolled, they could nonspecifically affect multiple downstream proteins. However, AKAPs provide signaling specificity by anchoring multi-protein complexes in close proximity to specific downstream substrates. Thus, AKAPs integrate multiple upstream signals into specific downstream events by organizing multi-protein signaling complexes at specific cellular locations.

In the heart, the signaling events coordinated by AKAPs control aspects of cardiac growth, remodeling [9,14,15], and physiology, including excitation/contraction (EC) coupling and calcium regulation [16,17]. The physiological roles of several AKAPs in coordinating EC coupling have been studied in isolated cardiomyocytes and whole organisms [18]. However, the roles of AKAPs in coordinating cellular growth and remodeling during cardiac hypertrophy have been limited to studies in isolated cardiomyocytes [9,14,19,20].

Interestingly, many of the signaling pathways involved in cardiac remodeling are also important in the developing heart.

We studied AKAP13 in mice because of its expression pattern, null mouse phenotype, and the well-characterized signaling pathway it coordinates in isolated cardiomyocytes. We first identified AKAP13 because its expression is up-regulated during mouse fetal development [21] and mouse embryonic stem (ES) cell differentiation [22] (Table 1.1; see Chapter 1). In addition, AKAP13 is highly expressed in the adult heart [23,24]. Second, a null allele of AKAP13 causes embryonic death and exhibits cardiac defects [11]. Finally, AKAP13 coordinates a signaling complex that transduces cardiac remodeling signals induced by G protein-coupled receptors (GPCRs) into hypertrophic responses in isolated cardiomyocytes [14,20].

AKAP13 is a large gene that encodes for three main transcripts, AKAP-Lbc [23], Brx [24], and Lbc [25], through the use of alternative promoters. The protein isoforms encoded by these three transcripts share a common carboxyl-terminal region that contains a guanine nucleotide exchange factor (GEF) domain and PKC and PKD binding domains (Figure 4.1). The unique amino-terminus of AKAP-Lbc encodes the PKA binding domain [23,26,27]. The roles these AKAP13 protein domains play during hypertrophic signaling have been well studied in isolated rat cardiomyocytes. Several GPCR ligands that signal through the G-protein pathways $G_{12/13}$ and G_q can activate the GEF domain of AKAP13 and AKAP13-bound PKC, respectively [14,20]. Once activated, the GEF domain activates RhoA, which leads to cardiomyocyte hypertrophy [20]. Activated PKC

activates co-bound PKD, which, through several additional steps, activates the transcription factor MEF2C and leads to hypertrophy [14,26,28].

The same signaling pathways coordinated by AKAP13 to regulate isolated cardiomyocyte hypertrophy could be required for cardiac development. Despite the finding that *Akap13*-null embryos die, likely from cardiovascular defects [11], the protein domains and coordinated signaling pathways of AKAP13 required for development remain unknown. Both the $G_{12/13}$ and G_q signaling pathways, which can signal upstream of AKAP13, are required for development of the mouse cardiovascular system [29,30]. In addition, proteins downstream of AKAP13 are required for proper development since mutant MEF2C and PKD mouse embryos die from heart formation defects and unknown causes, respectively [31,32].

In this study, we asked if the signaling events coordinated by AKAP13 in isolated cardiomyocytes were important for cardiac development and remodeling in mice. We hypothesized that the AKAP13 protein domains for Rho-GEF activity and PKC-PKD binding are required for mouse development. To test this hypothesis, we mated AKAP13 gene-trap mutant mouse lines and assessed them for viable offspring. Unexpectedly, we found that mice lacking the Rho-GEF and PKC-PKD binding domains had normal viability. These mice also had normal cardiac electrical activity, as assessed by 6-lead electrocardiograms (ECGs), and cardiac structure.

We then hypothesized that the Rho-GEF and PKC-PKD binding domains of AKAP13 are important for cardiac remodeling in response to β-adrenergic-induced cardiac hypertrophy. To test this hypothesis, we treated mice with

isoproterenol for 14 days, measured cardiac structural and functional changes by echocardiography, and analyzed heart size and structure by morphology and histology. Surprisingly, we found that AKAP13 Rho-GEF and PKC-PKD deficient mice failed to increase cardiac ejection fraction and fractional shortening despite a normal increase in heart size.

4.3 Results

4.3.1 Gene-trap events disrupt AKAP13 in multiple locations

Complete loss of AKAP13 causes embryonic death in mice, possibly from cardiac defects [11]. However, AKAP13 contains multiple protein domains, and it is unclear which domains are required for development. In addition, the AKAP13 gene locus utilizes alternative promoters to drive expression of at least three different isoforms, AKAP-Lbc, Brx, and Lbc.

To determine if the AKAP13 Rho-GEF and PKC-PKD binding domains are required for mouse development, we generated AKAP13 mutant mice from gene-trapped ES cells. The gene-trap construct uses a strong splice acceptor to create a fused mRNA of the upstream AKAP13 exons with the trapping cassette [33]. The resulting fusion protein contains the amino-terminus of AKAP13 fused to βGeo, which confers β-galactosidase activity and neomyocin resistance. These fusion proteins create truncation mutants that can be used to dissect the role of AKAP13 protein domains *in vivo*.

We used the International Gene Trap Consortium (IGTC) database (at

www.genetrap.org) [34] and the IGTC Sequence Tag Alignments track on the

UCSC Genome Browser [35] to select three gene-trap events at different

positions of the AKAP13 gene, ΔBrx (from ES cell line AG0213), ΔGEF

(CSJ306), and ΔPKC (CSJ288), for further analysis (Figure 4.1A). We confirmed

the splicing of upstream AKAP13 exons into the gene-trap cassette (Figure 4.1B)

by RT-PCR and sequencing from total ES cell RNA. We also identified the

insertion site of each gene-trap event by long-range PCR and designed

genotyping strategies for these mutant lines (Figure 4.1B, D). These three gene-

trap events create a mutational series that affects specific AKAP13 isoforms and

protein domains (Figure 4.1C). The ΔBrx mutation creates a fusion of the AKAP-

Lbc and Brx isoforms with βGeo that disrupts the Rho-GEF and PKC-PKD

binding domains for these two isoforms. However, the Lbc isoform should be

normally expressed. The ΔGEF mutation is expected to be the most severe as it

creates a fusion of all three isoforms that disrupts the Rho-GEF and PKC-PKD

binding domains. Finally, the ΔPKC mutation disrupts the PKC-PKD binding

domains of all three isoforms while the Rho-GEF domain remains intact. Male

chimeric mice were generated from these three gene-trap ES cell lines and

crossed to female C57Bl/6 mice to generate heterozygotes. We used these mice

to study the roles of AKAP13 Rho-GEF and PKC-PKD binding domains *in vivo*.
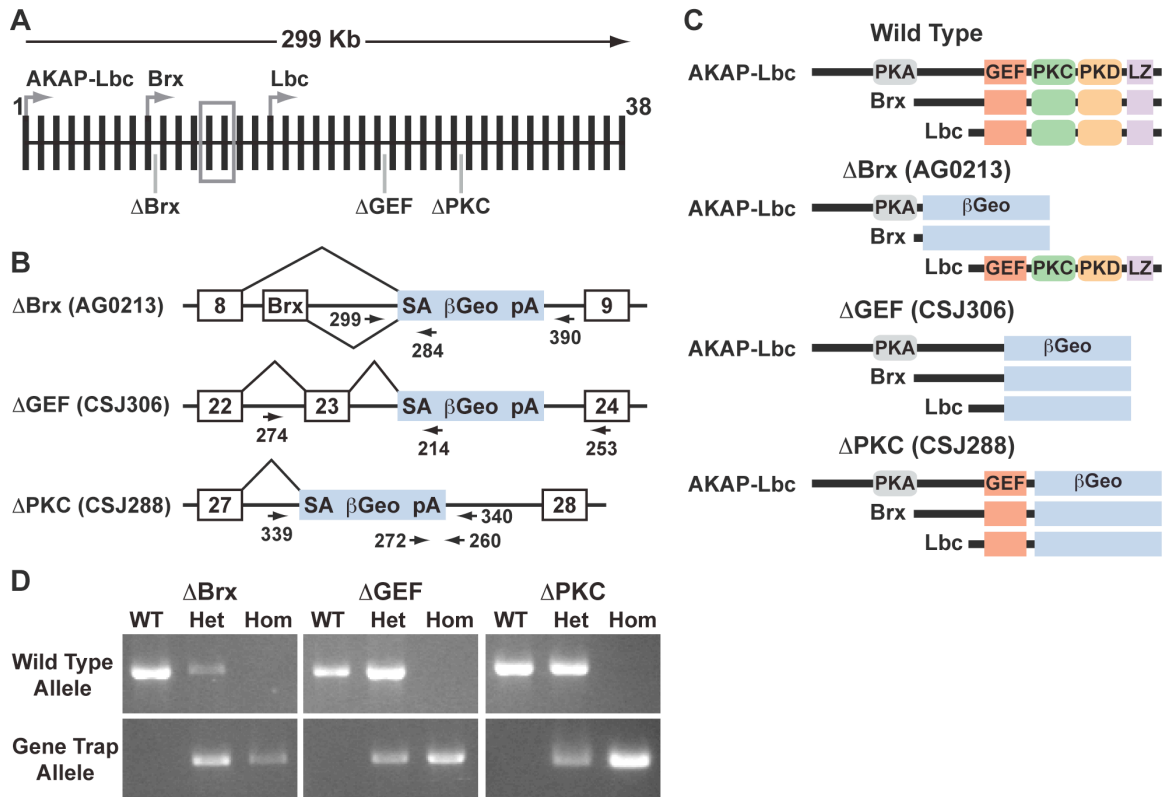
Figure 4.1. Gene-traps disrupt AKAP13 in multiple locations. (A) Schematic of the AKAP13 genomic locus. Exons are depicted with black bars, cassette exons with a grey box, and alternative promoters with arrows. The three gene-trap insertions are indicated. (B) Diagram of the gene-trap constructs (blue boxes) integrated between AKAP13 exons (open boxes with exon numbers). The gene-trap vector contains a strong splice acceptor (SA), βGeo cassette (β–galactosidase and neomyocin resistance genes), and stop codon as well as a polyadenylation (pA) sequence. The splicing events indicated were confirmed by RT-PCR and sequencing. Primers used to genotype the wild-type and gene-trap alleles are shown (black arrows). (C) Resulting protein fusions of AKAP-Lbc, Brx, and Lbc isoforms with βGeo for the gene-trap mutational series. PKA = protein kinase A binding domain, GEF = Rho-guanine nucleotide exchange factor domain, PKC = protein kinase C binding domain, PKD = protein kinase D binding domain, LZ = leucine zipper domain. (D) Sample genotyping of mouse tail clips for the AKAP13 gene-trap mutations using primers in (B). WT=Wild-type, Het=Heterozygote, Hom=Homozygote.

4.3.2 AKAP13 is broadly expressed during mouse development and in adult tissue

Despite the requirement of AKAP13 for mouse development, its expression pattern during this process is unknown. In addition to disrupting the AKAP13 protein, the gene-trap events report the expression pattern of AKAP13 because the endogenous AKAP13 promoters drive expression of the AKAP13-βGeo fusion proteins.

To determine the expression of AKAP13 during mouse development, we conducted X-Gal staining of AKAP13$^{+/\Delta GEF}$ embryos at E8.5, E9.5, E10.5, and E14.5 (Figure 4.2). We found X-Gal staining in the head folds, notochord, and somites of E8.5 embryos but little to no staining in the looping heart (Figure 4.2A, B). At E9.5, the staining pattern was broadly expanded with higher levels of expression in the heart (Figure 4.2C). There was also staining in the vasculature, eye, ear, somites, gut and brain. E10.5 embryos had a staining pattern similar to that of E9.5 embryos (Figure 4.2D). However, there was stronger staining throughout the heart (Figure 4.2D, E). E14.5 embryos had high levels of staining in the atrial and ventricular myocardium and endocardium, trabeculae, and outflow tract (Figure 4.2F-H). There was also staining in skeletal muscle, tongue, gut, kidney, lung, urinary system, and the choroid plexus of the brain (Figure 4.2F). Finally, the yolk sac and umbilical cord of mouse embryos stained positive with X-Gal (Figure 4.2I). We found the same staining patterns in AKAP13$^{+/\Delta Brx}$ and AKAP13$^{+/\Delta PKC}$ embryos, and no staining in wild-type embryos was detected. These results show that AKAP13 is broadly expressed during mouse

development with increasing levels of expression in the heart and outflow tract. They also show that AKAP13 is expressed in skeletal and smooth muscle throughout the developing embryo.

Previous studies using Northern blot analysis found AKAP13 to be highly expressed in human heart tissue with less expression in other tissues, including the lung and kidney [23,24]. However, the expression patterns of AKAP13 within these organs remain unknown. To determine the expression pattern of AKAP13 within adult mouse organs, we conducted X-Gal staining of AKAP13$^{+/\Delta GEF}$ heart, kidney, and brain samples (Figure 4.3). We found X-Gal staining throughout the entire heart and in the pulmonary arteries and aorta (Figure 4.3A). In the kidney, the cortex, arteries and ureter stained positive (Figure 4.3C). The vasculature of the brain, olfactory bulb, and part of the cerebellar cortex stained positive (Figure 4.3D). The same staining patterns were seen in kidney and brain from AKAP13$^{+/\Delta Brx}$ and AKAP13$^{+/\Delta PKC}$ adult mice. Surprisingly, AKAP13$^{+/\Delta PKC}$ hearts lacked staining in the ventricles; however, there was still staining in the atria, pulmonary arteries, aorta, and ventricular vasculature (Figure 4.3B). These results show that AKAP13 is highly expressed in the adult heart and vasculature and is expressed in specific regions of additional organs, including the kidney and brain.
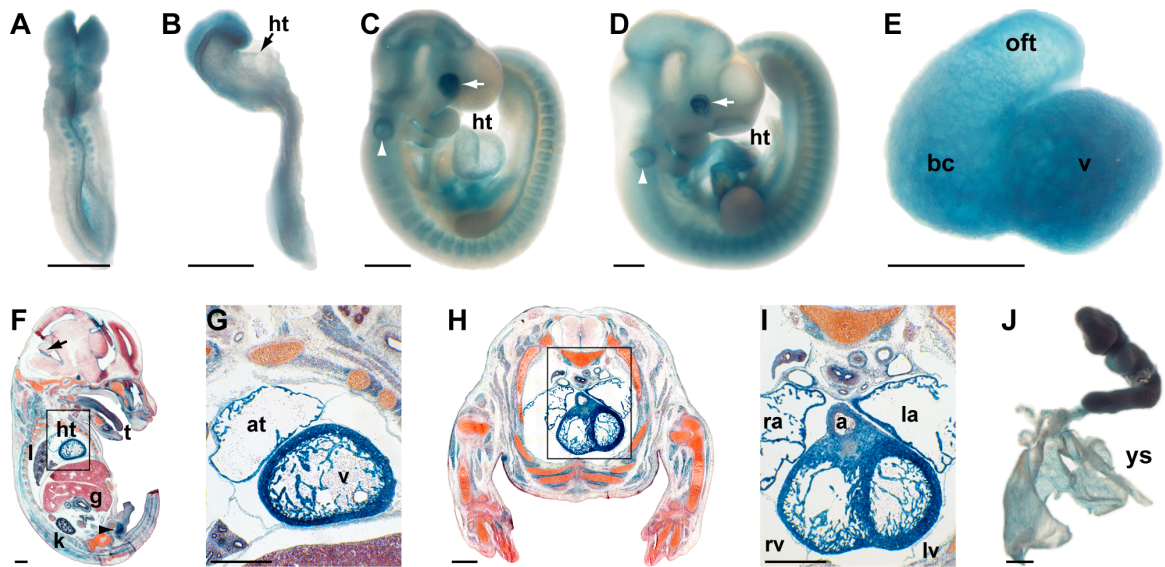
Figure 4.2. AKAP13 is broadly expressed during mouse development. (A–D) Whole-mount AKAP13$^{+/\Delta GEF}$ embryos stained with X-Gal (in blue) to identify AKAP13-βGeo expression at (A&B) E8.5, (C) E9.5, and (D) E10.5. (A&B) E8.5 embryos showed expression in the head folds, notochord, and somites. (C) Right side view of E9.5 embryo showed expression in the heart (ht), brain, eye (arrow), otic pit (arrowhead), gut, and somites. (D) Right side view of E10.5 embryo showed similar expression as in (C) with higher expression in the heart (ht). (E) Frontal view of an E10.5 heart showed high levels of expression in the ventricle (v), bulbous cordis (bc), and outflow tract (oft). (F) Sagittal and (H) transverse sections of E14.5 embryos stained with X-Gal and nucleofast red. E14.5 embryos showed expression in the heart (ht), tongue (t), lung (l), gut (g), kidney (k), skeletal muscle, brain (arrow), and urogenital region (arrowhead). (G&I) Close ups of the hearts boxed in F and H, respectively, showed expression in atrial (at), and ventricular (v) myocardium, endocardium and trabeculae. The right and left atria (ra & la) and ventricles (rv & lv) all showed expression with higher levels in the left ventricle (lv). There was also expression in the aorta (a). (J) X-Gal staining of E9.5 embryos with the yolk sac attached showed expression in the yolk sac (ys). Black scale bars are 0.5 mm.
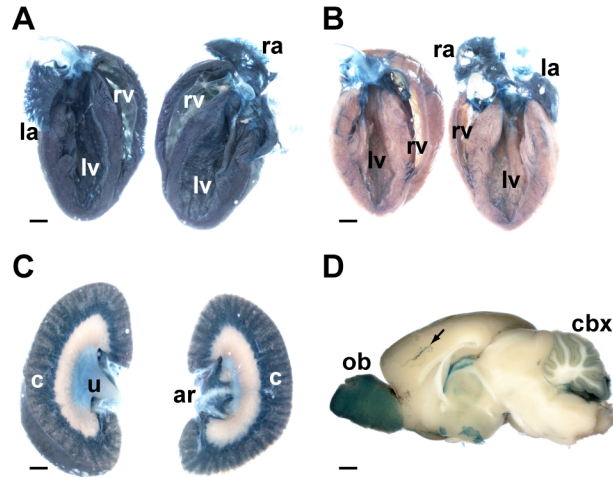
Figure 4.3. AKAP13 is expressed in adult heart, kidney, and brain. Adult AKAP13$^{+/\Delta GEF}$ organs were bisected and stained with X-Gal (in blue) to determine AKAP13-βGeo expression in heart (A), kidney (C) and brain (D). (A) The AKAP13-ΔGEF hearts showed strong staining throughout the entire heart, including the left (la) and right (ra) atria, left (lv) and right (rv) ventricles, pulmonary artery, and aorta. (B) AKAP13-ΔPKC hearts had staining in the atria pulmonary artery, and aorta, as expected, but lacked staining in the ventricles. The blood vessels of the ventricles stained positive. (C) The kidney cortex (c), ureter (u), and arteries (ar) stained positive. (D) The interior of the right hemisphere of the brain showed staining of the olfactory bulb (ob), vasculature (arrow), and part of the cerebellum (cbx). Black scale bars are 1 mm.

4.3.3 AKAP13 Rho-GEF and PKC-PKD binding domains are not required for mouse development

Recently, an *Akap13*-null mouse was reported to die at E9.5–E10.5 during embryonic development and it was proposed that this was due to a loss of Rho-GEF signaling [11]. Since AKAP13 also encodes for PKA, PKC, and PKD binding domains, we asked whether the AKAP13 Rho-GEF and PKC-PKD binding domains were required for mouse development. To answer this question, we conducted heterozygote crosses for the three mutant mouse lines and assessed the matings for viable offspring. We found that all of these matings produced homozygous mutant offspring at the expected Mendelian ratios (Table 4.1). In addition, the homozygous mutant mice lacked gross abnormalities, were fertile, and had normal viability.

Table 4.1. Genotypes of pups from heterozygous AKAP13 mutant matings

Genotype	Expected Mendelian Ratio %	Observed Ratios % (Number of Pups)		
		∆Brx	∆GEF	∆PKC
WT	25	23 (n = 39)	25 (n = 52)	25 (n = 64)
Het	50	54 (n = 91)	56 (n = 116)	54 (n = 141)
Hom	25	23 (n = 39)	19 (n = 39)	21 (n = 55)

WT = Wild-type, Het = Heterozygote, Hom = Homozygote

To verify that the gene-trap mutations disrupt full-length AKAP13 expression, we conducted quantitative PCR on total RNA from newborn pup heart and lung tissue (Figure 4.4). We used TaqMan probes to measure relative expression of the E4-5, Brx-9, and E37-38 exon-exon junctions (Figure 4.4A). As expected, we found that none of the gene-trap mutations changed the expression of the

AKAP13 E4-5 junction, which lies upstream of the three gene-trap insertion sites (Figure 4.4B). The expression of the Brx-9 junction was reduced in a dose-dependent manner only in ΔBrx mice, and AKAP13$^{\Delta Brx/\Delta Brx}$ mice completely lacked expression at this location (Figure 4.4C). These results were also expected because the ΔBrx insertion site lies between the Brx specific exon and exon 9, and the other two gene-trap insertions are downstream of this exon-exon junction. Finally, all three gene-trap mutations decreased expression of the E37-38 junction in a dose-dependent manner, as expected (Figure 4.4D). The ΔGEF mutation was particularly effective at reducing expression, as the AKAP13$^{\Delta GEF/\Delta GEF}$ mice completely lacked expression.

Contrary to our expectations, these results indicate that the AKAP13 gene-trap mutations do not affect development or viability. Specifically, the ΔBrx mutation eliminates expression of the Brx-9 exon-exon junction indicating that the Brx isoform of AKAP13 is not required for development or viability. Likewise, the ΔGEF mutation completely eliminates expression of E24-25 (data not shown) and E37-38. This region encodes for the AKAP13 Rho-GEF and PKC-PKD binding domains. Thus, these results show that the Rho-GEF and PKC-PKD binding domains are not required for development or viability.
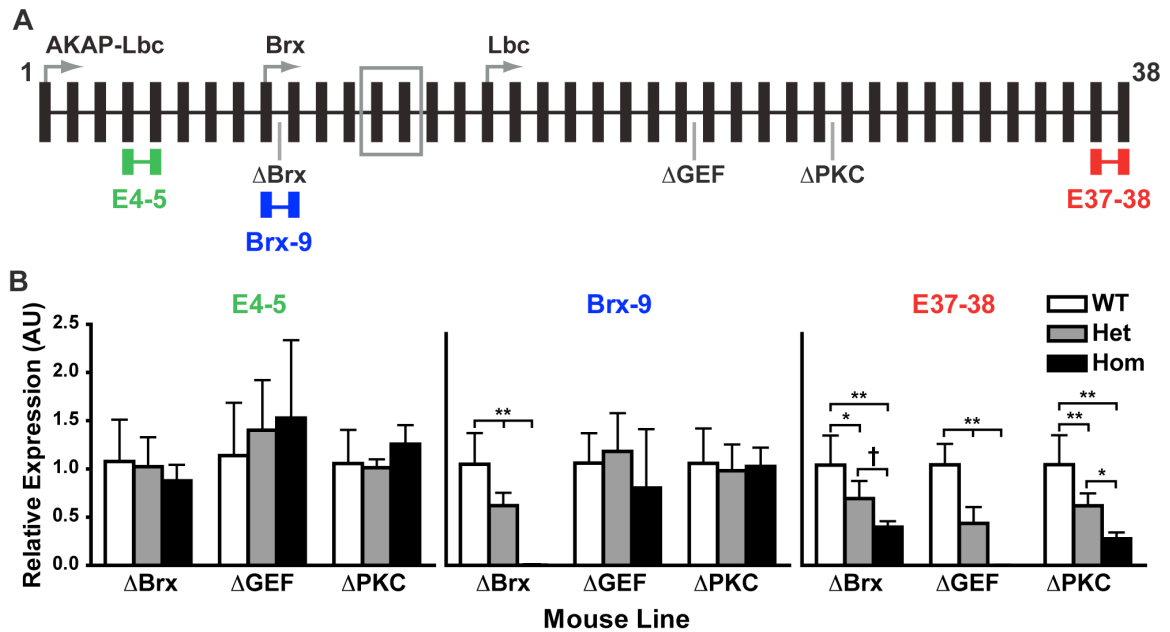
Figure 4.4. Full-length AKAP13 mRNA levels are reduced by the gene-trap events.
(A) TaqMan gene expression assays were used to measure the expression of AKAP13 transcripts at the indicated exon-exon junctions (E4-5, Brx-9, & E37-38). (B) Quantitative PCR analysis of wild-type (WT), heterozygote (Het) and homozygote (Hom) neonatal mouse heart and lung RNA for AKAP13 showed that none of the gene-trap mutations affected expression of the E4-5 exon-exon junction. The ΔBrx gene-trap dose dependently decreased expression of the Brx-9 exon-exon junction. Expression of the Brx-9 junction was eliminated in the AKAP13$^{\Delta Brx/\Delta Brx}$ mice. All three gene-traps decreased expression of the E37-38 exon-exon junction in a dose-dependent manner. Expression of the E37-38 junction was eliminated in the AKAP13$^{\Delta GEF/\Delta GEF}$ mice. The means and standard deviations are graphed for six mice per genotype. One-way ANOVA and Bonferroni's multiple comparison tests were conducted (Prism 5; GraphPad).
†, $p<0.10$; *, $p<0.05$; **, $p<0.01$.

4.3.4 Cardiac electrical activity and structure is normal in AKAP13 mutant mice

Since AKAP13 is highly expressed during cardiac development and throughout the adult heart (Figure 4.2 & 4.3) and regulates cardiomyocyte physiology [14,20], we asked whether the ΔGEF mutation affected adult cardiac electrical activity or structure. To address this, we conducted 6-lead ECG analysis and then harvested hearts from 16–18-week-old male homozygous mutant and wild-type control mice.

ECG analysis showed that heart rate (HR), PR interval, P wave duration, QRS interval, and corrected QT interval (QTc) of AKAP13$^{\Delta GEF/\Delta GEF}$ mice were indistinguishable from wild-type littermates (Table 4.2). Gross morphology showed that the ΔGEF hearts had normal atrial and ventricular structures (Figure 4.5A) and a properly formed pulmonary artery and aorta. Additionally, the wild-type and ΔGEF hearts were the same size as assessed by the heart weight to tibia length (HW/TL) ratios (Figure 4.5B). Hearts from AKAP13$^{\Delta Brx/\Delta Brx}$ and AKAP13$^{\Delta PKC/\Delta PKC}$ mice also had normal morphology and size (data not shown). Histological analysis of ΔGEF hearts by hematoxylin and eosin (H&E) staining showed proper cardiomyocyte organization and structure (Figure 4.5C). Finally, the ΔGEF hearts had normal levels of Masson's trichrome staining, indicating no change in cardiac fibrosis (Figure 4.5D). These results indicate that the loss of AKAP13 Rho-GEF and PKC-PKD binding domains does not affect cardiac electrical activity or structure under normal physiological conditions.

Table 4.2. Six-Lead ECG analysis of AKAP13-ΔGEF mutant mice

Genotype	Heart Rate	PR (ms)	P (ms)	QRS (ms)	QTc (ms)
WT	462.3 ± 30.6	38.4 ± 3.2	9.16 ± 1.14	11.3 ± 1.3	52.2 ± 3.5
ΔGEF	437.1 ± 17.9	39.1 ± 2.3	9.30 ± 0.61	11.5 ± 1.0	55.4 ± 5.7

Heart rate is in beats per minute, ms = milliseconds

Values are given as the mean ± standard deviation for six mice in each genotype.
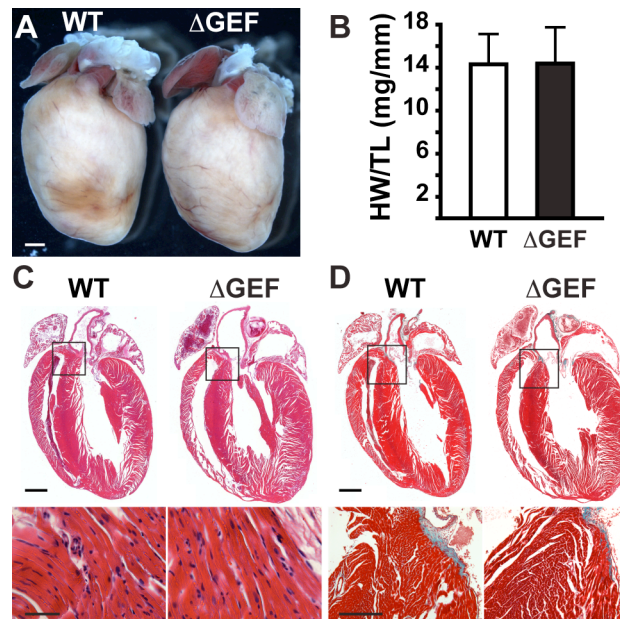
Figure 4.5. AKAP13-ΔGEF mutant mice had normal cardiac structure.

(A) Hearts isolated from six wild-type (WT) and six AKAP13$^{ΔGEF/ΔGEF}$ (ΔGEF) adult male mice at 16–18 weeks of age had normal gross morphology; representative images shown. White scale bar is 1 mm. (B) WT and ΔGEF hearts were the same size as measured by heart weight to tibia length (HW/TL) ratios (in milligrams per millimeter). Means and standard deviations are graphed for six hearts of each genotype. Hearts were sectioned for histology and stained with (C) H&E or (D) Masson's trichrome. The bottom panels of C&D are higher magnifications of the boxed regions in the top panels. (C) Cardiac structure was normal in ΔGEF hearts (top), and cardiomyocytes had proper organization (bottom). (D) ΔGEF hearts had normal levels of fibrosis as assessed by Masson's trichrome staining. Black scale bars in C&D are 1 mm (top), 50 µm (C bottom), and 250 µm (D bottom).

4.3.5 AKAP13 ΔGEF mice have a normal structural but not functional response to β-adrenergic induced cardiac hypertrophy

We then asked whether the AKAP13 Rho-GEF and PKC-PKD binding domains are required for a β-adrenergic induced cardiac hypertrophic response in mice. These AKAP13 domains transduce hypertrophic signaling events in isolated cardiomyocytes [14,20]; however, it is unclear if they are required for the hypertrophic response in mice. To answer this, we implanted mini-osmotic pumps into 22–32-week-old wild-type and AKAP13$^{\Delta GEF/\Delta GEF}$ littermate mice to infuse PBS vehicle (Veh) or isoproterenol (Iso; 60 mg/kg per day) for 14 days [36]. Iso activates β-adrenergic receptors to induce cardiac hypertrophy [37] partially through PKD signaling [31]. To assess the cardiac structural and functional response to β-adrenergic-mediated cardiac hypertrophy, we conducted echocardiography on mice in a blinded fashion. We recorded echocardiograms before pump implantation to obtain a baseline value and on day 13 of treatment. We then isolated the hearts from these mice on day 14 of treatment to further analyze cardiac structural changes.

M-Mode echocardiogram recordings on day 13 showed that Iso treatment increased left ventricular wall thickness in wild-type and AKAP13$^{\Delta GEF/\Delta GEF}$ mice. However, the degree of cardiac contraction was lower in the Iso-treated ΔGEF mice than wild-type mice (Figure 4.6A). Cardiac structural and functional changes were quantified from the echocardiogram recordings (Figure 4.6B–E). Iso treatment increased left ventricular mass (LV Mass) in both wild-type (51%) and ΔGEF (60%) mice from baseline values (Figure 4.6B). Left ventricular

anterior wall thickness at diastole (LVAW;d) increased in both wild-type (43%) and ∆GEF (34%) mice treated with Iso (Figure 4.6C). Left ventricular posterior wall thickness was increased similarly to LVAW (data not shown). There was no difference in LV Mass or LVAW;d between the wild-type and ∆GEF mice at baseline or after Iso treatment.

Despite normal structural changes, cardiac contractility did not increase in ∆GEF mice treated with Iso as compared to Veh controls (Figure 4.6D, E). Left ventricular fractional shortening was calculated from M-Mode echocardiogram recordings (Figure 4.6D). Fractional shortening (FS) was 15% greater in wild-type mice treated with Iso than Veh-treated controls. However, there was no change in FS between ∆GEF Veh- and Iso-treated mice. Similar results were obtained for left ventricular ejection fraction (EF), which was calculated from B-Mode echocardiogram recordings (Figure 4.6E). EF was 22% greater in wild-type mice treated with Iso than Veh-treated controls; however, EF did not change in the ∆GEF mice treated with Iso.
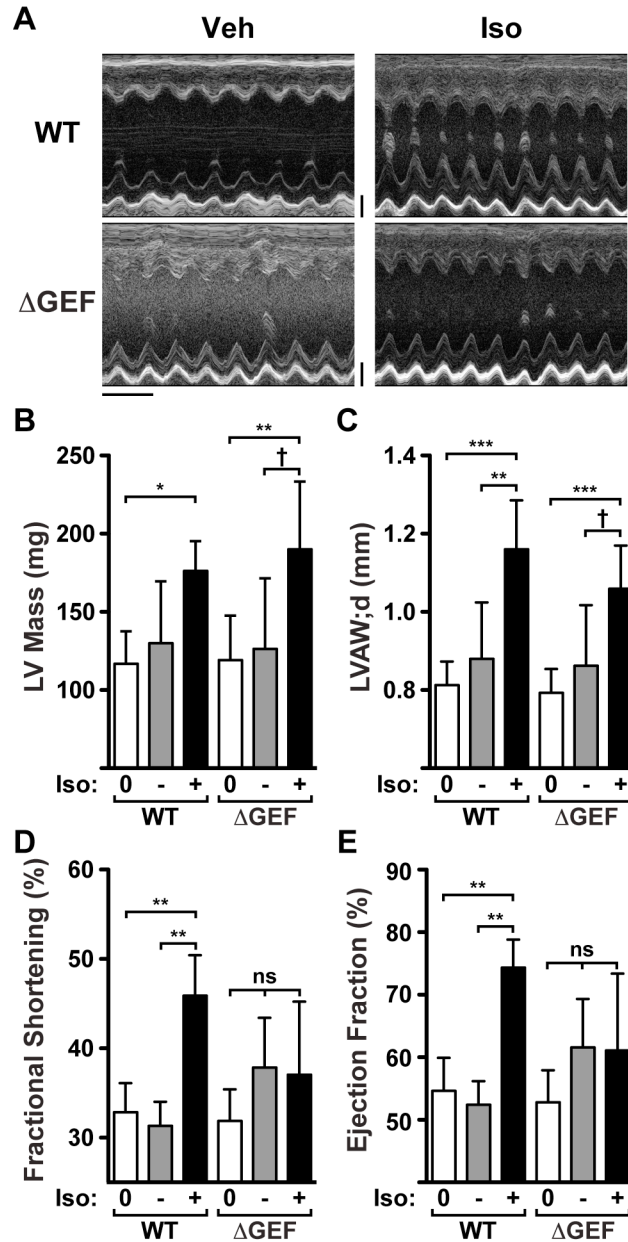
Figure 4.6. AKAP13-ΔGEF mutant mice failed to induce the expected cardiac functional response to β-adrenergic-induced hypertrophy.

(A) Representative M-Mode echocardiogram images showed a thicker left ventricular wall in wild-type (WT) and AKAP13$^{ΔGEF/ΔGEF}$ (ΔGEF) male mice treated with isoproterenol (Iso; 60 mg/kg per day for 13 days) than in those treated with PBS vehicle (Veh). Iso treatment increased the magnitude of contraction in WT mice but not in ΔGEF mice. The horizontal black scale bar is 200 ms; the vertical black scale bars are 1 mm. (B-E)

Quantification of echocardiography data for left ventricle structural and functional changes in response to Iso treatment. Echocardiograms were recorded the day before mini-osmotic pumps were implanted for baseline levels (0) and after 13 days of Iso (+) or Veh (-) treatment. (B) Both WT and ΔGEF mice increased left ventricular (LV) mass to the same level with Iso treatment. (C) LV anterior wall thickness at diastole (LVAW;d) was increased to the same level in both WT and ΔGEF mice treated with Iso. (D) The percent of fractional shortening (FS) increased in wild-type mice treated with Iso compared to baseline or Veh treatment. ΔGEF mice did not increase FS with Iso treatment. (E) The percent ejection fraction (EF) also increased in wild-type mice treated with Iso compared to baseline or Veh treatment. ΔGEF mice did not increase EF with Iso treatment. The means and standard deviations are graphed in B–E for seven WT and nine ΔGEF mice at baseline (0), three WT and three ΔGEF mice with Veh treatment, and four WT and six ΔGEF mice with Iso treatment. One-way ANOVA and Bonferroni's multiple comparison tests were conducted (Prism 5; GraphPad). †, $p < 0.10$; *, $p < 0.05$; **, $p < 0.01$; ***, $p < 0.001$.

Morphological analysis of whole hearts verified that Iso treatment induced cardiac hypertrophy in both wild-type and AKAP13$^{\Delta GEF/\Delta GEF}$ mice to a similar extent (Figure 4.7A). HW/TL increased in wild-type mice treated with Iso from a Veh-treated value of 11.97 ± 0.81 (mean ± SD, n=3) to 16.07 ± 2.01 mg/mm (n=4; p=0.022). Similarly, HW/TL increased in ΔGEF mice from a Veh-treated value of 12.47 ± 3.49 (n=3) to 15.58 ± 2.12 mg/mm (n=6; p=0.133). H&E staining of histological sections of these hearts showed that Iso treatment increased left ventricular wall thickness in both sets of mice (Figure 4.7B, top). Closer examination of the cardiomyocytes at the top of the left ventricular wall showed increased interstitial cells between the myocytes and a looser myocyte configuration in Iso-treated than Veh-treated hearts (Figure 4.7B, bottom). Iso treatment also increased fibrosis in the myocardium of both wild-type and ΔGEF

154

hearts as assessed by Masson's trichrome staining (Figure 4.7C). This fibrosis was interspersed within the myocardium. Qualitative analysis of these heart sections suggested that there was more fibrosis in the ΔGEF than wild-type hearts. Quantification of Masson's trichrome staining also suggested a trend for increased fibrosis in the ΔGEF hearts (10.11 ± 8.42%, n=6, for ΔGEF vs. 5.63 ± 2.10%, n=4, for wild-type; p=0.336). Interestingly, one of the Iso-treated ΔGEF hearts had a large area of fibrosis at the top of the right and left ventricular walls (>25% of myocardial area).

The echocardiography results showed that AKAP13$^{\Delta GEF/\Delta GEF}$ mice did not increase cardiac contractility in response to β-adrenergic stimulation. However, they did have a normal structural response to β-adrenergic-mediated cardiac hypertrophy. Thus, these results indicate that the AKAP13 Rho-GEF and PKC-PKD binding domains are not required for the structural changes induced by β-adrenergic-mediated cardiac hypertrophy. However, they are required for a proper cardiac functional response to β-adrenergic stimulation.
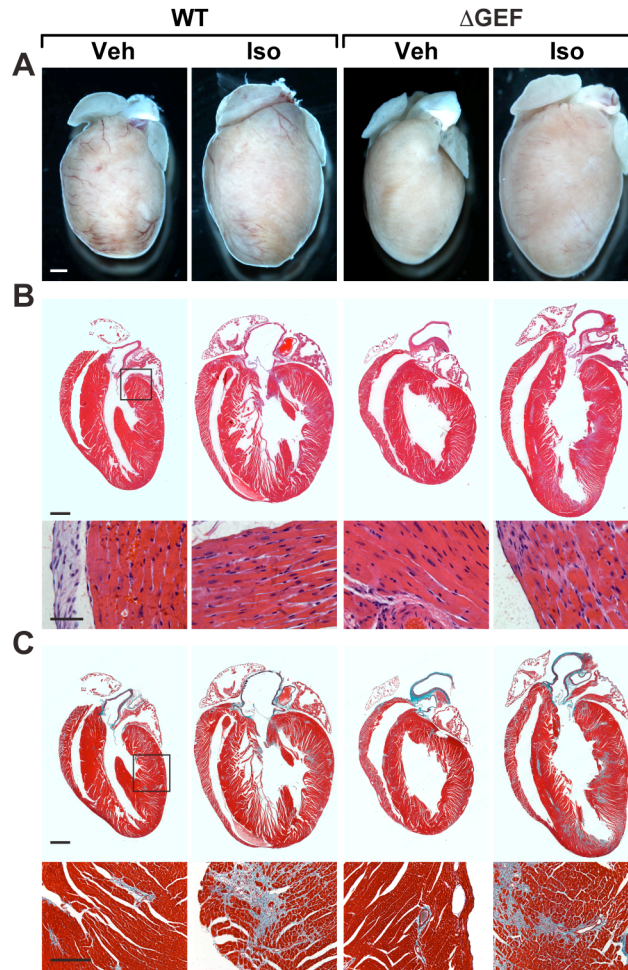
Figure 4.7. AKAP13-ΔGEF mutant mice induced cardiac hypertrophy in response to chronic isoproterenol treatment. (A) Hearts from wild-type (WT) and AKAP13$^{\Delta GEF/\Delta GEF}$ (ΔGEF) male mice showed hypertrophy with isoproterenol (Iso) treatment (60 mg/kg per day for 14 days). Three WT and three ΔGEF mice were treated with PBS vehicle (Veh) and four WT and six ΔGEF mice were treated with Iso; representative images are shown. White scale bar is 1 mm. Hearts were sectioned for histology and stained with (B) H&E or (C) Masson's trichrome. (B) WT and ΔGEF left ventricular walls were thickened by Iso treatment (top). Higher magnification of the upper left ventricular wall (box) showed disruption of myocyte organization in Iso-treated hearts (bottom). (C) Fibrosis increased throughout the WT and ΔGEF hearts as assessed by Masson's trichrome staining. Iso-treated ΔGEF hearts appeared to have more fibrosis than Iso-treated WT hearts. Higher magnification of the left ventricular wall (box) showed fibrosis within the myocardium (bottom). Black scale bars in B&C are 1 mm (top), 50 μm (B bottom), and 250 μm (C bottom).

4.4 Discussion

In this study, we investigated the roles of the Rho-GEF and PKC-PKD binding domains of AKAP13 in mouse development, adult cardiac physiology, and hypertrophic remodeling. Contrary to our expectations, our results show that these AKAP13 domains are not required for mouse development, normal adult cardiac architecture, or β-adrenergic-induced cardiac hypertrophy. Unexpectedly, the AKAP13 Rho-GEF and PKC-PKD binding domains are required for the proper cardiac functional response to β-adrenergic stimulation. In developing mice, AKAP13 was broadly expressed with high levels in the cardiovascular system, and in the adult heart, expression remained high. Despite the disruption of the AKAP13 Rho-GEF and PKC-PKD binding domains in AKAP13$^{\Delta GEF/\Delta GEF}$ mice, we found that these mice were born at a normal Mendelian ratio and had normal viability. Additionally, the mutant adult mice had normal ECGs, heart size, structure, and growth response to chronic isoproterenol treatment. However, the mutant adult mice did not increase fractional shortening or ejection fraction in response to chronic isoproterenol treatment.

Contrary to our expectations that the AKAP13-ΔGEF mutation would phenocopy *Akap13*-null mice, we found that AKAP13$^{\Delta GEF/\Delta GEF}$ mice developed normally. A previous study reported that *Akap13*-null embryos die at E9.5–10.5, display a thinned myocardium and loss of trabeculation, and have decreased expression of cardiac developmental genes [11]. The authors proposed that these phenotypes were due to the loss of AKAP13 Rho-GEF activity in the heart [11]. However, AKAP13 also coordinates a PKC-PKD signaling pathway, and

both the Rho-GEF and PKC-PKD pathways regulate cardiomyocyte hypertrophic growth [14,20]. We expected that eliminating both the Rho-GEF and PKC-PKD binding domains of AKAP13 would cause embryonic lethality and phenocopy the *Akap13*-null mutation. However, our results show that AKAP13-mediated Rho-GEF and PKC-PKD signaling are not required for mouse development. These results, combined with the published *Akap13*-null mouse phenotype, indicate that other AKAP13 protein domains are required for mouse development.

The PKA-binding domain of AKAP13 is an intriguing candidate for the developmentally required AKAP13 protein domain. The AKAP13-ΔGEF mutation used in this study fuses the amino-terminus of AKAP13, including the PKA binding domain, to the βGeo cassette. We confirmed that this mutation eliminates full-length AKAP13 mRNA but maintains expression of mRNA upstream of the gene-trap insertion. Thus, the AKAP13 region upstream of the ΔGEF mutation seems to be sufficient for mouse development, possibly through binding PKA. Currently, AKAP13-bound PKA is known to inhibit AKAP13-Rho-GEF activity [38] and enhance PKC-PKD signaling [14,26] in isolated cardiomyocytes. If PKA binding to AKAP13 were required for development, it would suggest a novel AKAP13-mediated signaling pathway. The requirement for AKAP13-PKA binding during development would not be unprecedented since proper regulation of PKA signaling is required for mouse development [39]. Moreover, the cardiac-specific disruption of a regulatory subunit of PKA, which holds the kinase in an inactive state until cyclic AMP activation, results in a thinning of the myocardium and loss of trabeculation [40]. Interestingly, the phenotype observed after cardiac

disruption of PKA regulation [40] is very similar to the phenotype described for the *Akap13*-null mouse [11]. Alternatively, an unappreciated AKAP13 protein domain could be required for development. Additional mutational analysis of the AKAP13 gene locus is required to fully investigate these possibilities.

AKAP13 is expressed in many tissues during mouse development, and we were surprised that the AKAP13$^{\Delta GEF/\Delta GEF}$ mice did not have any obvious developmental phenotypes. This suggests that additional proteins compensate for the loss of AKAP13-mediated Rho and PKC-PKD signaling. Several additional AKAP family members are expressed or up-regulated during mouse development. Two that might have compensatory roles are AKAP6 (mAKAP) and AKAP12 (Gravin). AKAP6 is expressed developmentally and becomes highly expressed in cardiac and skeletal muscle [41] to coordinate PKA, small GTPases [19], and calcium signaling events [42,43]. AKAP12 is broadly expressed in mouse embryos and in the adult heart [44] and is required for gastrulation in zebrafish [2]. AKAP12 coordinates PKA, PKC, and Raf signaling events to regulate cellular shape changes and movement [45]. Additionally, Rho signaling may be compensated for by the large Rho-GEF containing structural protein, Obscurin, which is required for proper cardiac, muscle, and brain development in zebrafish [46]. The roles of AKAP6, AKAP12, and Obscurin during mouse development are unknown, and disruption of these proteins may produce developmental defects. It would also be interesting to determine if these scaffolds provide redundancy for the loss of AKAP13 protein domains by creating double mutant mice.

AKAP13$^{\Delta GEF/\Delta GEF}$ mice had normal viability, and their adult cardiac structure and electrical activity were indistinguishable from wild-type littermates despite high levels of AKAP13 expression in the heart. These results indicate that AKAP13 Rho-GEF and PKC-PKD binding domains are not required for mouse survival or normal cardiac physiology. They further suggest that additional proteins provide redundancy in controlling Rho, PKC, and PKD signaling during heart maturation and normal physiology. The scaffolding molecules AKAP6 and AKAP12, as well as Obscurin, could again provide this redundant function. Additional Rho-GEF proteins, including p115RhoGEF and p63RhoGEF, are expressed in cardiomyocytes and could provide redundancy for RhoA signaling [47]. AKAP13 is also expressed in other organs such as the vasculature, kidney, lung, gut and brain. Since we did not detect gross phenotypes in these tissues, other proteins likely compensated for the loss of AKAP13 Rho-GEF and PKC-PKD signaling in these tissues as well.

We then decided to test the role of the Rho-GEF and PKC-PKD binding domains for cardiac remodeling in response to β-adrenergic-mediated cardiac hypertrophy. These AKAP13 domains are important for the induction of isolated cardiomyocyte hypertrophy in response to adrenergic, angiotensin, and endothelin receptor signaling [14,20]. Additionally, PKD is required for the cardiac hypertrophic response to several stresses, including isoproterenol activation of β-adrenergic receptors *in vivo* [31]. Thus, we were surprised that AKAP13$^{\Delta GEF/\Delta GEF}$ mice induced a normal structural response to β-adrenergic-mediated cardiac hypertrophy. This indicates that the Rho-GEF and PKC-PKD domains of AKAP13

are not required for β-adrenergic-mediated cardiac growth in mice and that another AKAP regulates these changes. AKAP6 could regulate the changes *in vivo* because it transduces adrenergic signaling events, such as isoproterenol stimulation, into cardiomyocyte hypertrophy *in vitro* [9]. Despite the normal cardiac structural response to isoproterenol, the AKAP13 Rho-GEF and PKC-PKD binding domains might be important for regulating phenylephrine, angiotensin II, and endothelin-1-induced cardiac structural changes. The pathways activated by these molecules signal through AKAP13 to induce hypertrophy in isolated cardiomyocytes [14,20]. Thus, the series of mutant mice described in this study provide a great resource to investigate the role of specific AKAP13 protein domains in regulating cardiac hypertrophy induced by these molecules *in vivo*.

Surprisingly, AKAP13$^{\Delta GEF/\Delta GEF}$ mice did not increase cardiac fractional shortening or ejection fraction in response to isoproterenol treatment. This indicates that the AKAP13 Rho-GEF and PKC-PKD domains are important for the cardiac functional response to chronic β-adrenergic stimulation. There are several possible models why the ΔGEF mouse hearts fail to increase cardiac contractility. One model might be that the signaling pathway regulating cardiac functional adaptation to chronic isoproterenol treatment may require the AKAP13 Rho-GEF or PKC-PKD binding domains for signaling. In agreement with this, increased cardiac contraction by isoproterenol treatment requires the β$_1$-adrenergic receptor, which activates Ca^{2+}/calmodulin-dependent kinase II (CaMKII) signaling [48,49]. Furthermore, PKC appears to activate CaMKII

signaling in response to α_1-adrenergic receptor signaling in cardiomyocytes [50].

Thus, AKAP13-bound PKC may be required for β-adrenergic activation of

CaMKII and increased cardiac contractility. Additionally, isoproterenol might

activate AKAP13-RhoA signaling to induce the formation of myofibrils in a

manner similar to angiotensin II [51], thus increasing contraction. An alternative

model might be that the Rho-GEF and PKC-PKD domains are required for

signaling through compensatory pathways, including additional adrenergic or

angiotensin pathways, activated during cardiac hypertrophy. Measuring cardiac

contractility during acute stimulation of α- and β-adrenergic and angiotensin

pathways in AKAP13 mutant mice could help delineate between these two

models. Finally, the effect of disrupted AKAP13-Rho-GEF and -PKC-PKD

signaling on heart failure remains unclear. The AKAP13-ΔGEF mice might reach

heart failure at an earlier point than the wild-type mice. In agreement with this,

the mutant mice seem to have a slightly higher level of fibrosis than wild-type

mice after chronic isoproterenol treatment. Future experiments will likely require

a stronger hypertrophic induction and continual monitoring of cardiac function

until full heart failure is reached.

The regulatory elements that control expression of AKAP13 isoforms in

specific tissues remain unknown. ΔPKC mice lacked AKAP13-βGeo expression

specifically in ventricular cardiomyocytes of adult hearts. This suggests that the

ΔPKC mutation disrupts a cis-regulatory element required for AKAP13

expression in ventricular cardiomyocytes. Furthermore, there are several

conserved elements within the ΔPKC-disrupted intron that could function as

162

ventricular myocyte enhancer elements. A detailed analysis of these possible

enhancer elements would be required to test this possibility. Additionally, a more

detailed characterization of the AKAP13 isoforms expressed during development

and in adult tissues could aid in designing future studies. Evidence of additional

splicing events from GenBank cDNAs and ESTs suggests alternative termination

and cassette exons that could result in functionally important protein isoforms for

development or adult physiology. In fact, the main AKAP13 isoforms appear to

localize to different subcellular sites with AKAP-Lbc localizing to the cytoplasm

and cytoskeleton and Brx localizing to the cytoplasmic and nuclear

compartments [11,24,52]. A closer examination of all the transcripts expressed

from the AKAP13 gene locus is needed to better understand the effects of certain

mutations on AKAP13 protein structure. Since AKAP13 undergoes extensive

alternative splicing to produce multiple protein isoforms, it may be necessary to

add back specific transcripts in an *Akap13*-null background to identify the unique

roles played by each isoform during mouse development and disease.

Finally, the mice created in this study should prove valuable for investigating

AKAP13 functions in additional tissues and diseases as well. Since AKAP13 is

highly expressed in the vasculature, it may transduce angiotensin II, or

endothelin-1 signals into vascular responses. Genome-wide studies have linked

AKAP13 to corneal thickness of the eye [53] and Alzheimer's disease-associated

tau phosphorylation [54]. Since we found AKAP13 expression in the eye and

specific regions of the brain during development, further investigation into the

role of AKAP13 in these processes is warranted. Additionally, AKAP13 may

function in regulating immunity as it mediates glucocorticoid signaling in lymphocytes [55] and Toll-like receptor 2 signaling in epithelial and leukemia cell lines [52]. Finally, AKAP13 has been associated with several types of cancer, including leukemia [25], breast cancer [24,56,57], and colorectal cancer [58]. From these studies, AKAP13 appears to have diverse functions in a multitude of tissues. Despite this, we do not see an obvious phenotype in unstressed mice that lack the Rho-GEF and PKC-PKD binding domains of AKAP13. Thus, we propose that these domains function to transduce acute signaling events in response to stresses.

In summary, we found that the Rho-GEF and PKC-PKD binding domains of AKAP13 are not required for mouse development, normal adult cardiac architecture, or β-adrenergic-induced cardiac hypertrophy. Surprisingly, we found that the AKAP13 Rho-GEF and PKC-PKD binding domains are required for the proper cardiac functional response to β-adrenergic stimulation. These findings suggest that additional AKAP13 protein domains are sufficient for regulating normal mouse development, but that AKAP13 is critical for transducing signaling events that regulate stress responses, such as regulating cardiac function during hypertrophy. The mice generated in this study provide an ideal system to investigate the roles of specific AKAP13 protein domains in mediating these stress responses. They could also be used to investigate the roles of AKAPs in pathological responses to injury, particularly in tissues expressing AKAP13, such as blood vessels, the eye, and the brain.

4.5 Materials and Methods

Ethics statement

All mouse studies were conducted in accordance with protocols approved by the

Institutional Animal Care and Use Committee and the Laboratory Animal

Research Center at the University of California, San Francisco. Protocol ID:

AN080925-02B.

Characterization of AKAP13 gene-trap ES cells

Gene-trap events within AKAP13 were identified from the International Gene

Trap Consortium (IGTC) database (at www.genetrap.org) and the IGTC

Sequence Tag Alignments track on the UCSC Genome Browser [34,35]. From

the sequence tag alignments, we identified ten uniquely trapped exons for

AKAP13. We then mapped these trapping events onto the AKAP13 protein to

identify the domains affected by the traps. The following cell lines were obtained

from the Mutant Mouse Regional Resource Centers: AG0213 (for AKAP13-ΔBrx),

CSJ306 (for AKAP13-ΔGEF), & CSJ288 (for AKAP13-ΔPKC) (Figure 4.1). The

feeder free gene-trap ES cell lines were cultured in normal growth media

supplemented with murine leukemia inhibiting factor as described [33]. Correct

splicing of AKAP13 exons into the gene-trap construct was verified by RT-PCR

and sequencing. Total RNA was extracted from ES cells with Trizol (Invitrogen),

and RT-PCR was conducted using the SuperScript III One-Step RT-PCR kit

(Invitrogen). Forward primers for RT-PCR were designed using Primer3 (Table

4.3A) [59]. The resulting products were sequence verified and confirmed the expected AKAP13–gene-trap splicing events.

The genomic insertion sites for the gene-trap events were identified by long-range PCR of genomic DNA using Phusion High-Fidelity DNA Polymerase (Finnzyme). In summary, Primer3 was used to design ~25mer forward and reverse primers with melting temperatures of 62–68°C throughout the introns containing the gene-trap insertions. These designed primers were used with common primers within the gene-trap construct to amplify genomic DNA (Table 4.3B). The PCR products were cloned into pCR-XL-TOPO (Invitrogen) and sequenced to identify the genomic insertion sites.

Mouse studies

Chimeric mice were generated by the Gladstone Transgenic Gene-Targeting Core by injecting C57Bl/6 blastocysts with the gene-trapped ES cell lines AG0213, CSJ306 and CSJ288. Male chimeric mice (N0) were backcrossed to C57Bl/6 (National Cancer Institute, National Institutes of Health) females and the resulting progeny (N1) were genotyped to identify heterozygotes carrying the gene-trap allele. Mice were genotyped from tail clips with a REDExtract-N-Amp Tissue PCR Kit (Sigma Aldrich) and the primer pairs listed in Table 4.3C. Heterozygous mice were inter-crossed to obtain homozygous mice, AKAP13$^{\Delta Brx/\Delta Brx}$ (from AG0213), AKAP13$^{\Delta GEF/\Delta GEF}$ (from CSJ306), AKAP13$^{\Delta PKC/\Delta PKC}$ (from CSJ288), for the three gene-trap mutational events, and litters were analyzed for Mendelian ratios at 3 weeks of age. All studies

performed in this report used littermate and age-matched control and mutant mice generated from heterozygous crosses.

These mouse lines will be available through the Mutant Mouse Regional Resource Center (MMRRC).

Table 4.3. Primer Sequences

A. RT-PCR primers for AKAP13-gene trap splicing

Primer Name	Location (Mutant)	Sequence (5'-3')	Size (bp)
MJS218	Exon 8 (ΔBrx For)	ACACCCAAGATGAAGCAAGG	441
MJS219	Exon Brx (ΔBrx For)	AATTTCGGACCTGTGTGAGC	573
MJS220	Exon 21-22 (ΔGEF For)	TGGAGTTGGCAATGATGAGA	674
AKAPlbc-F1_MS	Exon 27 (ΔPKC For)	TGAAGAGCACAACAGGAAGG	432
MJS213	Gene Trap (Univ. Rev)	TAATGGGATAGGTCACGT	

B. Long-Range PCR primers in the gene trap construct

Primer Name	Location	Sequence (5'-3')
MJS236	βGal (Rev)	CCCTGCCATAAAGAAACTGTTACCC
MJS237	Neo (For)	GTGGAGAGGCTATTCGGCTATGACT

C. Genotyping primers

Primer Name	Allele Identified	Sequence (5'-3')	Size (bp)
MJS299	Univ. ΔBrx (For)	TGGCATCTACCCAGGATCTC	
MJS390	WT ΔBrx (Rev)	CAAAGGCCATCTGCACACC	1697
MJS284	GT ΔBrx (Rev)	GTGAGGCCAAGTTTGTTTCC	1275
MJS274	Univ. ΔGEF (For)	TACCAAATAACAGTGCCTGCTCTCC	
MJS253	WT ΔGEF (Rev)	ATCTTGAGTGTGCGGATGTGATGTA	1533
MJS214	GT ΔGEF (Rev)	AGTATCGGCCTCAGGAAGATCG	1182
MJS339	WT ΔPKC (For)	TGTCTCTGGCCTGTTTGTGA	1112
MJS340	WT ΔPKC (Rev)	TCGGAAGAGGTTAAGGGACA	
MJS272	GT ΔPKC (For)	ACATTTCCCCGAAAAGTGC	435
MJS260	GT ΔPKC (Rev)	GGCTCACACTGGGTTCAATC	

(A) RT-PCR primers for verifying AKAP13 gene-trap splicing events are listed. The primer locations and mutant line verified are indicated. The size of the RT-PCR product is given in base pairs (bp). (B) The common long-range PCR primers within the gene-trap construct are listed. These primers were used with AKAP13 specific genomic DNA primers to identify the gene-trap insertion. (C) The genotyping primers used to identify the wild-type and mutant allele for the three mutant mouse lines are listed. The primer direction is also given: forward (For) and reverse (Rev). The size of the PCR product is given in base pairs (bp).

X-Gal staining of gene-trap embryos and adult tissue

To identify AKAP13 expression patterns during development, whole-mount embryos at E8.5, E9.5, and E10.5 and cryosectioned E14.5 embryos were stained with X-Gal. To determine embryonic ages, the morning a post-coital plug was identified was designated as E0.5. Whole embryos (E8.5, E9.5, and E10.5) were fixed in 2% formaldehyde (Sigma), 0.2% glutaraldehyde (Sigma), 0.02% sodium deoxycholate (Sigma), and 0.01% Nonidet P-40 substitute (Fluka) in PBS (Mediatech) for 15 to 45 min, depending on age, at 4°C. Embryos were permeabilized in 0.02% sodium deoxycholate and 0.01% Nonidet P-40 substitute in PBS at 4°C overnight. Embryos were stained in 5 mM potassium ferricyanide (Sigma), 5 mM potassium ferrocyanide (Sigma), 2 mM $MgCl_2$ (Sigma), 1 mg/ml X-Gal (Fermentas, AllStar Scientific, or Invitrogen), 0.02% sodium deoxycholate and 0.01% Nonidet P-40 substitute in PBS at 37°C for 5 hours. Embryos were post-fixed in 4% paraformaldehyde (PFA) at 4°C overnight. Images were obtained on a Leica MZ16F dissecting microscope with a Leica DFC500 camera and Leica Application Suite software.

E14.5 embryos were bisected and fixed in 4% PFA and 0.2% glutaraldehyde in PBS for 1 hour at 4°C. The embryos were sucrose protected and frozen in Tissue-Tek OCT (Sakura Finetek). Cryostat sections were stained with X-Gal and mounted. Mosaic images of entire sagittal and transverse sections were obtained using an inverted Axiovert 200M microscope and AxioCam HRc (Carl Zeiss) camera. Individual images were stitched together to create a mosaic image using AxioVision Software. Higher magnification images of specific

169

regions of interest were obtained using an upright Leica DM4000B microscope with a QImaging Retiga EXi Fast 1394 camera and Image-Pro Plus software.

Adult organs were obtained from euthanized 17–18-week-old mice. Mice were perfused with 10mM KCl (Sigma), followed by PBS, and finally with 4% PFA. Heart, kidney, and brain samples were bisected and organs were fixed in 4% PFA for 1 hour at 4°C. Organs were permeabilized in 2 mM $MgCl_2$, 0.01% sodium deoxycholate and 0.02% Nonidet P-40 substitute in PBS at 4°C overnight. They were stained in 5 mM potassium ferricyanide, 5 mM potassium ferrocyanide, 2 mM $MgCl_2$, 1 mg/ml X-Gal, 0.02% sodium deoxycholate and 0.01% Nonidet P-40 substitute in PBS at 37°C for 5 hours. Organs were post-fixed in 4% PFA at 4°C overnight. Images were obtained on a Leica MZ FLIII dissecting microscope with an AxioCam (Carl Zeiss) camera and Openlab 4.0.4 software.

Quantitative PCR analysis

Gene expression analysis was performed on total RNA isolated from neonatal mouse heart and lung tissue. Wild-type, heterozygous, and homozygous samples were collected from six mice each for the three mouse lines. Heart and lung samples were homogenized (4.5 mm Tissue Tearor, Research Products International) in Trizol (Invitrogen). cDNA was generated from 1 μg of TurboDNAse-treated (Ambion) total RNA with the SuperScript III First Strand Synthesis kit and random hexamers (Invitrogen) as described by the manufacturer. Expression was assessed using TaqMan probesets (Applied

Biosystems) for AKAP13 exon-exon junctions E4-5 (Mm01320101_m1), Brx-9 (Mm01318390_m1), and E37-38 (Mm01320099_m1) as well as GAPDH (Mm99999915_g1) and β-actin (Mm00607939_s1). Reactions were run on an Applied Biosystems 7900HT real-time thermocycler. Samples were assayed in technical triplicates and average AKAP13 expression levels were determined from GAPDH and β-actin normalized values. Relative expression was calculated against wild-type mouse samples. Means ± standard deviations were reported for six mice of each genotype. One-way ANOVA and Bonferroni's multiple comparison tests were conducted to determine significant differences (Prism 5; GraphPad).

Electrocardiographic analysis

Six-lead ECG analysis was conducted on 16–18-week-old wild-type and AKAP13$^{\Delta GEF/\Delta GEF}$ (ΔGEF) littermate male mice anesthetized with inhaled Isoflurane, USP (Baxter and Phoenix Pharmaceutical) [60]. In brief, anesthetized mice were placed on a heating pad, and body temperature was continually monitored to maintain at 36–37°C. Needle electrodes were implanted subcutaneously at each limb and ECGs were recorded for leads I, II, III, aVR, aVL, and aVF using the AD Instruments system: Dual BioAmp (ML135), PowerLab 4/30 (ML866) and Chart5 Pro (v5.4.2). ECG data were acquired for 15-45 seconds for each lead. The ECG recordings were analyzed using the mouse preset option in Chart5 Pro. The ECG signals were averaged within each lead and the temporal locations of P Start, P Peak, P End, QRS Start, QRS Max,

QRS End, T Peak, and T End were identified and manually adjusted as needed. Values were calculated for heart rate, PR interval, P wave duration, QRS interval, and corrected QT interval (using the provided Mitchell *et. al* calculation). These calculated values were averaged across all leads for a given mouse. Means ± standard deviations were reported for six mice of each genotype. Two-tailed student's t-test was conducted to determine significant differences (Excel).

Cardiac structural analysis

Hearts were isolated from the six wild-type and six ΔGEF littermate mice used for ECG analysis. Mice were weighed and euthanized and their hearts were collected and weighed. Hearts were washed with heparin (5 μg/ml) and PBS to remove the blood and incubated in 25 mM KCl to relax the cardiac muscle. The hearts were fixed in 4% PFA at 4°C overnight. The right tibia was removed and the length was measured using calipers (Scienceware). Hearts were imaged using a Leica MZ FLIII dissecting microscope with an AxioCam (Carl Zeiss) camera and Openlab 4.0.4 software. The hearts were then embedded in paraffin for sectioning. Five-micron sections were cut, deparaffinized, rehydrated, and stained with hematoxylin and eosin (H&E) and Masson's trichrome following standard protocols. Mosaic images of entire heart sections were obtained using an inverted Axiovert 200M microscope and AxioCam HRc (Carl Zeiss) camera. Individual images were stitched together to create a mosaic image using AxioVision Software. Higher magnification images of specific regions of interest

were obtained using an upright Leica DM4000B microscope with a QImaging
Retiga EXi Fast 1394 camera and Image-Pro Plus software.

Isoproterenol-induced cardiac hypertrophy

Cardiac hypertrophy was induced in 22–32-week-old wild-type and
$AKAP13^{\Delta GEF/\Delta GEF}$ (ΔGEF) littermate mice [36]. Mice were treated for 14 days with
isoproterenol (60 mg/kg per day; Sigma) diluted in PBS (Iso) or PBS alone
(vehicle; Veh) using mini-osmotic pumps (Alzet Model 2002) implanted
subcutaneously into the peritoneum. Three wild-type and three ΔGEF mice were
Veh-treated, four wild-type and six ΔGEF mice were Iso-treated. On day 14 after
initiating treatment, mice were weighed and euthanized. Their hearts were
collected, weighed, and processed for structural analysis as described above.
Sections were stained with H&E or Masson's trichrome. Fibrosis was quantified
from mosaic images of Masson's trichrome stained sections using Image-Pro
Plus software. Means ± standard deviations were reported. Two-tailed student's
t-test was conducted to determine significant differences (Excel and Prism 5;
GraphPad).

One additional ΔGEF mouse was treated with Iso and died on the fourth day
of treatment. Baseline echocardiography indicated that this mouse had enlarged
right and left atria.

Echocardiography

Baseline (before implantation of mini-osmotic pumps) and end-point (day 13) echocardiograms were recorded for each mouse as described [61]. M-Mode and B-Mode echocardiograms were recorded using the Vevo 770 Imaging System and RMV707B probe (VisualSonics). M-Mode measurements were taken for diastolic and systolic left ventricular anterior wall (LVAW;d & LVAW;s), internal diameter (LVID;d & LVID;s), and posterior wall (LVPW;d & LVPW;s). Corrected left ventricular mass (LV Mass; mg) was calculated from these measurements:

$$LV\ Mass = 0.8 \times (1.053 \times ((LVID;d + LVPW;d + LVAW;d)^3 - LVID;d^3))$$

Left ventricle fractional shortening (FS) was also calculated from these measurements:

$$FS\ (\%) = 100 \times \left(\frac{LVID;d - LVID;s}{LVID;d} \right)$$

Measurements were made on three separate heartbeats for each mouse.

B-Mode measurements were taken for endocardial area and major axis at diastole and systole (End Area;d, End Area;s, & End Major;d, End Major;s respectively). These B-Mode measurements were used to calculate endocardial volume at diastole and systole (End Vol;d & End Vol;s), left ventricular stroke volume (End SV), and left ventricular ejection fraction (EF):

$$End\ Vol;d = \frac{4\pi}{3} \times \frac{End\ Major;d}{2} \times \left(\frac{End\ Area;d}{\pi \left(\frac{End\ Major;d}{2} \right)} \right)^2$$

$$End\ Vol;s = \frac{4\pi}{3} \times \frac{End\ Major;s}{2} \times \left(\frac{End\ Area;s}{\pi \left(\frac{End\ Major;s}{2} \right)} \right)^2$$

$$End\ SV = End\ Vol;d\ -\ End\ Vol;s$$

$$EF(\%) = 100 \times \left(\frac{End\ SV}{End\ Vol;d} \right)$$

One set of B-Mode measurements were made per mouse.

Means ± standard deviations were reported. One-way ANOVA and Bonferroni's multiple comparison tests were conducted to determine significant differences (Prism 5; GraphPad).

Statistical analysis

Two-tailed student's t-tests were performed using Excel or Prism 5 (GraphPad) software. One-way ANOVA followed by Bonferroni's multiple comparison tests were performed using Prism 5 software (GraphPad).

4.6 Acknowledgments

The authors would like to thank Mark von Zastrow, Benoit Bruneau, Silvio Gutkind, Oren Shibolet, James Segars, Joshua Wythe, Trieu Nguyen, Jennifer Ng, Faith Kreitzer, Jill Dunham and Gary Howard for valuable discussions and technical advice. We would also like to thank Paul Swinton of the Gladstone Institutes Transgenic Gene-Targeting Core for microinjection of ES cells and Jo Dee Fish and Caroline Miller of the Gladstone Institutes Histology Core for histological sectioning and staining.

4.7 References

1. Klingbeil P, Frazzetto G, Bouwmeester T (2001) Xgravin-like (Xgl), a novel putative a-kinase anchoring protein (AKAP) expressed during embryonic development in Xenopus. Mech Dev 100: 323-326.
2. Weiser DC, Pyati UJ, Kimelman D (2007) Gravin regulates mesodermal cell behavior changes required for axis elongation during zebrafish gastrulation. Genes Dev 21: 1559-1571.

3. Newhall KJ, Criniti AR, Cheah CS, Smith KC, Kafer KE, et al. (2006) Dynamic anchoring of PKA is essential during oocyte maturation. Curr Biol 16: 321-327.

4. Rawe VY, Payne C, Navara C, Schatten G (2004) WAVE1 intranuclear trafficking is essential for genomic and cytoskeletal dynamics during fertilization: cell-cycle-dependent shuttling between M-phase and interphase nuclei. Dev Biol 276: 253-267.

5. Tunquist BJ, Hoshi N, Guire ES, Zhang F, Mullendorff K, et al. (2008) Loss of AKAP150 perturbs distinct neuronal processes in mice. Proc Natl Acad Sci U S A 105: 12557-12562.

6. Soderling SH, Guire ES, Kaech S, White J, Zhang F, et al. (2007) A WAVE-1 and WRP signaling complex regulates spine density, synaptic plasticity, and memory. J Neurosci 27: 355-365.

7. Soderling SH, Langeberg LK, Soderling JA, Davee SM, Simerly R, et al. (2003) Loss of WAVE-1 causes sensorimotor retardation and reduced learning and memory in mice. Proc Natl Acad Sci U S A 100: 1723-1728.

8. Tingley WG, Pawlikowska L, Zaroff JG, Kim T, Nguyen T, et al. (2007) Gene-trapped mouse embryonic stem cell-derived cardiac myocytes and human genetics implicate AKAP10 in heart rhythm regulation. Proc Natl Acad Sci U S A 104: 8461-8466.

9. Pare GC, Bauman AL, McHenry M, Michel JJ, Dodge-Kafka KL, et al. (2005) The mAKAP complex participates in the induction of cardiac myocyte hypertrophy by adrenergic receptor signaling. J Cell Sci 118: 5637-5646.

10. Chen L, Marquardt ML, Tester DJ, Sampson KJ, Ackerman MJ, et al. (2007) Mutation of an A-kinase-anchoring protein causes long-QT syndrome. Proc Natl Acad Sci U S A 104: 20990-20995.

11. Mayers CM, Wadell J, McLean K, Venere M, Malik M, et al. (2010) The Rho guanine nucleotide exchange factor AKAP13 (BRX) is essential for cardiac development in mice. J Biol Chem 285: 12344-12354.

12. Carnegie GK, Means CK, Scott JD (2009) A-kinase anchoring proteins: from protein complexes to physiology and disease. IUBMB Life 61: 394-406.

13. Wong W, Scott JD (2004) AKAP signalling complexes: focal points in space and time. Nat Rev Mol Cell Biol 5: 959-970.

14. Carnegie GK, Soughayer J, Smith FD, Pedroja BS, Zhang F, et al. (2008) AKAP-Lbc mobilizes a cardiac hypertrophy signaling pathway. Mol Cell 32: 169-179.

15. Diviani D, Baisamy L, Appert-Collin A (2006) AKAP-Lbc: a molecular scaffold for the integration of cyclic AMP and Rho transduction pathways. Eur J Cell Biol 85: 603-610.

16. Kamp TJ, Hell JW (2000) Regulation of cardiac L-type calcium channels by protein kinase A and protein kinase C. Circ Res 87: 1095-1102.

17. McConnell BK, Popovic Z, Mal N, Lee K, Bautista J, et al. (2009) Disruption of protein kinase A interaction with A-kinase-anchoring proteins in the heart in vivo: effects on cardiac contractility, protein kinase A phosphorylation, and troponin I proteolysis. J Biol Chem 284: 1583-1592.

18. Mauban JR, O'Donnell M, Warrier S, Manni S, Bond M (2009) AKAP-scaffolding proteins and regulation of cardiac physiology. Physiology (Bethesda) 24: 78-87.

19. Dodge-Kafka KL, Soughayer J, Pare GC, Carlisle Michel JJ, Langeberg LK, et al. (2005) The protein kinase A anchoring protein mAKAP coordinates two integrated cAMP effector pathways. Nature 437: 574-578.

20. Appert-Collin A, Cotecchia S, Nenniger-Tosato M, Pedrazzini T, Diviani D (2007) The A-kinase anchoring protein (AKAP)-Lbc-signaling complex mediates alpha1 adrenergic receptor-induced cardiomyocyte hypertrophy. Proc Natl Acad Sci U S A 104: 10140-10145.

21. Su AI, Wiltshire T, Batalov S, Lapp H, Ching KA, et al. (2004) A gene atlas of the mouse and human protein-encoding transcriptomes. Proc Natl Acad Sci U S A 101: 6062-6067.

22. Hailesellasse Sene K, Porter CJ, Palidwor G, Perez-Iratxeta C, Muro EM, et al. (2007) Gene function in early mouse embryonic stem cell differentiation. BMC Genomics 8: 85.

23. Diviani D, Soderling J, Scott JD (2001) AKAP-Lbc anchors protein kinase A and nucleates Galpha 12-selective Rho-mediated stress fiber formation. J Biol Chem 276: 44247-44257.

24. Rubino D, Driggers P, Arbit D, Kemp L, Miller B, et al. (1998) Characterization of Brx, a novel Dbl family member that modulates estrogen receptor action. Oncogene 16: 2513-2526.

25. Toksoz D, Williams DA (1994) Novel human oncogene lbc detected by transfection with distinct homology regions to signal transduction products. Oncogene 9: 621-628.

26. Carnegie GK, Smith FD, McConnachie G, Langeberg LK, Scott JD (2004) AKAP-Lbc nucleates a protein kinase D activation scaffold. Mol Cell 15: 889-899.

27. Klussmann E, Edemir B, Pepperle B, Tamma G, Henn V, et al. (2001) Ht31: the first protein kinase A anchoring protein to integrate protein kinase A and Rho signaling. FEBS Lett 507: 264-268.

28. Vega RB, Harrison BC, Meadows E, Roberts CR, Papst PJ, et al. (2004) Protein kinases C and D mediate agonist-dependent cardiac hypertrophy through nuclear export of histone deacetylase 5. Mol Cell Biol 24: 8374-8385.

29. Gu JL, Muller S, Mancino V, Offermanns S, Simon MI (2002) Interaction of G alpha(12) with G alpha(13) and G alpha(q) signaling pathways. Proc Natl Acad Sci U S A 99: 9352-9357.

30. Offermanns S, Zhao LP, Gohla A, Sarosi I, Simon MI, et al. (1998) Embryonic cardiomyocyte hypoplasia and craniofacial defects in G alpha q/G alpha 11-mutant mice. Embo J 17: 4304-4312.

31. Fielitz J, Kim MS, Shelton JM, Qi X, Hill JA, et al. (2008) Requirement of protein kinase D1 for pathological cardiac remodeling. Proc Natl Acad Sci U S A 105: 3059-3063.

32. Lin Q, Schwarz J, Bucana C, Olson EN (1997) Control of mouse cardiac morphogenesis and myogenesis by transcription factor MEF2C. Science 276: 1404-1407.

33. Skarnes WC (2000) Gene trapping methods for the identification and functional analysis of cell surface proteins in mice. Methods Enzymol 328: 592-615.

34. Nord AS, Chang PJ, Conklin BR, Cox AV, Harper CA, et al. (2006) The International Gene Trap Consortium Website: a portal to all publicly available gene trap cell lines in mouse. Nucleic Acids Res 34: D642-648.

35. Fujita PA, Rhead B, Zweig AS, Hinrichs AS, Karolchik D, et al. (2010) The UCSC Genome Browser database: update 2011. Nucleic Acids Res [Epub ahead of print].

36. Jaehnig EJ, Heidt AB, Greene SB, Cornelissen I, Black BL (2006) Increased susceptibility to isoproterenol-induced cardiac hypertrophy and impaired weight gain in mice lacking the histidine-rich calcium-binding protein. Mol Cell Biol 26: 9315-9326.

37. Zou Y, Komuro I, Yamazaki T, Kudoh S, Uozumi H, et al. (1999) Both Gs and Gi proteins are critically involved in isoproterenol-induced cardiomyocyte hypertrophy. J Biol Chem 274: 9760-9770.

38. Diviani D, Abuin L, Cotecchia S, Pansier L (2004) Anchoring of both PKA and 14-3-3 inhibits the Rho-GEF activity of the AKAP-Lbc signaling complex. Embo J 23: 2811-2820.

39. Amieux PS, Howe DG, Knickerbocker H, Lee DC, Su T, et al. (2002) Increased basal cAMP-dependent protein kinase activity inhibits the formation of mesoderm-derived structures in the developing mouse embryo. J Biol Chem 277: 27294-27304.

40. Yin Z, Jones GN, Towns WH, 2nd, Zhang X, Abel ED, et al. (2008) Heart-specific ablation of Prkar1a causes failure of heart development and myxomagenesis. Circulation 117: 1414-1422.

41. McCartney S, Little BM, Langeberg LK, Scott JD (1995) Cloning and characterization of A-kinase anchor protein 100 (AKAP100). A protein that targets A-kinase to the sarcoplasmic reticulum. J Biol Chem 270: 9327-9333.

42. Kapiloff MS, Jackson N, Airhart N (2001) mAKAP and the ryanodine receptor are part of a multi-component signaling complex on the cardiomyocyte nuclear envelope. J Cell Sci 114: 3167-3176.

43. Kapiloff MS, Schillace RV, Westphal AM, Scott JD (1999) mAKAP: an A-kinase anchoring protein targeted to the nuclear membrane of differentiated myocytes. J Cell Sci 112 (Pt 16): 2725-2736.

44. Gelman IH, Tombler E, Vargas J, Jr. (2000) A role for SSeCKS, a major protein kinase C substrate with tumour suppressor activity, in cytoskeletal architecture, formation of migratory processes, and cell migration during embryogenesis. Histochem J 32: 13-26.

45. Su B, Bu Y, Engelberg D, Gelman IH (2010) SSeCKS/Gravin/AKAP12 inhibits cancer cell invasiveness and chemotaxis by suppressing a protein kinase C-Raf/MEK/ERK pathway. J Biol Chem 285: 4578-4586.

46. Raeker MO, Bieniek AN, Ryan AS, Tsai HJ, Zahn KM, et al. (2010) Targeted deletion of the zebrafish obscurin A RhoGEF domain affects heart, skeletal muscle and brain development. Dev Biol 337: 432-443.

47. Porchia F, Papucci M, Gargini C, Asta A, De Marco G, et al. (2008) Endothelin-1 up-regulates p115RhoGEF in embryonic rat cardiomyocytes during the hypertrophic response. J Recept Signal Transduct Res 28: 265-283.

48. Wang W, Zhu W, Wang S, Yang D, Crow MT, et al. (2004) Sustained beta1-adrenergic stimulation modulates cardiac contractility by Ca2+/calmodulin kinase signaling pathway. Circ Res 95: 798-806.

49. Yoo B, Lemaire A, Mangmool S, Wolf MJ, Curcio A, et al. (2009) Beta1-adrenergic receptors stimulate cardiac contractility and CaMKII activation in vivo and enhance cardiac dysfunction following myocardial infarction. Am J Physiol Heart Circ Physiol 297: H1377-1386.

50. O-Uchi J, Komukai K, Kusakari Y, Obata T, Hongo K, et al. (2005) alpha1-adrenoceptor stimulation potentiates L-type Ca2+ current through Ca2+/calmodulin-dependent PK II (CaMKII) activation in rat ventricular myocytes. Proc Natl Acad Sci U S A 102: 9400-9405.

51. Aoki H, Izumo S, Sadoshima J (1998) Angiotensin II activates RhoA in cardiac myocytes: a critical role of RhoA in angiotensin II-induced premyofibril formation. Circ Res 82: 666-676.

52. Shibolet O, Giallourakis C, Rosenberg I, Mueller T, Xavier RJ, et al. (2007) AKAP13, a RhoA GTPase-specific guanine exchange factor, is a novel regulator of TLR2 signaling. J Biol Chem 282: 35308-35317.

53. Vitart V, Bencic G, Hayward C, Skunca Herman J, Huffman J, et al. (2010) New loci associated with central cornea thickness include COL5A1, AKAP13 and AVGR8. Hum Mol Genet 19: 4304-4311.

54. Azorsa DO, Robeson RH, Frost D, Meec hoovet B, Brautigam GR, et al. (2010) High-content siRNA screening of the kinome identifies kinases involved in Alzheimer's disease-related tau hyperphosphorylation. BMC Genomics 11: 25.

55. Kino T, Souvatzoglou E, Charmandari E, Ichijo T, Driggers P, et al. (2006) Rho family Guanine nucleotide exchange factor Brx couples extracellular signals to the glucocorticoid signaling system. J Biol Chem 281: 9118-9126.

56. Bonuccelli G, Casimiro MC, Sotgia F, Wang C, Liu M, et al. (2009) Caveolin-1 (P132L), a common breast cancer mutation, confers mammary cell invasiveness and defines a novel stem cell/metastasis-associated gene signature. Am J Pathol 174: 1650-1662.

57. Wirtenberger M, Tchatchou S, Hemminki K, Klaes R, Schmutzler RK, et al. (2006) Association of genetic variants in the Rho guanine nucleotide exchange factor AKAP13 with familial breast cancer. Carcinogenesis 27: 593-598.

58. Hu JK, Wang L, Li Y, Yang K, Zhang P, et al. (2010) The mRNA and protein expression of A-kinase anchor proteins 13 in human colorectal cancer. Clin Exp Med 10: 41-49.

59. Rozen S, Skaletsky H (2000) Primer3 on the WWW for general users and for biologist programmers. Methods Mol Biol 132: 365-386.

60. Nuyens D, Stengl M, Dugarmaa S, Rossenbacker T, Compernolle V, et al. (2001) Abrupt rate accelerations or premature beats cause life-threatening arrhythmias in mice with long-QT3 syndrome. Nat Med 7: 1021-1027.

61. Zhang Y, Takagawa J, Sievers RE, Khan MF, Viswanathan MN, et al. (2007) Validation of the wall motion score and myocardial performance indexes as novel techniques to assess cardiac function in mice after myocardial infarction. Am J Physiol Heart Circ Physiol 292: H1187-1192.

Chapter 5

Summary and Discussion

5.1 A summary of our results studying the physiological functions of AKAP13

This dissertation was designed to elucidate specific G-protein-signaling cascades that regulate cardiovascular development and physiology. Since G-proteins can activate multiple signaling cascades, we focused on the scaffolding molecules A-kinase anchoring proteins (AKAPs), which organize signaling complexes to integrate G-protein signals into specific physiological effects [1].

Through analysis of gene expression studies and literature, we identified AKAP13 as a top candidate to regulate aspects of cardiovascular development and physiology. Expression analysis revealed that AKAP13 is up-regulated during developmental processes and is highly expressed in mouse embryonic stem (ES) cells (Chapter 1). Literature analysis revealed that AKAP13 is highly expressed in the adult heart [2,3], coordinates signaling cascades that induce hypertrophic growth in isolated cardiomyocytes [4,5], and appears to be required for cardiovascular development [6]. To identify the developmental processes regulated by AKAP13, we used RNA interference (RNAi), a loss of function technique, to knock down AKAP13 expression (Figure 5.1 A-1) Despite our expectations, we found that AKAP13 knockdown did not affect mouse ES cell differentiation into functional cardiomyocytes or expression of endodermal or endothelial marker genes (Chapter 2). Additionally, AKAP13 knockdown did not

affect angiogenic processes, such as wound healing, tube formation, and VEGF-activation of protein kinase D (PKD), in human umbilical vein endothelial cells (HUVECs) (Chapter 3). We used AKAP13 truncation mutant mice, derived from gene-trap events, to determine the developmental functions of the Rho-guanine nucleotide exchange factor (Rho-GEF) and protein kinase C- (PCK) PKD binding domains (Chapter 4). Although these domains mediate the only known signaling processes downstream of AKAP13, they were not required for embryonic development or mouse survival and the mutant mice lacked obvious phenotypes under basal conditions (Figure 5.1 A-2). Finally, we used the AKAP13 truncation mutant mice to determine the physiological functions of these domains during β-adrenergic-induced cardiac hypertrophy (Chapter 4). These protein domains are not required for the increase in heart size, but are required for normal cardiac functional response to chronic β-adrenergic stimulation (Figure 5.1 B).

A

1

AKAP13

PKA   GEF   PKC PKD P   LZ

RhoA

Knockout Embryos

Early embryonic death (E9.5)
and cardiovascular defects
The mice we analyzed lacked the proper targeting
event - we could not verify the phenotype
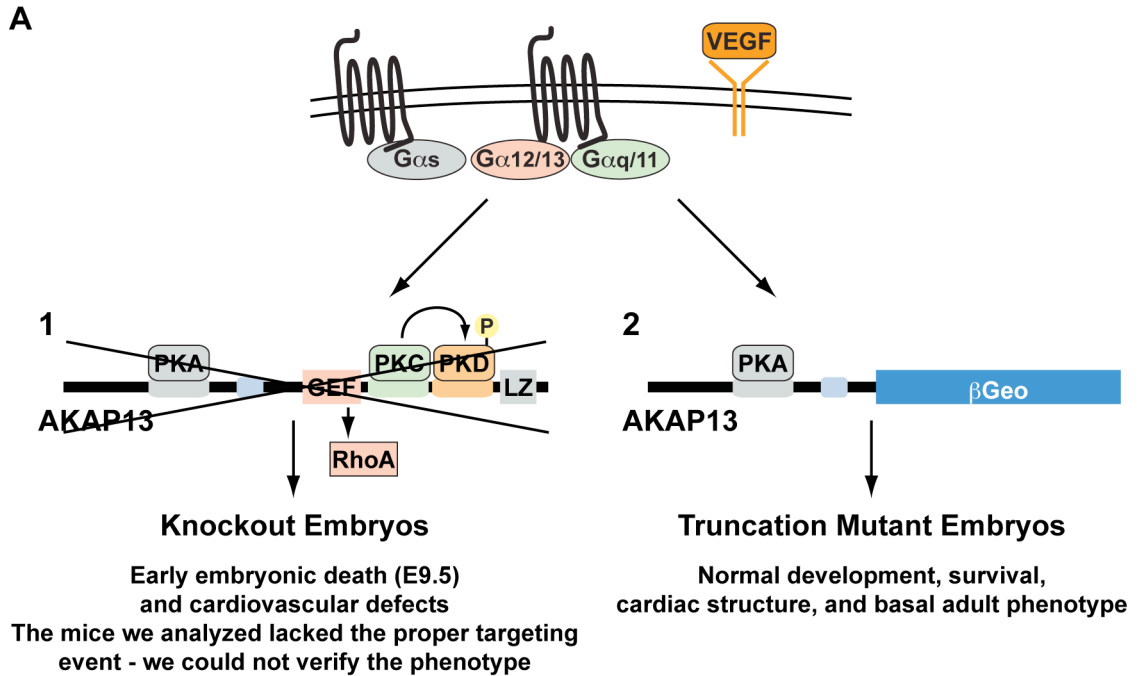
RNAi in ES Cells

Normal ES cell maintenance and differentiation
(cardiomyocyte, endoderm, and endothelial cell)

RNAi in HUVECs

Normal angiogenic processes: wound healing,
tube formation, and VEGF-activation of PKD

2

AKAP13

PKA   βGeo

Truncation Mutant Embryos

Normal development, survival,
cardiac structure, and basal adult phenotype

B

Iso

Gαs   Gα12/13 Gαq/11

cAMP

1

AKAP13

PKA   GEF   PKC PKD P   LZ

RhoA

Wild-Type Adult

Increased heart weight, size,
fractional shortening, and ejection fraction

2

AKAP13

PKA   βGeo

Truncation Mutant Adult

Increased heart weight and size
No change in fractional shortening or
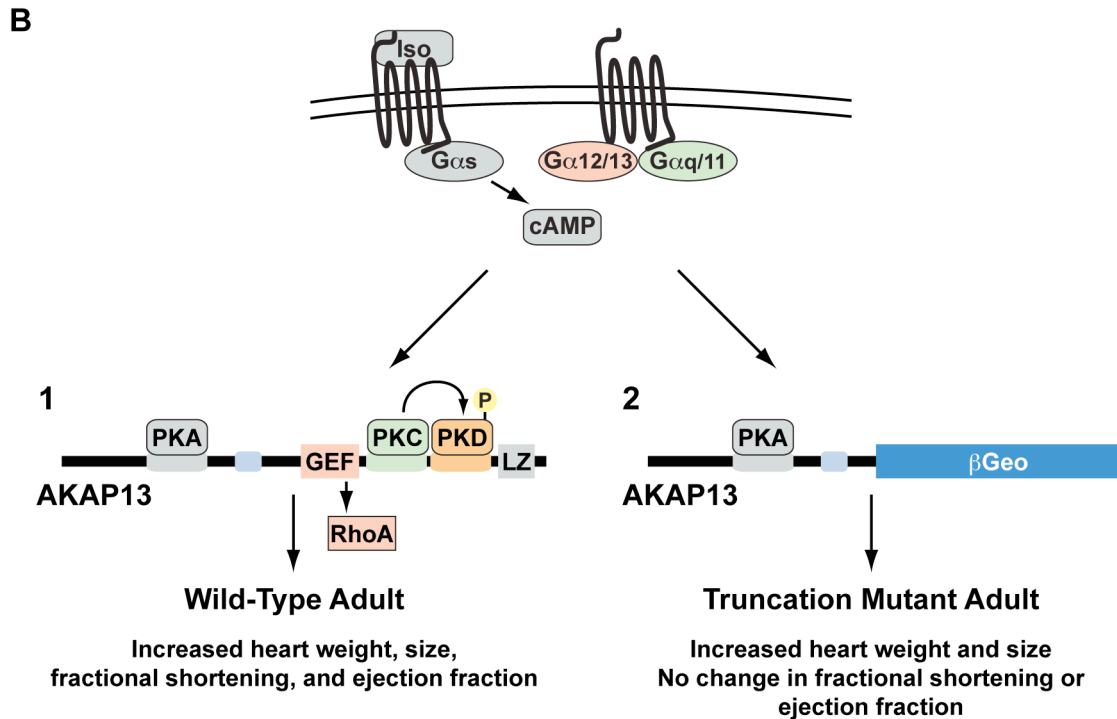ejection fraction

184

Figure 5.1. Summary of our AKAP13 loss of function and truncation mutant studies during cardiovascular development and physiology. (A) We tested the role of AKAP13 in mediating cardiovascular development by (1) loss of function and (2) truncation mutant approaches. (A-1) *Akap13*-null (i.e., Knockout) mice were reported do die at about embryonic day 9.5 and they appeared to display cardiovascular defects [6]. We obtained these mice to further investigate the phenotype, but were unable to obtain homozygous mutant mice. We found that the mice we were working with did not contain the proper *Akap13*-targeting event. We knocked down AKAP13 expression with RNAi in mouse ES cells and HUVECs. Reduced AKAP13 expression did not affect mouse ES cell differentiation into functional cardiomyocytes or the expression of endodermal, endothelial, or cardiac structural marker genes. Reduced AKAP13 expression did not affect angiogenic processes, such as wound healing, tube formation, or VEGF-mediated activation of PKD in HUVECs. (A-2) We breed AKAP13 Rho-GEF and PKC-PKD binding domain deficient mice (i.e., Truncation Mutant) to homozygosity and found that they developed normally, had normal adult survival, cardiac structure and function, and lacked obvious phenotypes under basal conditions. (B) We then treated the wild-type and truncation mutant mice with isoproterenol (Iso) to induce β-adrenergic-mediated cardiac hypertrophy. (B-1) Wild-type mice displayed an increase in heart weight and size as well as an increase in the cardiac functional parameters, fractional shortening and ejection fraction. (B-2) Truncation mutant mice displayed the same increase in heart weight and size. However, these mice did not increase the cardiac functional parameters. Fractional shortening and ejection fraction were the same in Iso and vehicle treated truncation mutant mice.

Embryonic development requires the orchestration of multiple biological processes, including cellular differentiation, cell migration and tissue morphogenesis, and the incorporation of properly functioning tissue. Despite the indication that AKAP13 is required for cardiovascular development, the specific biological processes it regulates are unknown. Two lines of evidence suggested that AKAP13 might regulate differentiation into functional cardiomyocytes. First, the initial description of *Akap13*-null embryos indicated that these embryos die early during development and display underdeveloped hearts with fewer cardiomyocytes than normal [7]. Second, the AKAP13-bound signaling molecule, PKC [8,9], and the downstream class II histone deacetylase (HDAC)–myocyte enhancer factor 2 (MEF2) signaling cascade [10,11] regulate cardiomyocyte differentiation.

To determine if AKAP13 regulates differentiation into functional cardiomyocytes, we developed an RNAi assay to disrupt gene expression during mouse ES cell differentiation (Chapter 2). A similar assay has been very useful for identifying genes required for ES cell maintenance [12,13], and our assay should have similar utility for identifying genes involved in early developmental process (i.e., cellular differentiation). We used our assay to assess the differentiation and maturation of certain cell types and the ability of functional cardiomyocytes to form and create areas of rhythmically contracting cells. AKAP13-deficient ES cells were differentiated into embryoid bodies (EBs) and analyzed for Nkx2.5-positive (i.e., cardiac mesodermal) cells, functionally contracting cardiomyocytes, and expression of cell-type marker genes. From

these studies, we found that AKAP13-deficient ES cells had normal differentiation into Nkx2.5-positive cells and expression of marker genes for cardiomyocytes, endothelial cells, and endoderm. Additionally, these cells formed areas of contracting cardiomyocytes at normal levels. These results indicate that AKAP13 is not required for differentiation into cardiac or endothelial cells or for the formation of functional cardiomyocytes. Furthermore, they suggest that the *Akap13*-null mouse phenotype is not due to defective cellular differentiation or cardiomyocyte function. However, the ES cell differentiation model is not ideal for studying developmental processes that require cellular migration or tissue morphogenesis. Thus, defects in these processes could cause the *Akap13*-null embryos to die.

Cellular migration and tissue morphogenesis during development are best studied in an *in vivo* system. Thus, we initiated a collaboration with Dr. James Segars (at the NICHD) to further investigate the *Akap13*-null developmental phenotype. The goal of this collaboration was to compare age-matched embryos and to identify the defects that block further development and lead to embryonic death. Despite much time and effort, we never obtained *Akap13*-null embryos from the mice imported from the Segars Lab. Subsequently, Southern blot analysis indicated that the mice we were working with did not have the proper *Akap13* targeting event. Thus, we discontinued our work on this mouse line and focused our *in vivo* studies on the AKAP13 gene-trap mutant mice we generated. Further analysis of embryos with the proper targeting event remains to be done.

Since AKAP13 knockdown did not effect cellular differentiation and we were unable to obtain *Akap13*-null embryos to identify the defected tissues, we did not know which tissues and cell types could require AKAP13 for development. To identify these tissues and cell types, we determined the expression pattern of AKAP13 with the gene-trap encoded β-galactosidase reporter cassette [14] (Chapters 3 & 4). From this analysis, we found that AKAP13 is broadly expressed during embryonic development with expression in the heart, brain, lung, gut, kidney, muscle, and vasculature. Since *Akap13*-null embryos appear to die early during development, around embryonic day E9.5, the vascular expression of AKAP13 was very intriguing. This is because the cardiovascular system is the first functioning organ system required for embryonic survival and defects in this system can cause early embryonic death. Additionally, both cardiac and vascular defects can give rise to edema as seen in the *Akap13*-null embryos [6]. Thus, the *Akap13*-null phenotype could be caused by either cardiac or vascular defects.

To determine if AKAP13 mediates vascular development or function, we conducted RNAi in HUVECs, a common *in vitro* model for endothelial cell biology and angiogenic processes (Chapter 3). We used the HUVEC model system to investigate the role of AKAP13 in endothelial cell attachment to extracellular matrices, cytoskeletal organization, wound healing, tube formation, and the signaling response to vascular endothelial growth factor (VEGF). Despite the indications that AKAP13 may regulate aspects of angiogenesis, we found that AKAP13-deficient HUVECs had normal cellular properties, tube formation, and

188

VEGF-induced wound healing and activation of PKD. These results indicate that AKAP13 does not regulate normal endothelial cell biology or angiogenic processes. Furthermore, they suggest that AKAP13 is not required for vascular formation during embryonic development.

AKAP13 integrates three upstream G-protein signaling pathways to induce at least two downstream signaling cascades, and the complete loss of AKAP13 results in embryonic death. However, the specific AKAP13-coordinated signaling pathways required for development are unknown. The AKAP13 signaling complex induces two downstream signaling cascades by activating the small GTPase RhoA [3] or a PKC–protein kinase D (PKD) cascade [15]. Since *Akap13*-null mouse embryos die, we wanted to identify the specific AKAP13-mediated signaling cascade required for development. To determine this, we generated truncation mutant mice from gene-trap mutations that disrupt specific AKAP13 protein domains (Chapter 4). One of these truncations eliminates the PKC and PKD binding domains and the second truncation eliminates the Rho–guanine nucleotide exchange factor (GEF) domain, as well as the PKC and PKD binding domains. We mated these mutant mice to determine if these AKAP13-domain deficient mice recapitulate the *Akap13*-null phenotype. Surprisingly, we found that both sets of truncation mutant mice survive normally and do not show phenotypes under normal conditions. These results indicate that the AKAP13 Rho-GEF and PKC-PKD binding domains are not required for embryonic development or survival. Furthermore, they suggest that an unknown AKAP13-coordinated signaling pathway may be required for embryonic development.

Since the AKAP13 Rho-GEF and PKC-PKD binding domains are not required for mouse development or survival, we were able to investigate the role of these AKAP13 protein domains in adult mice. We looked at the gross morphology of organs and conducted an in-depth analysis of cardiac structure and electrical activity by electrocardiography (ECG). The organs from Rho-GEF and PKC-PKD binding domain–deficient mice were morphologically normal. Additionally, these mice had normal cardiac structure and ECGs. Finally, we investigated the role of AKAP13 in mediating a cardiac hypertrophic stress response. The AKAP13 Rho-GEF and PKC-PKD binding domains regulate cardiomyocyte hypertrophic growth *in vitro* [4,5], and we wanted to know if they also regulate cardiac hypertrophic responses *in vivo*. To determine this, we treated AKAP13 Rho-GEF and PKC-PKD deficient mice with the common hypertrophic-inducing drug isoproterenol to stimulate the β-adrenergic receptor (Iso; Chapter 4). We found that these AKAP13-mutant mice had a normal increase in heart size in response to chronic β-adrenergic stimulation by Iso. Unexpectedly, these mice did not display a normal increase in cardiac ejection fraction or fractional shortening in response to chronic Iso treatment. These results indicate that the AKAP13 Rho-GEF and PKC-PKD binding domains do not mediate β-adrenergic-induced cardiac hypertrophy. However, these domains are required for proper cardiac functional responses to hypertrophic signals.

5.2 A systematic approach to identify the developmental and physiological functions of AKAP13

These studies were designed to provide a systematic analysis of AKAP13 function during development and physiology. Initially, our aims were twofold: (1) to identify the specific developmental processes regulated by AKAP13 and (2) to identify the AKAP13-mediated signaling cascade(s) required for development.

We conducted multiple studies to try and identify the developmental processes regulated by AKAP13. We were initially surprised that the AKAP13-deficient ES cells had a normal differentiation potential and were able to differentiate into functional cardiomyocytes. However, when we obtained more information about the *Akap13*-null embryos, we noticed that they form a heart that contains cardiomyocytes and does not have gross structural abnormalities [6]. Combined, the ES cell and *Akap13*-null embryo results indicate that AKAP13 does not regulate differentiation into cardiomyocytes or other important cell types, such as endothelial cells. Additionally, the relatively normal cardiac structure of *Akap13*-null embryos indicates that AKAP13 is not required for early cardiac morphogenesis. This suggests that AKAP13 may be required for morphogenesis of other tissues or for proper cardiovascular function. Unfortunately, the mice we were working with to study the *Akap13*-null developmental phenotype did not contain the proper targeting event. Thus, we were unable to analyze age-matched mutant embryos to identify the defects caused by the loss of AKAP13. Furthermore, the embryos compared in the published *Akap13*-null paper appear to be at different developmental stages (i.e., contain different numbers of somites) [6]. This could explain the decreased expression of cardiac markers in the *Akap13*-null embryos and suggests that

these expression changes are secondary to the primary *Akap13*-null defect. Thus, a much more detailed analysis of somite matched *Akap13*-null and wild-type embryos needs to be conducted to identify the true cause of embryonic lethality.

The *Akap13*-null mouse line has a global disruption of AKAP13, so the cell and tissue types that require AKAP13 during development are unknown. Our expression analysis showed that AKAP13 is broadly expressed during development and is highly expressed in the heart as well as endothelial cells and the vascular system. The cardiovascular system is the first functional organ system required for embryonic development, and either heart or vascular defects could result in the early lethality seen in *Akap13*-null embryos. We determined that AKAP13 was not required for ES cell differentiation into functional cardiomyocytes or endothelial cells. Additionally, we determined that AKAP13 was not required for endothelial cell biology, angiogenic processes, or VEGF-induced signaling in HUVECs. These results suggest that AKAP13 does not regulate cardiac or vascular differentiation or morphogenesis. However, our experiments did not investigate the role of AKAP13 in cardiovascular function. Thus, the *Akap13*-null embryos might die from defective cardiac or vascular function. Since AKAP13 mediates RhoA signaling, one possible role could be regulating vascular barrier integrity. To investigate this, future studies should determine if AKAP13 regulates the formation and maintenance of endothelial cell-cell junctions under normal conditions. Additionally, AKAP13 may transduce signaling events that regulate these cellular junctions and modulate vascular

integrity. Finally, a conditional *Akap13*-null allele is needed to identify the tissue type(s) that requires it for development. This will help focus future experiments to delineate the tissue-specific developmental processes mediated by AKAP13.

The second aim of our study was to identify the AKAP13-mediated signaling cascade(s) required for development. AKAP13 organizes multiple signaling molecules into a complex to integrate upstream G-protein signaling events and activate downstream pathways. In isolated cardiomyocytes, AKAP13 coordinates the activation of two signaling cascades that can induce cardiomyocyte growth and hypertrophy. One of these pathways transduces $G\alpha_{12/13}$ signals through the AKAP13 Rho-GEF domain to activate RhoA [4]. The other pathway transduces $G\alpha_{q/11}$ signaling to activate AKAP13-bound PKC and PKD, which induce gene expression changes at least in part through the de-repression of the transcription factor MEF2 [5]. The activation of these two signaling pathways is believed to be the main function of AKAP13 and the $G\alpha_s$-PKA signaling pathway modulates these two pathways [15,16]. Intriguingly, each of the three upstream G-protein pathways ($G\alpha_s$, $G\alpha_{12/13}$, and $G\alpha_{q/11}$) are required for cardiovascular development and embryonic survival in mice [17,18,19]. Similarly, many of the signaling molecules in the AKAP13-coordinated complex also regulate aspects of cardiovascular development. For instance, the Rho family of GTPases is required for cardiac morphogenesis and cardiomyocyte proliferation in mice [20], and more specifically, RhoA is required for cardiac morphogenesis in chick embryos [21]. Additionally, PKD is required for embryonic survival [22], and MEF2 is required for cardiac morphogenesis, myogenesis, and vascular development

[23,24]. These facts suggest that either of the AKAP13-coordinated signaling pathways (Rho-GEF or PKC-PKD) could be required for mouse development. Since the *Akap13*-null mouse is believed to eliminate all protein and signaling events, this mouse does not provide any information on the specific AKAP13-mediated signaling cascades required for development.

The AKAP13-truncation mutant mice we generated from gene-trap events were used to determine if the AKAP13-mediated PKC-PKD cascade alone or both the GEF-RhoA and PKC-PKD cascades are required for development (see Chapter 4). These gene-trap events disrupt the AKAP13 PKC and PKD binding domains (ΔPKC mouse line) or the Rho-GEF and PKC-PKD binding domains (ΔGEF mouse line). Thus, if the function of AKAP13 is solely to active the GEF-RhoA and PKC-PKD signaling cascades, then the ΔGEF mouse line should phenocopy the *Akap13*-null mouse line. Similarly, if the AKAP13-mediated PKC-PKD signaling cascade is required for development, the ΔPKC mouse line should have embryonic lethality. Additionally, comparing the embryonic phenotypes of the ΔGEF and ΔPKC mouse lines could provide information on the developmental processes regulated by the two pathways. Contrary to our expectations, the ΔGEF and ΔPKC mutations did not phenocopy the *Akap13*-null mouse line as they had normal development and survival. This indicates that the GEF-RhoA and PKC-PKD signaling cascades are not required for mouse development. Furthermore, this suggests that an additional AKAP13-mediated signaling cascade is required for mouse development. A top candidate for this required signaling cascade is AKAP13-mediated PKA signaling which could

regulate developmental processes through an unidentified pathway. Future studies will need to determine if the loss of AKAP13 binding to PKA phenocopies the *Akap13*-null mouse line.

The lack of any developmental or structural defect in the ΔGEF mice casts some doubt on the described *Akap13*-null mouse line. As mentioned previously, the mice we obtained to further investigate the *Akap13*-null phenotype did not contain the correct targeting event. It is possible that the mouse line we analyzed was not the same as the *Akap13*-null line described. Thus, validation of the phenotype in embryos that contain the proper targeting event remains to be done. Despite this, if the ΔGEF mice eliminate all of the AKAP13-mediated signaling pathways, then the phenotypic disparity between the two mouse lines suggest that the *Akap13*-null described embryonic lethality and cardiovascular defects may not be due to the loss of AKAP13. Thus, future studies need to validate the finding that AKAP13 is required for cardiovascular development and embryonic survival.

Since mice lacking the AKAP13 Rho-GEF and PKC-PKD binding domains survived normally and did not display obvious phenotypes under normal conditions, we developed a third aim: to determine if these protein domains are required for cardiac hypertrophy *in vivo*.

Both of the AKAP13-mediated GEF-RhoA and PKC-PKD signaling cascades induce hypertrophy in isolated cardiomyocytes [4,5]. However, it is unknown if AKAP13 is required for the induction of cardiac hypertrophy in a mouse. Cardiac hypertrophy can be induced in mice through several pathways, including

pressure overload by thoracic aortic constriction (TAC) or chronic activation of the angiotensin II (Ang II) or adrenergic pathways. Interestingly, all three of these pathways require PKD expression in cardiomyocytes to induce the full cardiac hypertrophic response [22]. To determine if AKAP13-mediated signaling was required for the cardiac hypertrophic response, we chronically stimulated the β-adrenergic receptor with Iso. We chose to activate this pathway because it gives a quick and very robust cardiac hypertrophic response, is easier and quicker than TAC, and generates a larger effect than Ang II treatment. If AKAP13 mediates signaling events downstream of the β-adrenergic receptor to induce hypertrophy, we expected the ΔGEF mice to display a reduced growth response to Iso treatment. Contrary to this expectation, Iso treatment increased heart size similarly for wild-type and ΔGEF mice. Unexpectedly, however, the ΔGEF mice did not increase cardiac functional parameters in response to Iso treatment. This indicates that AKAP13 does not regulate the growth response but does regulate the functional response to β-adrenergic induced cardiac hypertrophy. It is not clear if the lack of a functional response indicates that the ΔGEF mice are more or less likely to progress to heart failure. Future studies will need to further investigate the role of AKAP13 in the physiological and pathological response to hypertrophic stimuli. Additionally, the ΔGEF and ΔPKC mice offer an ideal mutational series to investigate the importance and unique functions of the AKAP13-mediated GEF-RhoA and PKC-PKD signaling pathways during β-adrenergic induced hypertrophy. Future studies should also use these mice to delineate the functions of AKAP13 during cardiac hypertrophy induced by other

pathways, including TAC, Ang II and endothelin-1. These studies will improve our understanding of the signaling processes involved in mediating cardiac hypertrophy and could lead to the identification of new therapeutic targets for the treatment of pathological hypertrophy.

My studies reveal the importance of conducting thorough and systematic investigations of the physiological functions of complex genes. Through these studies, we determined that AKAP13 does not regulate differentiation into cardiac or endothelial cells. Additionally, AKAP13 is not required for the formation of functional cardiomyocytes or for endothelial cells to mediate angiogenic processes. We also determined, to our surprise, that the known AKAP13-mediated signaling pathways, GEF-RhoA and PKC-PKD, are not required for development. Finally, we found that these AKAP13 domains are not required for the structural response to β-adrenergic induced cardiac hypertrophy. However, they are required for the proper cardiac functional response to β-adrenergic stimulation. A much more complete assessment of the *Akap13*-null phenotype and an independent *Akap13*-null mouse line are required to better understand the developmental processes regulated by AKAP13. In-depth analysis of the AKAP13 ΔGEF and ΔPKC mouse responses to multiple cardiac hypertrophic stimuli is also required to understand the physiological processes mediated by AKAP13.

5.3 Future directions for delineating AKAP13 function

197

The work described in this dissertation can be used as a starting point for many studies to further investigate the functions of AKAP13 during development and in adult physiology. Future work will need to verify that AKAP13 is required for development and identify the affected processes and tissues that cause lethality. Once the affected developmental processes are better understood, additional mutagenesis can be conducted to dissect out the AKAP13-mediated signaling cascades required for them. Future studies should also take advantage of the AKAP13 gene-trap mutant mice developed in this work. These truncation mutant mice can be used to determine the specific AKAP13-mediated signaling cascades required for the physiological responses to stresses.

Our results that AKAP13 Rho-GEF and PKC-PKD binding domain–deficient mice survive are in discordance with *Akap13*-null embryonic lethality. There are two possible reasons for this discordance: (1) AKAP13 is not required for embryonic development or (2) AKAP13 coordinates an unidentified signaling process that is required for development. The best way to distinguish between these two possibilities is to generate a novel *Akap13*-null allele through gene targeting and determine if homozygous embryos die during development. If the second *Akap13*-null allele confirms the embryonic lethal phenotype, then additional studies to identify the affected developmental processes and required protein domains are warranted. However, if this second set of *Akap13*-null embryos survive, then the original lethal phenotype is not due to the loss of AKAP13 but to some confounding effect.

The tissue types that require AKAP13 for development and the processes regulated by AKAP13 will need to be further understood. We found that AKAP13 is broadly expressed during embryonic development with high levels of expression in the heart, endocardium, and endothelial cells. This suggests that AKAP13 could be required in cardiomyocytes and/or endothelial cells for cardiovascular development and function. To determine which of these cell types requires AKAP13 during development, a floxed *Akap13* conditional allele will need to be generated. This floxed *Akap13* allele could then be crossed to *Cre*-expressing mouse lines to eliminate AKAP13 specifically in cardiomyocytes with *Nkx2.5-Cre* [25,26] or endothelial cells with *Tie2-Cre* [27,28]. These studies will aid in identifying and characterizing the developmental processes regulated by AKAP13.

The AKAP13 protein domains required for development need to be identified. Our annotation of the *Akap13* gene locus revealed that this is a very complicated gene that encodes for multiple transcripts, and these transcripts encode for different sets of protein domains. This complexity needs to be kept in mind when creating mutations and interpreting phenotypic results. The three major AKAP13 transcripts (i.e., *AKAP-lbc*, *Brx*, and *Lbc*) encode for a common set of protein domains, including the Rho-GEF and PKC-PKD binding domains. Our results indicate that these common domains are not required for development. This suggests that the PKA binding domain, which is specific to the *AKAP-lbc* transcript, is required. The requirement for the PKA binding domain could be tested for using a gene-trap truncation mutant (i.e., AE0301) or targeted

disruption of the *AKAP-lbc* transcript. If these mutants phenocopy the *Akap13*-null embryos, it indicates that the PKA binding domain is required for development. However, these mutants may not phenocopy the *Akap13*-null embryos because of redundancy provided by the *Brx* and *Lbc* transcripts. If this is the case, it may be necessary to add back specific AKAP13 transcripts into an *Akap13*-null background to identify the transcripts and protein domains sufficient for development.

The gene-trap mutant mouse lines we generated should provide very useful reagents for studying the roles of AKAP13 in mediating responses to stresses. We found that despite a normal increase in cardiac size, mice lacking the Rho-GEF and PKC-PKD binding domains of AKAP13 (ΔGEF mouse line) do not increase cardiac ejection fraction or fractional shortening in response to β-adrenergic stimulation by Iso. This indicates that these AKAP13 protein domains are not required for β-adrenergic-induced cardiac hypertrophy but are required for a proper cardiac functional response to β-adrenergic stimulation. Cardiac hypertrophy is a complex process that involves multiple signaling pathways, feedback loops, and cellular processes. Thus, it is unclear if β-adrenergic receptors signal directly through AKAP13 or if compensatory signaling pathways require AKAP13 to increase these functional parameters. To determine the signaling pathway(s) that requires AKAP13, the cardiac functional response to acute stimulation of β-adrenergic and other signaling pathways could be measured. Another possibility is that the β-adrenergic-stimulated ΔGEF mice may be at a more advanced stage of heart failure than the wild-type mice. To

determine if the AKAP13-ΔGEF mice progress to heart failure more quickly than wild-type mice, the effect of β-adrenergic stimulation on cardiac functional parameters could be monitored over a time course of heart failure. Finally, to identify which AKAP13-mediated signaling cascade (i.e., Rho-GEF or PKC-PKD) is required for the cardiac functional response to β-adrenergic stimulation, AKAP13-ΔPKC mice could be analyzed for their β-adrenergic-induced cardiac hypertrophic response.

The set of AKAP13 gene-trap mutant mice can also be used to dissect the functional roles of specific AKAP13 protein domains during other stresses. The Rho-GEF and PKC-PKD binding domains of AKAP13 transduce Ang II and endothelin-1 (ET-1) signals into cardiomyocyte hypertrophy *in vitro* [4,5]. The AKAP13 mutant mouse lines could be used to test the hypothesis that Ang II and ET-1 require the AKAP13 Rho-GEF and PKC-PKD protein domains to induce cardiac hypertrophy *in vivo*. AKAP13 may also play important roles in mediating stress responses in other tissues as we found expression in endothelial cells, vasculature, kidney, lung, and brain. This expression pattern suggests that AKAP13 could mediate vasoconstriction in response to Ang II and ET-1 stimulation. The ΔGEF and ΔPKC mice could be used to investigate the role of AKAP13-mediated signaling in regulating this vascular response. These mice could also be used to study the importance of AKAP13 signaling in maintaining vascular integrity and inducing vascular leak in response to thrombin. AKAP13 has also been associated with leukemia [29], breast [2,30,31], and colorectal [32] cancers. AKAP13 might have a cell autonomous role in cancer formation, but

AKAP13-mediated signaling in the vasculature might also help to promote tumor growth. Future studies should look at the importance of AKAP13-mediated signaling in promoting tumor formation and growth. In conclusion, these studies should provide valuable insight into the many functions of AKAP13 in the mammalian system.

5.4 A perspective on the future of mouse and ES cell mutational studies

The pace of technological advances for studying gene function and disease in mice [33] and pluripotent (ES and induced pluripotent stem, iPS) cell systems [34] has been incredibly quick. Just over 20 years ago, the first gene targeting events by homologous recombination were conducted in mouse ES cells [35,36]. The isolation of mouse ES cells [37,38] was incredibly important because these cells could be used to generate an entire adult mouse, and thus, mice could be generated from mouse ES cells containing the targeting events [39]. Since then, the generation of gene knockouts by targeted homologous recombination has become the standard technique for studying gene function in mice.

The traditional gene knockout approach generates a null allele for the targeted gene throughout the entire mouse. This technique is great for studying the general functions of a gene, but there are a couple of caveats to this approach. First, studying the tissue specific functions of a widely expressed gene can be difficult because of confounding defects in other tissues. Second, the adult functions of a gene cannot be studied if the gene is required for development. Conditional knockout strategies (i.e., Cre/loxP and Flp/FRT)

alleviate these issues by allowing researchers to control the disruption of a gene in a tissue and temporal manner [40,41,42,43]. This approach allows for a more detailed analysis of gene function in specific cell and tissue types and can be used to avoid embryonic lethal phenotypes that prohibit studying gene function in adults. The generation of gene knockouts has been greatly sped up by large-scale international collaborations, including the mouse knockout project (KOMP; www.knockoutmouse.org) and the international gene trap consortium (IGTC; www.genetrap.org), which are working towards the goal of knocking out every gene in the mouse genome. These resources will make it much easier to study the overall function of any gene and the KOMP strategy even includes a method for generating conditional knockouts.

The generation of null alleles through gene knockouts gives a global picture of gene function. However, studying specific protein isoforms and domains is necessary to truly understand the biological processes mediated by certain genes. As my project demonstrates, this method can reveal new and unexpected results that are missed using a global knockout mouse. Many genes encode for multiple transcripts and protein isoforms through the use of alternative promoters and splicing events, and these unique isoforms can regulate distinct physiological processes. Additionally, many proteins contain multiple protein domains, and these domains could regulate unique functions. Finally, most diseases do not result from the complete loss of a gene's function but from the loss, gain, or mis-regulation of a portion of the genes activity. Thus, future research will need to

use truncation and hypomorphic alleles in conjunction with null alleles and tissue specific knockouts to systematically study gene function.

The IGTC is a great resource for obtaining truncation and hypomorphic alleles. This consortium has used gene-trap constructs to generate random mutational events in ES cells [44]. In this technique, the gene-trap construct randomly integrates into the ES cell genome [14,45]. If this integration occurs within an expressed gene, the gene-trap construct uses its strong splice acceptor to create a fused mRNA with the upstream exons of the endogenous gene. The fused mRNA is then translated into a fusion protein that contains the amino-terminus of the endogenous gene fused to βGeo, which confers β-galactosidase activity and antibiotic resistance. This fusion produces a truncation of the endogenous protein and, depending on the affected protein domains and severity of the truncation, can result in a variety of mutant alleles including null, hypomorphic, and dominant negative alleles. The gene-trap construct used for most of the IGTC resource requires ES cell expression of the endogenous gene for antibiotic selection of the gene-trap event. In fact, the probability of a gene being trapped can be modeled using gene length and ES cell expression levels [46]. Thus, large, highly expressed genes, such as AKAP13, are often trapped multiple times throughout the gene locus. These multiple gene-trap lines can be used as a series of truncation mutants to delineate the role of specific protein domains in mediating the gene's function(s). Genes not expressed in ES cells will not be trapped, but the same methodology can be applied to these genes. In this case, a series of targeting constructs can be used to generate specific truncation

mutants. This method of using multiple mutant alleles will be very powerful in delineating the function(s) of specific protein domains, dissecting apart complicated protein complexes, and modeling disease *in vivo*.

Additional strategies are likely to play complementary roles in delineating the functions of specific transcripts and their encoded protein isoforms in mediating biological processes. RNAi has great potential for identifying the functions of specific isoforms in regulating biological processes [47]. RNAi can be used to decrease the expression of a specific protein isoform by targeting a unique region of the mRNA transcript [48]. Additionally, a lentiviral-mediated RNAi approach has been used to study gene function in the epithelium of developing mice [49]. This approach allows for a very rapid assessment of gene function *in vivo* and alleviates the need for time and resource intensive gene-targeting methods. The results from this study suggest that lentiviral-mediated RNAi could also be used to study gene function in the whole mouse embryo. For this to be possible, lentiviral transduction into the embryo will need to be optimized. Finally, combining embryo-wide lentiviral transduction with a Cre-regulated RNAi expression system could be used to knock down gene or transcript expression in a specific tissue [50].

An additional strategy that has great promise for studying gene and transcript expression and function *in vivo* is the generation of tagged protein isoforms. Again, as my project showed, identifying the expression pattern of AKAP13 during development and in adult tissues has suggested possible roles AKAP13 might play during development, in adult physiology, and during disease.

205

Determining the expression pattern of a gene is often the first step in identifying gene function. The gene-trap construct encodes for β-galactosidase activity and faithfully reports endogenous gene expression patterns by LacZ staining [14]. Thus, the gene-trap ES cells [51,52] and derived mice [53] can be used to determine the tissue expression pattern of any trapped gene. Similarly, the targeting construct being used by most of the KOMP project also includes a β-galactosidase reporter cassette to report tissue expression [54,55]. However, LacZ staining for the β-galactosidase reporter cannot be used for *in vivo* imaging and does not report the subcellular localization of trapped proteins. Thus, it would be ideal to have all mammalian proteins tagged with a fluorescent or luciferase molecule similar to the yeast resource [56]. This would allow investigators to follow the expression of a gene *in vivo*, identify the subcellular distribution of proteins, and determine if different protein isoforms of the same gene localize to unique subcellular regions. Determining the subcellular distributions of proteins will help identify the potential cellular processes regulated by these proteins. A large set of the current gene-trap ES cell lines can be modified to generate a fusion of the endogenous protein with a fluorescent protein or a different tag by a floxin approach [57]. The fusion proteins can then be used to reveal the subcellular localization of the tagged proteins and for other biochemical techniques such as co-immunoprecipitation. These assays could be performed in ES cells, ES cell-derived cell types, or mouse lines. This strategy for modifying the gene-trapped loci should also be applicable to the loci targeted by KOMP. In

summary, these methods should further aid in identifying the functions of these gene-trapped genes and proteins.

Both the KOMP and IGTC resources disrupt a single allele in mouse ES cells and these ES cells are used to generate mouse lines where the homozygous mutant phenotypes can be studied. The generation of mouse lines from these heterozygous ES cells takes a significant amount of time and money. However, an increasing number of studies have used ES cells, ES cell differentiation, and ES cell-derived cell types to study gene function during developmental processes and physiology. These approaches offer several advantages over the generation of mouse lines. First, studies in ES cells can be done much quicker and more cheaply than studies in mice. Second, these properties allow for a larger number of genes to be studied and for more high-throughput analysis to be conducted. Finally, human ES and iPS cells, which cannot be used to make a whole organism, can be used to study gene functions and disease processes in human cell types.

There are several methods that can be used to disrupt gene expression and function in pluripotent ES and iPS cells. RNAi has become the "go-to" approach for disrupting gene expression in these cells because it is quick, easy, and inexpensive [58]. As described in Chapter 2, lentiviral-mediated RNAi is a great method for obtaining continued gene knockdown in ES cells and has been used to disrupt gene expression in undifferentiated ES cells [12,13] as well as during ES cell differentiation [59]. Additionally, lentiviral-mediated RNAi can be used to dissect the functions of unique transcripts and protein isoforms from a single

gene because RNAi is very specific and only requires a target sequence of 19 nucleotides [48]. Lentiviral-mediated RNAi can also been conducted efficiently in human ES and iPS cells, while gene targeting by homologous recombination has proven quite difficult in these cells [60]. There are several caveats to the use of RNAi knockdown techniques. First, RNAi reduces but does not completely eliminate expression of the target gene. Second, the lentivirus used to express the short hairpin RNA (shRNA) can be silenced as the ES cells differentiate thus reducing the level of knockdown. Finally, RNAi methods alone do not replace the need for truncation or disease mutations to conduct a systematic analysis of protein function. Thus, additional techniques are needed to compliment the RNAi approach.

An ideal method for complete, stable, and rational mutagenesis in ES cells is to generate homozygous gene targeted ES cells. As previously mentioned, mouse ES cells have been extensively used for gene targeting. Gene targeting can also be conducted in human ES [61] and iPS [62] cells, and methods, such as the use of zinc finger nucleases, have been developed to increase the low targeting efficiency and the selection of targeting events in these cells [63,64]. Several methods have been used to generate homozygous mutant ES cell lines. One method used in mouse ES cells is to select for cells that underwent loss of heterozygosity by increasing the antibiotic concentration [65,66]. This selects for cells that contain two copies for the resistance gene instead of just one and have become homozygous for the mutational event. This approach could be used for the randomly generated gene-trap events for which specific targeting constructs

do not exist. However, this approach could create deleterious effects and loss of heterozygosity at other genomic loci especially in human ES and iPS cells, which are heterozygous at many loci. Another method that has been used in both mouse and human ES cells is to serially target both alleles. In this approach, a conditional knockout cell line can be made using the same targeting construct and antibiotic resistance gene to target both alleles [54,67]. Alternatively, the same targeting construct containing different antibiotic resistance genes can be used to target both alleles [68]. This serial targeting method can use the targeting constructs designed by KOMP and should be applicable to most other targeting constructs as well. Homozygous gene targeted ES and iPS cells will be great resources for systematically studying gene function during development, physiology, and disease. Furthermore, the gene targeting strategies will be incredibly valuable for introducing human disease mutations into a controlled genetic background (i.e., into a normal human ES or iPS cell lines) and for verifying the role of disease associated mutations in the molecular or cellular defect (i.e., rescue experiments in disease-specific human iPS cell lines).

In summary, these strategies offer many advantages and provide more efficient and systematic methods for conducting disease- and physiological-centric as well as gene-centric research. *In vitro* and *in vivo* RNAi approaches have and will continue to be an efficient method for identifying genes that functionally regulate disease and physiological processes. Additionally, human ES and disease-specific iPS cells will greatly enhance our understanding of disease processes and provide insight into novel disease associated pathways.

These disease-specific cell lines should also provide a great system for identifying drug targets to treat the disease. Moreover, truncation mutant mice and homozygous pluripotent cell lines will allow for a much more systematic dissection of gene functions and will provide a detailed description of the physiological and molecular processes regulated by specific protein domains.

5.5 Acknowledgements

5.6 References

1. Wong W, Scott JD (2004) AKAP signalling complexes: focal points in space and time. Nat Rev Mol Cell Biol 5: 959-970.
2. Rubino D, Driggers P, Arbit D, Kemp L, Miller B, et al. (1998) Characterization of Brx, a novel Dbl family member that modulates estrogen receptor action. Oncogene 16: 2513-2526.

3. Diviani D, Soderling J, Scott JD (2001) AKAP-Lbc anchors protein kinase A and nucleates Galpha 12-selective Rho-mediated stress fiber formation. J Biol Chem 276: 44247-44257.

4. Appert-Collin A, Cotecchia S, Nenniger-Tosato M, Pedrazzini T, Diviani D (2007) The A-kinase anchoring protein (AKAP)-Lbc-signaling complex mediates alpha1 adrenergic receptor-induced cardiomyocyte hypertrophy. Proc Natl Acad Sci U S A 104: 10140-10145.

5. Carnegie GK, Soughayer J, Smith FD, Pedroja BS, Zhang F, et al. (2008) AKAP-Lbc mobilizes a cardiac hypertrophy signaling pathway. Mol Cell 32: 169-179.

6. Mayers CM, Wadell J, McLean K, Venere M, Malik M, et al. (2010) The Rho guanine nucleotide exchange factor AKAP13 (BRX) is essential for cardiac development in mice. J Biol Chem 285: 12344-12354.

7. Wadell JL, McLean, K., Driggers, P., Sarber, K., Jackson, R., Moorman, A., Westphal, H., Segars, J. Elucidation of the role of AKAP-Brx, an activator of RhoA, in murine cardiac morphogenesis.; 2006; Santa Fe, New Mexico. pp. 75.

8. Ventura C, Zinellu E, Maninchedda E, Fadda M, Maioli M (2003) Protein kinase C signaling transduces endorphin-primed cardiogenesis in GTR1 embryonic stem cells. Circ Res 92: 617-622.

9. Ventura C, Zinellu E, Maninchedda E, Maioli M (2003) Dynorphin B is an agonist of nuclear opioid receptors coupling nuclear protein kinase C activation to the transcription of cardiogenic genes in GTR1 embryonic stem cells. Circ Res 92: 623-629.

10. Karamboulas C, Dakubo GD, Liu J, De Repentigny Y, Yutzey K, et al. (2006) Disruption of MEF2 activity in cardiomyoblasts inhibits cardiomyogenesis. J Cell Sci 119: 4315-4321.

11. Karamboulas C, Swedani A, Ward C, Al-Madhoun AS, Wilton S, et al. (2006) HDAC activity regulates entry of mesoderm cells into the cardiac muscle lineage. J Cell Sci 119: 4305-4314.

12. Gaspar-Maia A, Alajem A, Polesso F, Sridharan R, Mason MJ, et al. (2009) Chd1 regulates open chromatin and pluripotency of embryonic stem cells. Nature 460: 863-868.

13. Grskovic M, Chaivorapol C, Gaspar-Maia A, Li H, Ramalho-Santos M (2007) Systematic identification of cis-regulatory sequences active in mouse and human embryonic stem cells. PLoS Genet 3: e145.

14. Skarnes WC, Auerbach BA, Joyner AL (1992) A gene trap approach in mouse embryonic stem cells: the lacZ reported is activated by splicing, reflects endogenous gene expression, and is mutagenic in mice. Genes Dev 6: 903-918.

15. Carnegie GK, Smith FD, McConnachie G, Langeberg LK, Scott JD (2004) AKAP-Lbc nucleates a protein kinase D activation scaffold. Mol Cell 15: 889-899.

16. Diviani D, Abuin L, Cotecchia S, Pansier L (2004) Anchoring of both PKA and 14-3-3 inhibits the Rho-GEF activity of the AKAP-Lbc signaling complex. Embo J 23: 2811-2820.

17. Yu S, Yu D, Lee E, Eckhaus M, Lee R, et al. (1998) Variable and tissue-specific hormone resistance in heterotrimeric Gs protein alpha-subunit (Gsalpha) knockout mice is due to tissue-specific imprinting of the gsalpha gene. Proc Natl Acad Sci U S A 95: 8715-8720.

18. Offermanns S, Zhao LP, Gohla A, Sarosi I, Simon MI, et al. (1998) Embryonic cardiomyocyte hypoplasia and craniofacial defects in G alpha q/G alpha 11-mutant mice. Embo J 17: 4304-4312.

19. Offermanns S, Mancino V, Revel JP, Simon MI (1997) Vascular system defects and impaired cell chemokinesis as a result of Galpha13 deficiency. Science 275: 533-536.

20. Wei L, Imanaka-Yoshida K, Wang L, Zhan S, Schneider MD, et al. (2002) Inhibition of Rho family GTPases by Rho GDP dissociation inhibitor disrupts cardiac morphogenesis and inhibits cardiomyocyte proliferation. Development 129: 1705-1714.

21. Kaarbo M, Crane DI, Murrell WG (2003) RhoA is highly up-regulated in the process of early heart development of the chick and important for normal embryogenesis. Dev Dyn 227: 35-47.

22. Fielitz J, Kim MS, Shelton JM, Qi X, Hill JA, et al. (2008) Requirement of protein kinase D1 for pathological cardiac remodeling. Proc Natl Acad Sci U S A 105: 3059-3063.

23. Lin Q, Lu J, Yanagisawa H, Webb R, Lyons GE, et al. (1998) Requirement of the MADS-box transcription factor MEF2C for vascular development. Development 125: 4565-4574.

24. Lin Q, Schwarz J, Bucana C, Olson EN (1997) Control of mouse cardiac morphogenesis and myogenesis by transcription factor MEF2C. Science 276: 1404-1407.

25. Moses KA, DeMayo F, Braun RM, Reecy JL, Schwartz RJ (2001) Embryonic expression of an Nkx2-5/Cre gene using ROSA26 reporter mice. Genesis 31: 176-180.

26. McFadden DG, Barbosa AC, Richardson JA, Schneider MD, Srivastava D, et al. (2005) The Hand1 and Hand2 transcription factors regulate expansion of the embryonic cardiac ventricles in a gene dosage-dependent manner. Development 132: 189-201.

27. Kisanuki YY, Hammer RE, Miyazaki J, Williams SC, Richardson JA, et al. (2001) Tie2-Cre transgenic mice: a new model for endothelial cell-lineage analysis in vivo. Dev Biol 230: 230-242.

28. Koni PA, Joshi SK, Temann UA, Olson D, Burkly L, et al. (2001) Conditional vascular cell adhesion molecule 1 deletion in mice: impaired lymphocyte migration to bone marrow. J Exp Med 193: 741-754.

29. Toksoz D, Williams DA (1994) Novel human oncogene lbc detected by transfection with distinct homology regions to signal transduction products. Oncogene 9: 621-628.

30. Bonuccelli G, Casimiro MC, Sotgia F, Wang C, Liu M, et al. (2009) Caveolin-1 (P132L), a common breast cancer mutation, confers mammary cell invasiveness and defines a novel stem cell/metastasis-associated gene signature. Am J Pathol 174: 1650-1662.

31. Wirtenberger M, Tchatchou S, Hemminki K, Klaes R, Schmutzler RK, et al. (2006) Association of genetic variants in the Rho guanine nucleotide exchange factor AKAP13 with familial breast cancer. Carcinogenesis 27: 593-598.

32. Hu JK, Wang L, Li Y, Yang K, Zhang P, et al. (2010) The mRNA and protein expression of A-kinase anchor proteins 13 in human colorectal cancer. Clin Exp Med 10: 41-49.

33. Guan C, Ye C, Yang X, Gao J (2010) A review of current large-scale mouse knockout efforts. Genesis 48: 73-85.

34. Stadtfeld M, Hochedlinger K (2010) Induced pluripotency: history, mechanisms, and applications. Genes Dev 24: 2239-2263.

35. Doetschman T, Gregg RG, Maeda N, Hooper ML, Melton DW, et al. (1987) Targetted correction of a mutant HPRT gene in mouse embryonic stem cells. Nature 330: 576-578.

36. Thomas KR, Capecchi MR (1987) Site-directed mutagenesis by gene targeting in mouse embryo-derived stem cells. Cell 51: 503-512.

37. Evans MJ, Kaufman MH (1981) Establishment in culture of pluripotential cells from mouse embryos. Nature 292: 154-156.

38. Martin GR (1981) Isolation of a pluripotent cell line from early mouse embryos cultured in medium conditioned by teratocarcinoma stem cells. Proc Natl Acad Sci U S A 78: 7634-7638.

39. Thompson S, Clarke AR, Pow AM, Hooper ML, Melton DW (1989) Germ line transmission and expression of a corrected HPRT gene produced by gene targeting in embryonic stem cells. Cell 56: 313-321.

40. Birling MC, Gofflot F, Warot X (2009) Site-specific recombinases for manipulation of the mouse genome. Methods Mol Biol 561: 245-263.

41. Wang Y, Krushel LA, Edelman GM (1996) Targeted DNA recombination in vivo using an adenovirus carrying the cre recombinase gene. Proc Natl Acad Sci U S A 93: 3932-3936.

42. Sauer B (1998) Inducible gene targeting in mice using the Cre/lox system. Methods 14: 381-392.

43. Feil R, Brocard J, Mascrez B, LeMeur M, Metzger D, et al. (1996) Ligand-activated site-specific recombination in mice. Proc Natl Acad Sci U S A 93: 10887-10890.

44. Nord AS, Chang PJ, Conklin BR, Cox AV, Harper CA, et al. (2006) The International Gene Trap Consortium Website: a portal to all publicly available gene trap cell lines in mouse. Nucleic Acids Res 34: D642-648.

45. Skarnes WC (2000) Gene trapping methods for the identification and functional analysis of cell surface proteins in mice. Methods Enzymol 328: 592-615.

46. Nord AS, Vranizan K, Tingley W, Zambon AC, Hanspers K, et al. (2007) Modeling insertional mutagenesis using gene length and expression in murine embryonic stem cells. PLoS One 2: e617.

47. Martin SE, Caplen NJ (2007) Applications of RNA interference in mammalian systems. Annu Rev Genomics Hum Genet 8: 81-108.

48. Salomonis N, Schlieve CR, Pereira L, Wahlquist C, Colas A, et al. (2010) Alternative splicing regulates mouse embryonic stem cell pluripotency and differentiation. Proc Natl Acad Sci U S A 107: 10514-10519.

49. Beronja S, Livshits G, Williams S, Fuchs E (2010) Rapid functional dissection of genetic networks via tissue-specific transduction and RNAi in mouse embryos. Nat Med 16: 821-827.

50. Stern P, Astrof S, Erkeland SJ, Schustak J, Sharp PA, et al. (2008) A system for Cre-regulated RNA interference in vivo. Proc Natl Acad Sci U S A 105: 13895-13900.

51. To C, Epp T, Reid T, Lan Q, Yu M, et al. (2004) The Centre for Modeling Human Disease Gene Trap resource. Nucleic Acids Res 32: D557-559.

52. Hirashima M, Bernstein A, Stanford WL, Rossant J (2004) Gene-trap expression screening to identify endothelial-specific genes. Blood 104: 711-718.

53. Wurst W, Rossant J, Prideaux V, Kownacka M, Joyner A, et al. (1995) A large-scale gene-trap screen for insertional mutations in developmentally regulated genes in mice. Genetics 139: 889-899.

54. Tate PH, Skarnes WC (2011) Bi-allelic gene targeting in mouse embryonic stem cells. Methods.

55. Testa G, Schaft J, van der Hoeven F, Glaser S, Anastassiadis K, et al. (2004) A reliable lacZ expression reporter cassette for multipurpose, knockout-first alleles. Genesis 38: 151-158.

56. Huh WK, Falvo JV, Gerke LC, Carroll AS, Howson RW, et al. (2003) Global analysis of protein localization in budding yeast. Nature 425: 686-691.

57. Singla V, Hunkapiller J, Santos N, Seol AD, Norman AR, et al. (2010) Floxin, a resource for genetically engineering mouse ESCs. Nat Methods 7: 50-52.

58. Heidersbach A, Gaspar-Maia A, McManus MT, Ramalho-Santos M (2006) RNA interference in embryonic stem cells and the prospects for future therapies. Gene Ther 13: 478-486.

59. Liu Y, Asakura M, Inoue H, Nakamura T, Sano M, et al. (2007) Sox17 is essential for the specification of cardiac mesoderm in embryonic stem cells. Proc Natl Acad Sci U S A 104: 3859-3864.

60. Giudice A, Trounson A (2008) Genetic modification of human embryonic stem cells for derivation of target cells. Cell Stem Cell 2: 422-433.

61. Zwaka TP, Thomson JA (2003) Homologous recombination in human embryonic stem cells. Nat Biotechnol 21: 319-321.

62. Hockemeyer D, Soldner F, Beard C, Gao Q, Mitalipova M, et al. (2009) Efficient targeting of expressed and silent genes in human ESCs and iPSCs using zinc-finger nucleases. Nat Biotechnol 27: 851-857.
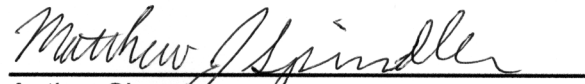
63. Hockemeyer D, Jaenisch R (2011) Gene Targeting in Human Pluripotent Cells. Cold Spring Harb Symp Quant Biol.

64. Tenzen T, Zembowicz F, Cowan CA (2010) Genome modification in human embryonic stem cells. J Cell Physiol 222: 278-281.

65. Lefebvre L, Dionne N, Karaskova J, Squire JA, Nagy A (2001) Selection for transgene homozygosity in embryonic stem cells results in extensive loss of heterozygosity. Nat Genet 27: 257-258.

66. Mortensen RM, Conner DA, Chao S, Geisterfer-Lowrance AA, Seidman JG (1992) Production of homozygous mutant ES cells with a single targeting construct. Mol Cell Biol 12: 2391-2395.

67. Bu L, Gao X, Jiang X, Chien KR, Wang Z (2010) Targeted conditional gene knockout in human embryonic stem cells. Cell Res 20: 379-382.

68. Song H, Chung SK, Xu Y (2010) Modeling disease in human ESCs using an efficient BAC-based homologous recombination system. Cell Stem Cell 6: 80-89.
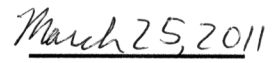
Publishing Agreement

It is the policy of the University to encourage the distribution of all theses, dissertations, and manuscripts. Copies of all UCSF theses, dissertations, and manuscripts will be routed to the library via the Graduate Division. The library will make all theses, dissertations, and manuscripts accessible to the public and will preserve these to the best of their abilities, in perpetuity.

Please sign the following statement:
I hereby grant permission to the Graduate Division of the University of California, San Francisco to release copies of my thesis, dissertation, or manuscript to the Campus Library to provide access and preservation, in whole or in part, in perpetuity.

_____   March 25, 2011
Author Signature   Date